

Grid-connected microgrids: Evaluation of benefits and challenges for the distribution system operator

Master's thesis in Electric Power Engineering

Charlie Jägerhag
Vishal Shende

MASTER'S THESIS 2018

**Grid-connected microgrids: Evaluation of benefits
and challenges for the distribution system
operator**

Charlie Jägerhag and Vishal Shende



CHALMERS
UNIVERSITY OF TECHNOLOGY

Department of Electrical Engineering
Division of Electric Power Engineering
CHALMERS UNIVERSITY OF TECHNOLOGY
Gothenburg, Sweden 2018

Grid-connected microgrids: Evaluation of benefits and challenges for the distribution system operator
Charlie Jägerhag
Vishal Shende

© Charlie Jägerhag and Vishal Shende, 2018.

Supervisors:

Kyriaki Antoniadou-Plytaria, Department of Electrical Engineering, Chalmers University of Technology

Erika Antonsson, Göteborg Energi

Ferruccio Vuinovich, GENAB

Examiner:

Tuan Anh Le, Department of Electrical Engineering, Chalmers University of Technology

Master's Thesis Report 2018
Department of Electrical Engineering
Division of Electric Power Engineering
Chalmers University of Technology
SE-412 96 Gothenburg

Cover: Illustrative figure of a distribution grid with a grid-connected microgrid.

Grid-connected microgrids: Evaluation of benefits and challenges for the distribution system operator

Charlie Jägerhag and Vishal Shende

Department of Electrical Engineering

Chalmers University of Technology

Abstract

A microgrid is low or medium voltage that includes and operates its own distributed energy resources. From the viewpoint of the distribution system, it can be seen as single entity, which is connected to the distribution network at a point of common coupling. The aim of this project was to evaluate the effects on, e.g., grid losses and grid loading of the operation of a grid-connected microgrid in the distribution grid. A linear programming model has been developed for the optimal operation of a microgrid. The model has been applied on a real distribution grid that supplies an area in Gothenburg. The microgrid which is a 400 V network consisting of 78 villas includes various energy resources with the focus put on renewable energy generation and energy storage systems. Photovoltaic systems, wind turbines, batteries, a hydrogen energy storage system, and a combined heat and power generation plant are among the resources used in the microgrid. Five cases of different energy resources mixes were simulated to investigate the impacts of a microgrid in the distribution system. Two different operational objectives have been examined for the optimal scheduling of these resources: minimizing energy cost and minimizing energy exchange between the microgrid and the main grid at the point of common coupling.

The results showed that the operation of the proposed grid-connected microgrid in the distribution system could reduce the energy losses in the upstream 10 kV distribution network by up to 8.1 %. It was also shown that the microgrid could help reduce congestion by reducing the energy import from the upstream 135 kV network by up to 6.3 %. This reduction in power import could provide an opportunity to the distribution system operator to release network capacity, which could support the supply of more loads in the future. The operation of the microgrid does not have a significant impact on the steady-state voltage at the point of common coupling. The results of the thesis can provide suggestions both for the distribution system operation and the microgrid operation. i) The simulations showed that a fee that penalizes high peak import of power into the microgrid would be mutually beneficial for the microgrid and the distribution system operator. ii) In terms of investment and energy cost, a solar and battery based microgrid seemed to be the best option for this network, since after a 30-year period this microgrid could have saved up to 6 MSEK. However, the operation of the microgrid is also important and should be taken into consideration as results vary a lot. iii) Between the two operational objectives that were applied, the minimization of the energy exchange proved to be the most viable in terms of the lifetime of the batteries.

Keywords: Microgrid, Energy storage system, distributed generation, distributed

energy resources, optimal energy management, optimal power flow, electrical network modelling.

Acknowledgements

The authors would like to thank the examiner, Tuan A. Le, Lecturer at Department of Electrical Engineering, for giving proper guidance throughout the thesis work and help in structuring the planning of the project. The authors would also like to thank Ferruccio Vuinovich, GENAB, for helping in the selection of the area for the microgrid implementation and also for supplying the required grid data. Next, the authors wish to thank Kyriaki Antoniadou-Plytaria, PHD student at Chalmers Department of Electrical Engineering, for her immense support in the modelling, helping in proper structuring of the master thesis report, and also helping in giving guidance with the software used in the process of completing the thesis. Finally, the authors would like to thank Erika Antonsson, supervisor at Göteborg Energi, for her support and guidance in formulating the thesis idea.

Charlie Jägerhag and Vishal Shende, Gothenburg, June 2018



Contents

List of Figures	xv
------------------------	-----------

List of Tables	xvii
-----------------------	-------------

1 Introduction	1
1.1 Background and Motivation	1
1.2 Aim	2
1.3 Objectives	2
1.4 Specific Tasks	2
1.5 Scope and Limitations	3
1.6 Thesis Structure	3
2 Technical Background	5
2.1 Microgrid Concept	5
2.2 Control and Operation of Microgrids	6
2.2.1 Primary Control	7
2.2.2 Secondary Control	7
2.2.3 Tertiary Control	8
2.2.3.1 Energy Management System	8
2.3 Microgrid Projects	9
2.3.1 E.ON Microgrid Project in Simris Sweden	9
2.3.2 ABB Microgrid Project on Robben Island South Africa	9
2.4 Resources and Components in a Microgrid	9
2.4.1 Distributed Generation	10
2.4.1.1 Wind Turbines	10
2.4.1.2 Photovoltaic System	10
2.4.1.3 Combined Heat and Power Generation Plant	11
2.4.2 Distributed Energy Storage System	11
2.4.2.1 Battery Banks	12
2.4.2.2 Flywheels	12
2.4.2.3 Supercapacitors	13
2.4.2.4 Compressed Air Energy Storage	13
2.4.2.5 Pumped Hydro Energy Storage System	14
2.4.2.6 Hydrogen Energy Storage System	15
2.4.3 Controllable Loads	16
2.4.3.1 Electrified Vehicles	16

2.5	Optimization Applications in Power Systems	17
2.5.1	Mathematical Programming	17
3	Mathematical Formulation and Solution Methodology	19
3.1	Objective Functions	19
3.2	Electric Network	20
3.2.1	Line Modelling	20
3.2.2	Power Flow Equations	21
3.3	Linearization	22
3.3.1	Linearized Power Flow Equations	22
3.3.1.1	Linearized Current Constraints	24
3.4	Resource modelling	25
3.4.1	Energy Storage System	25
3.4.2	Photovoltaic System	26
3.4.3	Wind Turbines	26
3.4.4	Combined Heat and Power Generation Plant	27
3.5	Solution Approach	27
3.5.1	Software	27
4	Microgrid Scenario	29
4.1	Location of Microgrid	29
4.2	Energy Cost and Fees	32
4.3	Resources	33
4.3.1	Battery	33
4.3.2	Hydrogen Energy Storage System	33
4.3.3	Photovoltaic System	33
4.3.4	Wind Turbine	35
4.3.5	Combined Heat and Power Generation Plant	37
4.4	Investment Costs and Cost Analysis	38
4.4.1	Battery	38
4.4.2	Hydrogen Energy Storage System	38
4.4.3	Photovoltaic System	38
4.4.4	Wind Turbine	39
4.4.5	Combined Heat and Power Generation Plant	39
4.4.6	Grid Ownership and Operation	39
4.5	Cases	39
5	Result and Analysis	41
5.1	Base Case	41
5.2	Case 1	42
5.3	Case 2	44
5.3.1	Energy Cost Minimization Considering the Household Fee	44
5.3.2	Energy Cost Minimization Considering the Microgrid Fee	46
5.3.3	Minimization of Energy Exchange	48
5.4	Case 3	50
5.5	Case 4	52
5.6	Case 5	55

5.7	Cost Analysis	57
5.8	Accuracy of Linearization	59
5.9	Summary	60
6	Discussion	63
6.1	Network Losses	63
6.2	Energy Storage System Strategies	63
6.3	Microgrid Operational Strategies	63
6.4	Microgrid Economics	64
6.5	Off-grid Operation	64
7	Conclusions and Future Work	67
7.1	Conclusions	67
7.2	Future Work	68
A	Line Data	I
B	GAMS Code Case 5	V

List of Figures

1.1	Brief overview of the tasks done.	2
2.1	Microgrid central controller.	7
2.2	Hierarchical control levels of a microgrid.	8
2.3	Photovoltaic system.	10
2.4	Working flow of a CHP plant.	11
2.5	Storage of energy using flywheels.	13
2.6	Working flow of compressed air energy storage.	14
2.7	Pumped hydro energy storage system.	15
2.8	Hydrogen energy storage system.	16
3.1	Equivalent π -model of a line.	20
3.2	Piecewise linearization of a circle.	25
3.3	Microgrid GAMS and MATLAB simulation.	28
4.1	The 10 kV distribution grid that was used for the development of the microgrid model.	30
4.2	The 400 V distribution grid that was used for the development of the microgrid model.	31
4.3	Spot price for the year 2017.	32
4.4	Power production from 25 Sharp PV panels.	34
4.5	Power production from 25 Sharp PV panels with 30° tilt.	35
4.6	Power output as function of wind speed for the production data from the data sheet of the wind turbine and for a polynomial fitted curve.	36
4.7	Calculated power production from Bergey wind turbine for the year 2017.	37
5.1	Power import for the base case for year 2017.	41
5.2	Average power import for the base case for a day.	42
5.3	Annual power import for case 1.	43
5.4	Average power import for a day for case 1.	43
5.5	Annual power import when energy cost is minimized considering the household fee (case 2).	45
5.6	Daily average power import and battery usage when energy cost is minimized considering the household fee (case 2).	45
5.7	Power import for 2017 for case 2 minimizing cost with microgrid fee.	47

5.8	Average power import and battery usage for daily energy cost minimization considering the microgrid fee for case 2.	47
5.9	Power import for a year when minimizing energy exchange for case 2.	49
5.10	Average power import and battery usage for a day when minimizing energy exchange for case 2.	49
5.11	Power import for a year considering minimization of energy exchange for case 3.	51
5.12	Average daily power import for minimization of the energy exchange for case 3.	51
5.13	Power import for a year for case 4.	53
5.14	Average daily power import for the minimization of energy exchange for case 4.	53
5.15	Stored energy in the hydrogen tank in case 4.	54
5.16	Power import for a year for minimization of energy exchange for case 5.	55
5.17	Power production for a year from the CHP plant.	56
5.18	Stored energy in hydrogen tank in case 5.	56
5.19	Cost analysis comparison.	58
5.20	The total of present worth of energy and investment costs for a each year for 30 year period.	59

List of Tables

4.1	Energy subscription fees.	32
4.2	Scaling factor of solar panels for different tilt angles.	34
4.3	Factors for polynomial fitted curves.	36
4.4	Cases used in simulating the operation of the low voltage network. . .	39
5.1	Annual results for the base case.	42
5.2	Annual results for case 1.	44
5.3	Annual results for energy cost minimization considering the household fee for case 2.	46
5.4	Annual results for energy cost minimization considering the microgrid fee for case 2.	48
5.5	Annual results for minimization of energy exchange for case 2.	50
5.6	Annual results for the minimization of energy exchange for case 3. . .	52
5.7	Annual results for the minimization of energy exchange for case 4. . .	54
5.8	Components of the Hydrogen energy storage system.	55
5.9	Annual results for the minimization of energy exchange for case 5. . .	57
5.10	Present worth of energy and investment costs for a 30-year period. . .	58
5.11	Average absolute value of the error of linearized model compared to non-linear model.	60
5.12	Maximum voltage deviation for different test cases in percentage. . .	60
5.13	Summary of the key results for different test cases.	61
A.1	10 kV network line data.	I
A.2	400 V network line data.	II

1

Introduction

1.1 Background and Motivation

The climate is changing and one of the major challenges that the world is facing today is global warming. This is mainly due to large dependence on conventional sources, such as fossil fuels, for the production of a large portion of the electricity. To combat this challenge, the generation of electricity should shift from conventional sources to renewable energy sources (RES). The integration of RES into the existing power system, however, does pose some challenges regarding control and stability due to the intermittent nature of most RES [1]. A solution could be to integrate RES locally, i.e., as distributed generation (DG) and to control it separately which would make a local grid a microgrid. This means that the local grid would have separate control structures and can work in an islanded mode, i.e., disconnected from the main grid. In short, a microgrid is a collection of distributed controllable resources within the distribution network, either at low voltage level or medium voltage level [2].

Microgrids could be the key in providing reliable and sustainable energy to the society. The application of the microgrid concept might help to decrease power losses, reduce energy cost, minimize power import and, therefore, increase efficiency of the distribution systems. Multiple microgrids in connection to the distribution systems might also help to decrease the loading in the distribution lines and can help utilize the flexibility of customers (demand response) for supporting the operation of distribution systems as well as the overlaying transmission grids. Microgrids have a lot of benefits that may help advocate the use of sustainable power generation at the local level, as the integration of distributed energy resources (DER) would become easier. There is a strong interest in understanding the interactions between distribution systems and microgrids. And also analyzing how microgrids can benefit in improving the overall performance of the distribution systems.

Many DSOs are interested in understanding the effects of integrating a microgrid in their distribution system. They have a goal of integrating more sustainable energy and microgrids can promote the company's goal and enhance the penetration of RES in the distribution grid.

1.2 Aim

The aim of the thesis is to evaluate the benefits and the challenges of grid-connected microgrids in the distribution grid in terms of reduction of power losses, energy cost and economic viability. Moreover, the impact on the energy import and the steady-state voltage level before and after integration of a microgrid are examined as well.

1.3 Objectives

The objectives of this project are to:

- Estimate the investment cost for the implementation of a microgrid.
- Evaluate the effects of a microgrid operating under different objectives (power exchange minimization, and energy cost minimization) on the distribution system.
- Estimate the reduction in the energy cost for the microgrid customers under different cases and energy fees applied by the DSO.
- Propose a strategy for the DSO to address any negative effects or to take advantage of any positive effects.

1.4 Specific Tasks

Figure 1.1 shows how the specific tasks were carried out in order to achieve the objectives of the project.

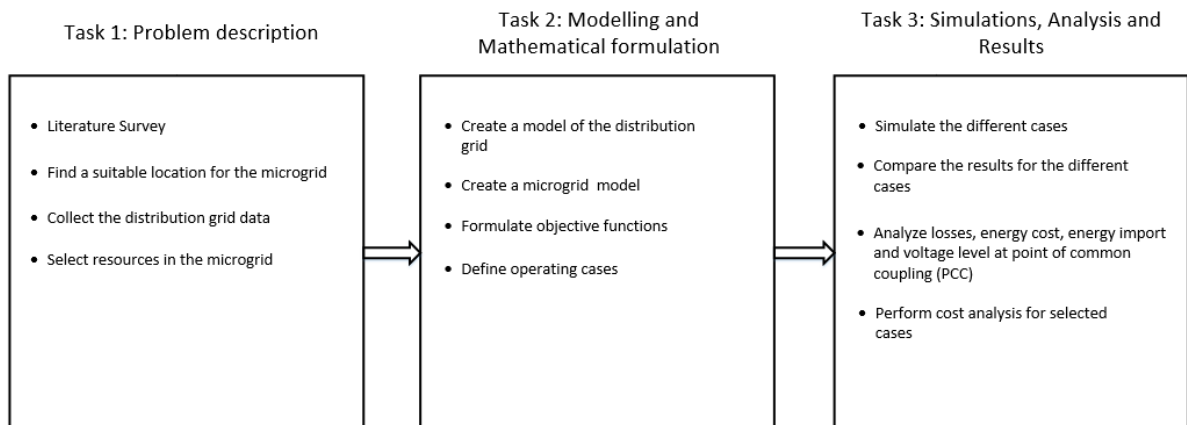


Figure 1.1: Brief overview of the tasks done.

A literature survey was done in order to gather knowledge about microgrids. A suitable location for the microgrid implementation was chosen and grid data were gathered for this area. A grid model based on the data was created and then a model of a microgrid was created by selecting among various energy resources. Two operational objectives and five cases with different energy resources mix were used. The results from all the different cases were then compared to each other, and a cost analysis was done for the cases with the most promising economical viability.

1.5 Scope and Limitations

The grid data required for this project were acquired from GENAB. This project applied steady-state simulations which means that dynamic simulations such as transient stability, fault analysis, and fault detection have not been considered. The project considers steady-state simulations over specific time periods. This project focuses on the power flow and losses in the distribution network. Moreover, this project is limited to a specific area of the distribution network in Gothenburg. The effects are evaluated by the simulations and a real site demonstration is suggested as a part of future work.

1.6 Thesis Structure

- **Technical Background:** This chapter explains the microgrid concept, its operation and presents some ongoing microgrid projects. This chapter also highlights the components and resources used in microgrid. A brief introduction to mathematical programming, which is used in the modelling, is also included in this chapter.
- **Mathematical Formulation and Solution Methodology:** This chapter presents the mathematical formulation of the optimization problem that was solved for the simulation of the microgrid operation. It presents the network modelling for the main distribution network and the microgrid as well as the mathematical models of the controllable resources. Furthermore, the solution approach is explained.
- **Microgrid Scenario:** This chapter presents the grid data that are used in the network model as well as the data for the parameters used in the resource modelling. This chapter also presents the microgrid cases and the mix of resources, that are used in the simulations.
- **Result and Analysis:** This chapter illustrates the results for all the microgrid cases. The analysis of the results is also carried out in this section. Lastly, the cost analysis is presented.
- **Discussion:** This chapter discusses the results and analysis and explains the impacts of the found results.
- **Conclusions and Future Work:** This section includes the conclusion remarks of the project and it also offers suggestions for future work on the area.

2

Technical Background

This chapter explains the microgrid concept, its operation and presents some ongoing microgrid projects. This chapter also highlights the components and resources used in microgrid. A brief introduction to mathematical programming, which is used in the modelling, is also included in this chapter.

2.1 Microgrid Concept

Energy production from fossil fuels can have various environmental issues. Using renewable energy sources (such as wind, solar, etc.) in the electrical system is a promising solution to these issues [3]. As the integration of RES increases in the distribution network, a microgrid can be formed. A microgrid can be a low or a medium voltage distribution network which is located downstream and connected with the distribution grid through a point of common coupling (PCC). Microgrids can be built with a number of various components which may comprise of distributed generation (DG), energy storage system devices (ESS) and controllable loads [4]. The main idea of a microgrid is local control of local resources that enables the microgrid to operate, at least during a limited time, in an islanded mode. ABB defines a microgrid as "distributed energy resources and loads that can be operated in a controlled and coordinated way; they can be connected to the main power grid, operate in "islanded" mode or be completely off-grid" [5]. Another close definition is the one given by the Consortium for Electric Reliability Technology Solutions (CERTS) who defines the concept of microgrids as "an aggregation of loads and microsources operating as a single system providing both power and heat. The majority of the microsources must be power electronic based to provide the required flexibility to insure operation as a single aggregated system. This control flexibility allows the CERTS MicroGrid to present itself to the bulk power system as a single controlled unit that meets local needs for reliability and security" [6]. Based on the proposed definition by CERTS, microgrids have been suggested for improving the power quality, reliability, efficiency, resiliency and for reducing environmental impact i.e reduction in CO₂ emissions [7].

The purpose of the microgrid operation varies depending on where a microgrid is built. Off-grid microgrids are built in remote locations where there is little possibility to import power. This type of microgrid has been employed to, e.g, ensure a reliable power supply. It could also be a cheaper alternative compared to building long transmission lines.

A microgrid can also be a part of the distribution system. A distribution network which incorporates microgrids would still include centralized conventional sources of energy. However, the microgrid would have its own local sources of energy and could independently manage and distribute its power to other consumers in that area. This type of microgrid mainly operates in connection with the main distribution grid but they are also capable of functioning autonomously from the main grid by switching to the islanded mode. Therefore, the consumers within the microgrid could have constant power supply even during faults such as power outages in the distribution network [8].

The recent advances in energy storage and power electronics facilitate an economic and reliable operation for the microgrid, which can promote the microgrid as a viable solution [8].

2.2 Control and Operation of Microgrids

As stated in section 2.1, a microgrid can have two operational modes, the interconnected mode also called the grid-connected mode of operation and the islanded mode also referred to as autonomous mode of operation. In the interconnected mode, the microgrid is linked with the distribution grid at the PCC whereas in the islanded mode, the microgrid is isolated from the distribution grid [9].

A microgrid can consist of e.g, DG, energy storage system (ESS), wind turbines, photovoltaic systems (PV), and controllable loads. However, the islanded microgrids are weaker and have smaller inertia than the conventional main distribution grid. This makes the microgrid more sensitive and vulnerable to voltage and frequency deviations. This is mainly due to the fact that the penetration of intermittent sources of renewable generation is large in microgrids [10, 11]. Secure, cost-effective, and steady operation of microgrids in both modes require a proper control system [12]. In order to enhance the controllability, security and flexibility of the whole distribution system, a microgrid can be controlled in a hierarchical approach [13]. The hierarchical control of the microgrid has three levels depending on time response and communication requirement, which will be discussed in Sections 2.2.1, 2.2.2 and 2.2.3 [13, 14].

Microsource controller (MC) and load controllers are local controllers (LC) used for controlling the loads and microsources and also for sharing needed information (such as load or consumption status) with the microgrid grid central controller (MGCC) by a communication link. LC are utilized for controlling the loads during emergency situations such as load shedding and MC is used to control the active and the reactive power of all the microsource devices. LCs are responsible for the primary control in microgrids. Figure 2.1 shows the typical design of a microgrid central controller. A microgrid is connected with the main distribution grid at the point of common coupling (PCC) and with MGCC for proper control of the microgrid. The MGCC is used for controlling the microgrid centrally.

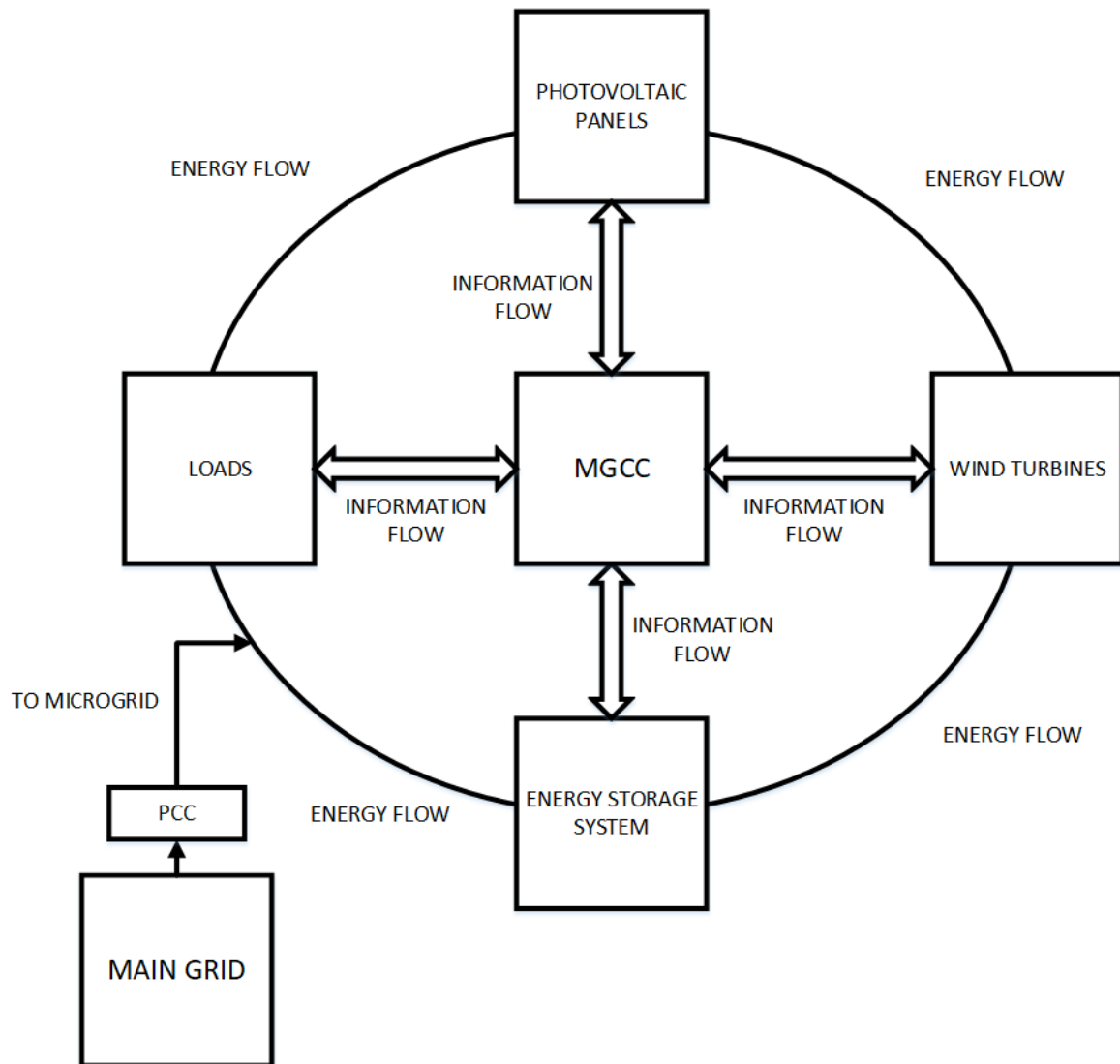


Figure 2.1: Microgrid central controller.

2.2.1 Primary Control

The first level of control hierarchy is primary control, also called local or internal control. This control is designed to operate independently and to respond instantaneously to local events. The primary control maintains the voltage and the frequency stability of the microgrid even after the islanding process [12]. The power flow control avoids undesired circulating currents among the DERs.

2.2.2 Secondary Control

Secondary control is the second level of the control hierarchy. The main function is to perform corrective measures to compensate for the unwanted frequency and voltage deviations which may have occurred during the primary level control. This control can be implemented and carried out either centrally by MGCC or locally by

MCs [9]. This control coordinates primary control within the microgrid in the time span of a few minutes.

2.2.3 Tertiary Control

The highest level of control in a hierarchical approach is tertiary control. Tertiary control coordinates the operation of one or multiple microgrids interacting with each other in the network and is also used to ensure that the requirements from the main grid such as voltage support and frequency control are fulfilled [14]. This control level operates within several minutes and then provides signals to the secondary control level at the microgrid. The tertiary control is not only the part of microgrid but also the main grid. It is used in both grid-connected and islanded mode as shown in Figure 2.2. This control also manages the power flow between the main grid and the microgrid.

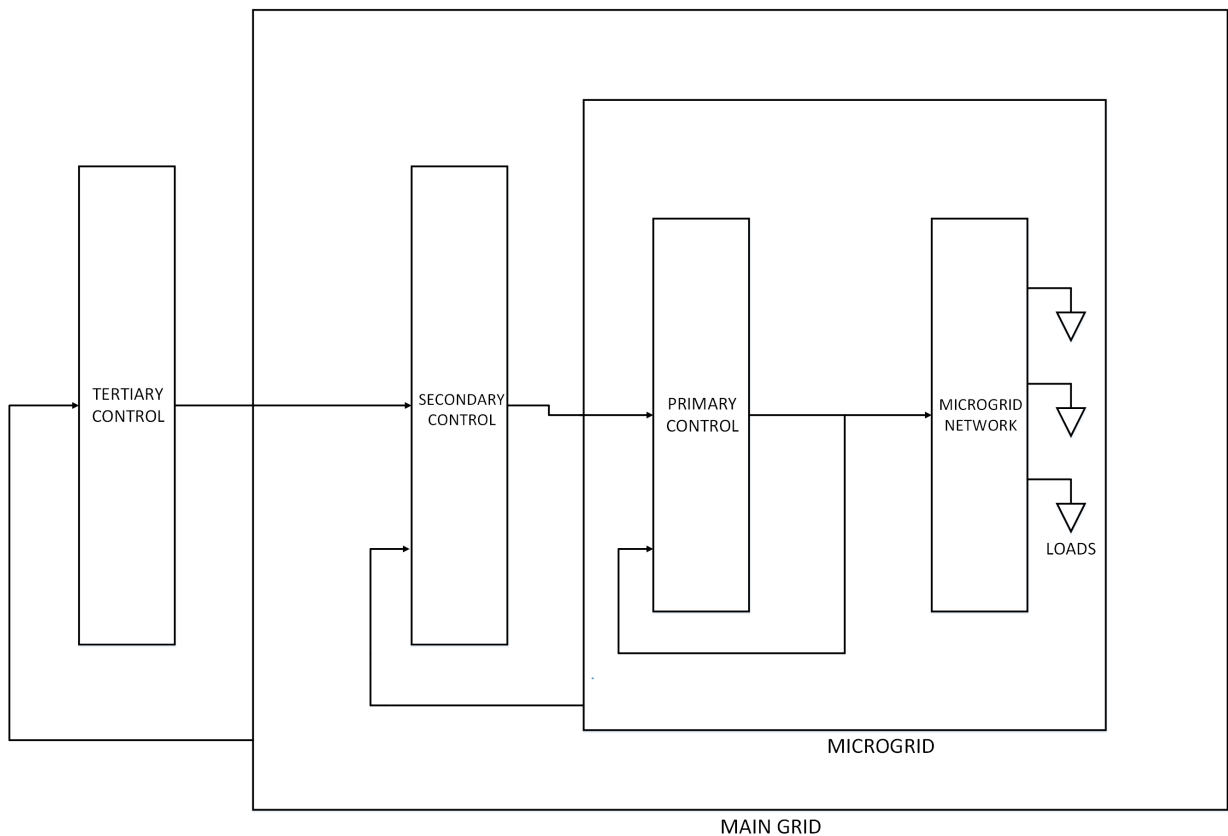


Figure 2.2: Hierarchical control levels of a microgrid.

2.2.3.1 Energy Management System

Tertiary control is responsible for controlling the power flow between the microgrid and the main distribution grid in the grid-connected mode [13]. For proper operation and scheduling of the power output among the various DG units of the microgrid and the loads, the energy management system (EMS) is required. The EMS is a controller which can control the DER units, optimally distribute the power

between the DER units, schedule the controllable loads in a cost-effective way and can automatically enable the system re-synchronization whenever there is a need for switching between the interconnected and the islanded modes [4].

2.3 Microgrid Projects

In this section, some ongoing microgrid projects will be presented. One of the microgrid is located in Sweden and the other in South Africa.

2.3.1 E.ON Microgrid Project in Simris Sweden

Simris is a small village on the east coast of Skåne in Sweden. This village is the location of a pre-existing grid that was transformed into a microgrid by E.ON. It is a test project to research the viability of microgrids and is part of the EU project InterFlex. The energy production is a mix of 440 kW capacity of PV, a 500 kW wind power plant, a 480 kW biogas reserve generator, and a battery of 833 kW nominal power and with 333 kWh storage capacity. The PV accounts for 20 % of the annual energy production, wind for 65 %, and the reserve generator for 15 %. The battery is used for voltage and frequency regulation and also to mitigate load peaks as well as store excessive energy. The battery never fully discharges or charges in order to ensure that it always has the possibility to control the power balance in the grid. The microgrid operates in islanded mode every fifth week. The investment cost of this project was 35 million SEK. The main purpose of this project was to understand how a closed electrical system can be made of fully weather dependent renewable production and controllable storage while also keeping the system in balance [15].

2.3.2 ABB Microgrid Project on Robben Island South Africa

Robben island is a remote island located in Table Bay about 9 km north west off the coast of Cape town. This island is operated by ABB. The main purpose of this project is to increase penetration of solar energy and reduce the use of fossil fuels. A solar park with peak power of 667 kW combined with ABB's solar inverters have been installed. A 500 kVA/ 837 kWh ABB Ability PowerStore battery is connected to the solar park. Cloud-based wireless networks are used to remotely operate the grid. Solar power is used to power the island for a minimum of 9 months a year. This project promotes high penetration of renewables in this area. The consumption of fossil fuel is reduced by 75 % which corresponds to approximately 600,000 litres annually [16].

2.4 Resources and Components in a Microgrid

In this section, some of the different DERs that can be used in forming a microgrid will be presented. The main focus is on the sustainable DERs. The suitable resources in forming a microgrid are highly dependent on the microgrids location.

2.4.1 Distributed Generation

The local source of energy in a microgrid is DG. The type of generation that is possible to install varies depending on the location.

2.4.1.1 Wind Turbines

The power generation from wind turbines is a DG which can be installed in a microgrid. The kinetic energy of the wind is converted to electric energy. The production of energy from wind is dependent on weather conditions and is, therefore, intermittent in nature. Wind turbines have a downside of generating noise that can create problems or complaints from the people living nearby. The power capacity of a wind turbine can vary from 50 W to 8.8 MW, an offshore wind turbine of 8.8 MW is the biggest wind turbine up to date [17]. Wind turbines requires a lot of space, and a rough estimate of the minimum needed distance between two wind turbines in order for them to not negatively affect their power outputs and performance is 10 times the rotor diameter [18].

2.4.1.2 Photovoltaic System

The photovoltaic system (PV) uses the energy in the sun rays to produce electric energy. In a similar way as wind power, the power production is dependent on weather conditions and can not be relied upon to produce continuous power all times of the year. As PV panels can be easily mounted on house roofs, they are considered as a promising DG for installation in microgrids. The working principle of PV energy generation is explained in Figure 2.3. As the sun rays hit the PV panels, it generates a DC power which can be directly fed to a battery storage device or else it can be converted to AC power through an inverter in order to feed the AC loads connected in the network. The typical efficiency of a PV panel is about 15 % [19].

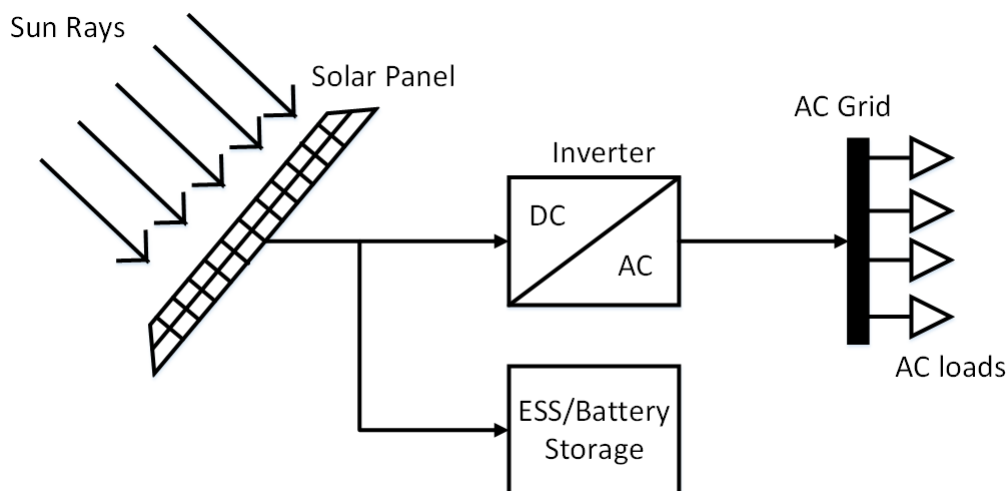


Figure 2.3: Photovoltaic system.

2.4.1.3 Combined Heat and Power Generation Plant

A combined heat and power generation plant (CHP), also known as cogeneration plant, produces heat and electricity simultaneously. Unlike conventional power plants, where only electricity is produced and the heat is wasted, a CHP plant also makes use of the heat in the form of hot water. CHP plants produce electricity in different ways using different heat engines. Smaller CHP plants use internal combustion engines to drive turbines along with heat exchangers to recover the waste heat. Larger CHP plants use gas and steam turbines. The efficiency of a CHP plant depends on how efficiently it uses the produced heat. CHP plants are more efficient and flexible than the conventional power plants since the heat is carried as hot water instead of being wasted [20]. The working flow of a typical CHP plant is illustrated in Figure 2.4.

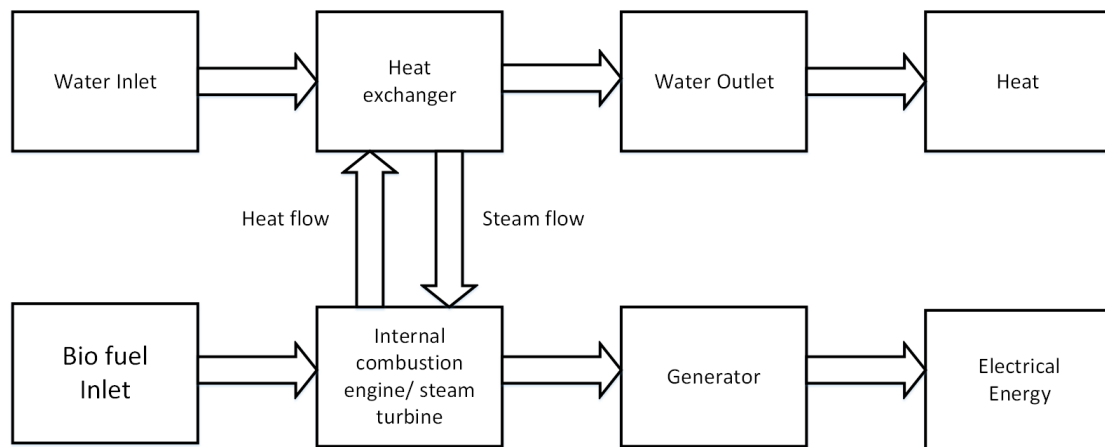


Figure 2.4: Working flow of a CHP plant.

In an internal combustion engine or steam turbine, a fuel, such as biomass or bio fuel, is burnt to generate heat and then this heat is used for boiling the water through the heat exchanger. The steam produced from heating water is used to rotate the turbine. This turbine then drives the generator and the generator produces electrical energy. The heat (hot water) from the heat exchanger can also be supplied to the consumers.

2.4.2 Distributed Energy Storage System

The power output of renewable energy such as wind and solar is highly dependent on weather conditions. It is hard to predict the power production due to the intermittent nature of most of the RES. Unlike conventional power sources, such as nuclear, the power output cannot be controlled. By using distributed energy storage systems (DESS), the power output of RES can be controlled by storing excess energy and using it later when needed. A non-dispatchable RES can be turned into a dispatchable energy source if it is integrated with DESS. In this section, different type of energy storage systems will be presented.

The purpose of DESS in a microgrid is to store energy when the energy from the

main distribution grid is cheap or when there is excessive generation in the microgrid [4]. The DESS can also function as energy sources and provide energy when demand is higher than generation. The EMS controls the power flow by dispatching the stored energy in the microgrid. ESS may be used for energy arbitrage which is the strategy of buying energy from the main grid when the price is low and to sell it when the price is high [21].

2.4.2.1 Battery Banks

Batteries can provide high efficiency, which leads to low energy losses. Batteries have limited storage size compared to their cost. There are a lot of options regarding the choice of battery technology. Two of the most common battery technologies are lead-acid and lithium-ion [22]. These batteries are different in terms of lifetime, efficiency, power density, and cost. Lithium-ion batteries have excellent efficiency (95%-98%), power density, and lifetime. However, they are expensive to produce. Lead-acid batteries have good efficiency (80%-90%), lifetime, and are cheap to produce. Lead-acid batteries have a low power density but when using a battery for energy storage inside a microgrid, the power density is irrelevant. It does not matter if the battery is heavy because there is no need for mobility. This makes the lead-acid battery, a suitable battery to integrate in a microgrid since it performs well for a low cost. The lithium-ion battery is also a suitable choice because of the higher efficiency that results in reduced losses. The efficiency of the battery is one of the most important specifications of a battery for an energy storage system. Battery storage systems are suitable for energy arbitrage. This is done by scheduling the batteries based on forecasted price.

2.4.2.2 Flywheels

Flywheels are another type of DESS. The main components of a flywheel are a massive rotating cylinder (the flywheel) storing kinetic energy, bearings, and a transmission device which is built in such a way that the motor or the generator is mounted on a stator. This is illustrated in Figure 2.5. The transmission device controls the energy charging and discharging and it controls the speed of the rotating cylinder to manage the energy in the flywheel. The speed at which the moving cylinder rotates denotes the amount of energy which is stored [22].

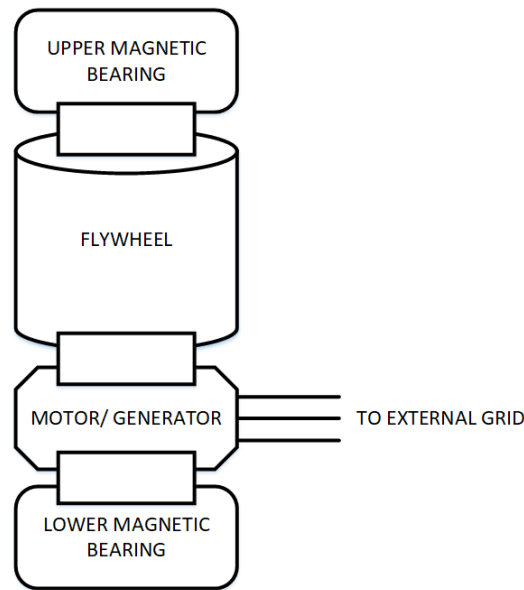


Figure 2.5: Storage of energy using flywheels.

For instance, an increase in speed of the moving cylinder means that a higher amount of energy is stored. For increasing speed of the flywheel, electricity can be supplied through the transmission device which is mounted on the stator. When the speed of the flywheel is reduced, electricity can be transmitted through the same transmission device. Durability, low maintenance need, a high power density are the main features of flywheels. However, it has a high self discharge rate due to air resistance and losses in the bearings.

2.4.2.3 Supercapacitors

A supercapacitor (SC), which is also called ultra capacitor or electric double-layer capacitor (EDLC), functions similarly to normal capacitors in which the energy can be stored by the separation of charges in an electric field. However, supercapacitors have a much higher capacitance as compared to normal capacitors.

2.4.2.4 Compressed Air Energy Storage

Compressed air energy storage system (CAES) stores energy by compressing air and is another effective type of DESS. Electricity is used to compress air which is later stored in either underground or above ground structures. Caves and old mines are an example of typical storage locations. To use the compressed air for producing electricity, the air is released from its storage location through a recuperator into a pressure turbine which is then connected to a generator. This is illustrated in Figure 2.5.

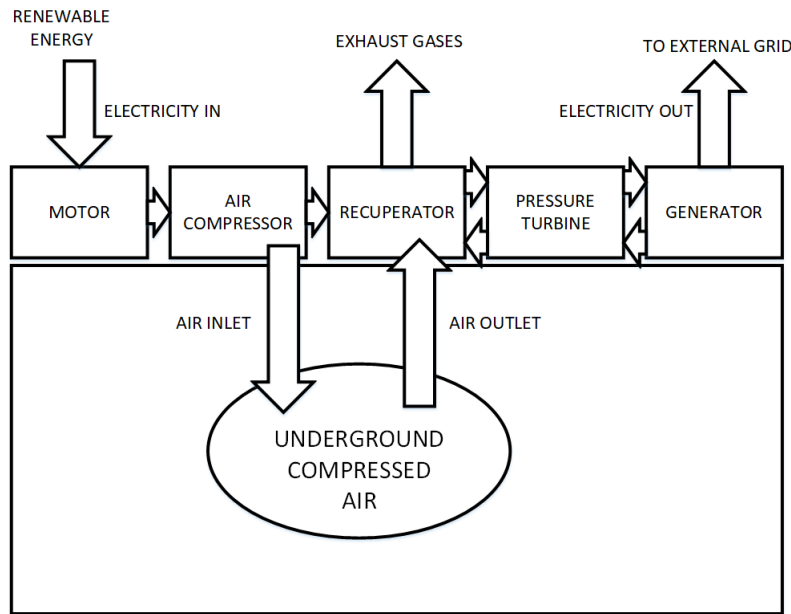


Figure 2.6: Working flow of compressed air energy storage.

The advantage of CAES is that it has large capacity. Low round trip efficiency and location requirements are some of its limitations [22].

2.4.2.5 Pumped Hydro Energy Storage System

Pump hydro energy storage system (PHESS) is constructed in such a way that there are two reservoirs located at two different elevations separated by significant altitudes, as shown in Figure 2.7. During off peak period, often during night time, the water is pumped upwards to the reservoir situated at the higher elevation where water can be stored whenever there is low power demand. In peak period, the water can be released from the upper reservoir and allowed to flow towards the lower reservoir. This flowing water is used for rotating the turbine which is connected to the generator in order to produce electricity.

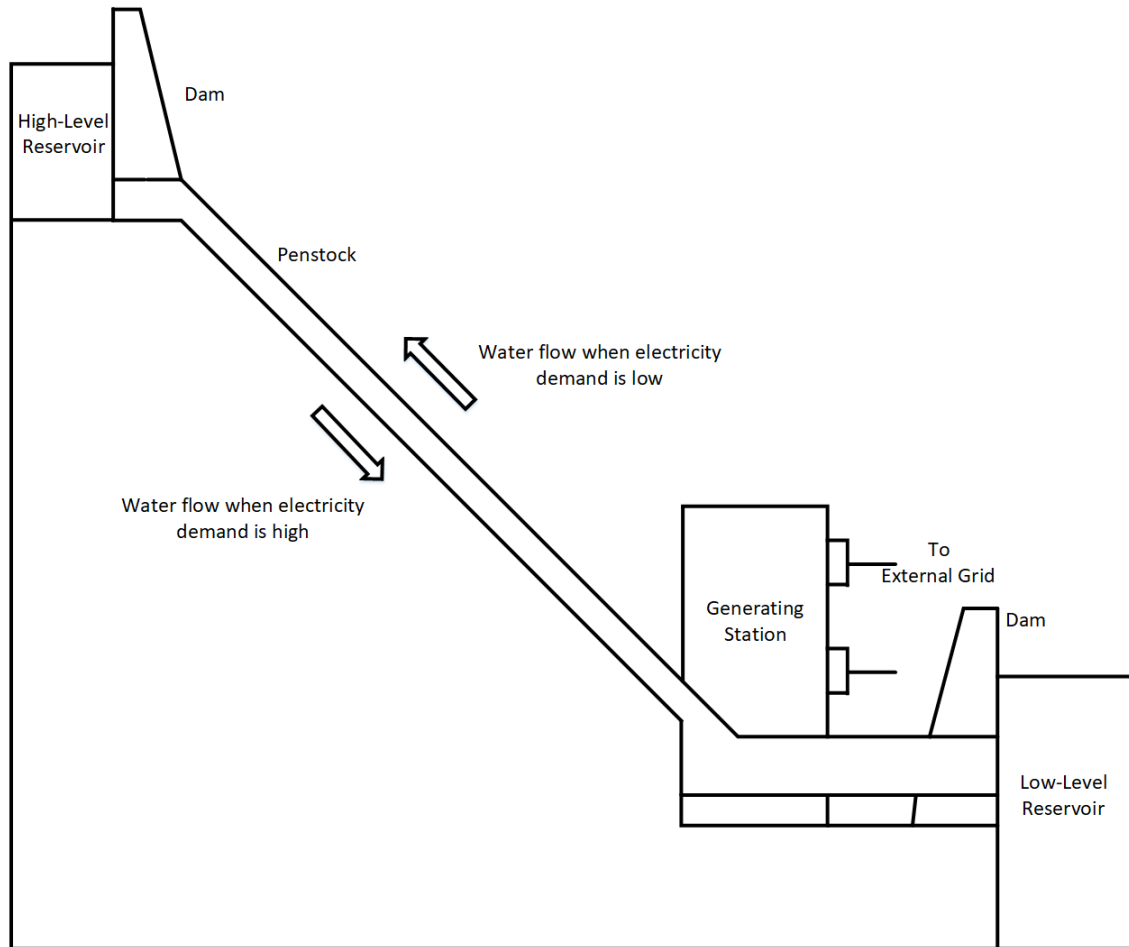


Figure 2.7: Pumped hydro energy storage system.

The typical round-trip efficiency of pumped hydro storage plant is around 70% [22]. A PHS plant has a very long lifetime. One of the main drawbacks is that it requires a large amount of space for its construction and installation.

2.4.2.6 Hydrogen Energy Storage System

The main objective of a hydrogen energy storage system is to make use of surplus electricity to produce hydrogen by electrolysis of water. Once hydrogen is produced by electrolysis, it can be used to generate electricity. Although the overall efficiency of hydrogen storage is lower than other storage technologies it has an incredibly large storage capacity, up to hundreds of MWh, which makes it appealing for certain applications [22]. Figure 2.8 shows a typical hydrogen storage setup.

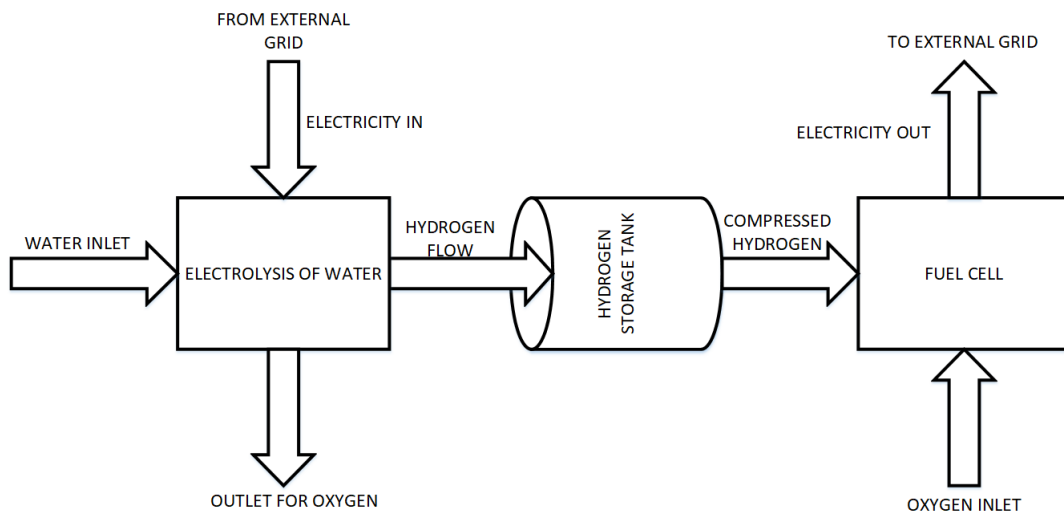


Figure 2.8: Hydrogen energy storage system.

As seen in the figure, the hydrogen storage system comprises of a hydrogen storage tank, a fuel cell and an electrolyzer. An electrolyzer splits the water into hydrogen and oxygen by using electricity. This splitting is an endothermic process, which means that heat is required during the chemical reaction. The produced hydrogen can then be stored in a gas tank under high pressure for an almost unlimited time. The produced oxygen is not stored in any gas tank for practical and economic reason and vented out to the atmosphere through pipes. Oxygen is taken directly from the atmosphere for generating electricity. Electricity is produced in the fuel cell where both hydrogen and oxygen are released. In the fuel cell an electro-chemical reaction takes place where the compressed hydrogen and the oxygen directly coming from the atmosphere react to produce water. In this chemical reaction, heat is released and electricity is generated.

2.4.3 Controllable Loads

Controllable loads can adjust and control their own electricity usage depending on the different real-time set points [4]. These loads are usually linked with demand side management (DSM) concepts or demand response (DR).

2.4.3.1 Electrified Vehicles

Plug-in hybrid electric vehicles (PHEVs) and plug-in electric vehicles (PEVs) can operate as controllable loads and can also be used as DESS. Unlike other controllable loads electric vehicles can frequently change their connection point and vary a lot in terms of both space and time. There is a concept called vehicle to grid (V2G) which purpose is to control and schedule the charging or discharging of electrical vehicles in order to help the operation of the grid [4].

2.5 Optimization Applications in Power Systems

To ensure that the resources within a power system are used in the most effective way, resource scheduling is often treated as an optimization problem. This could be economic load dispatch, i.e., optimal economic dispatch of available generation or an optimal power flow problem in order to minimize, e.g., losses or energy cost. In this thesis, the optimization problem that is formulated is optimal energy management within the microgrid.

2.5.1 Mathematical Programming

Mathematical programming is the use of numerical algorithms to solve mathematical optimization problems. There are different kinds of mathematical optimization problems and different kinds of variables that can be used, e.g., continuous, integer, binary, mixed continuous and integer. Some mathematical programming problems are: linear programming (LP), non linear programming (NLP), and mixed integer linear programming (MILP). Non linear programming problems are computationally heavy to solve and they are also "hard" to solve meaning that there are no algorithms that can handle all kinds of NLP. The problem is that even if a NLP is solved, there is no way to know if the solution is a local optimum or a global optimum. This often gives incentive for linearizing to create a LP which is the simplest form of mathematical programming and which can always be solved. The general formulation of a mathematical optimization problem is that there is an objective function

$$z = f(x) \tag{2.1}$$

where

$$x = (x_1, x_2, \dots, x_n) \tag{2.2}$$

and whose value should either be maximized or minimized with regards to given constraints of the variables x_1, x_2, \dots, x_n [23]. The constraints can be formulated as

$$g(x) \leq 0 \tag{2.3}$$

2. Technical Background

3

Mathematical Formulation and Solution Methodology

This chapter presents the mathematical formulation of the optimization problem that was solved for the simulation of the microgrid operation. It presents the network modelling for the main distribution network and the microgrid as well as the mathematical models of the controllable resources. Furthermore, the solution approach is explained.

3.1 Objective Functions

The energy scheduling of the micro-grid is solved as an optimization problem. Two different operational objectives have been used. One is minimizing power exchange with the main grid at the PCC and the other is minimizing energy cost. The microgrid power flow is solved separately from the distribution grid and therefore, the power import and export is modelled as the swing bus of the microgrid system. The first operational objective is formulated as

$$P_{MG,exchange} = \sum_t (P_{MG,imp}(t) + P_{MG,exp}(t) + K_{ESS} \cdot (P_{Discharge}(t) + P_{Charge}(t)) + K_{CHP} \cdot P_{CHP}(t)) \quad (3.1)$$

where $P_{MG,imp}(t)$ and $P_{MG,exp}(t)$ are the power import and export. The parameter K_{ESS} is a priority factor for discharging or charging the ESS. The variables $P_{Discharge}$ and P_{Charge} , represents the discharging and charging of the ESS and they are both positive variables. The variable P_{CHP} is the power output of the CHP plant and K_{CHP} is a priority factor for using the CHP plant. These priority factors are used to set the priority order of the resources. The lower limit of the priority factor for ESS is used to ensure that the ESS does not charge and discharge at the same time, the lower limit will be explained in more detail in Section 3.4.1. The priority factors are set as

$$\frac{1-n}{1+n} < K_{ESS} < 1 \quad (3.2)$$

and

$$K_{CHP} < 1 \quad (3.3)$$

where n is the round trip efficiency of the storage system. The upper limit of 1 in (3.2) and (3.3) is used to ensure that microgrid prefers to store energy rather

than exporting it, and produce its own energy rather than importing it. The other operational objective of the microgrid is to minimize energy trading cost

$$Cost = \sum_t \left(P_{MGimp}(t) \cdot (\pi_p(t) + \pi_{fb}) - P_{MGexp}(t) \cdot (\pi_p(t) + \pi_{fs}) \right) + \hat{P}_{MGimp} \cdot \pi_{pd} \quad (3.4)$$

where $\pi_p(t)$ is the spot price, and π_{fb} and π_{fs} is the buy and sell fee. \hat{P}_{MGimp} is the daily peak import and π_{pd} is the cost of the daily power import peak. $P_{MGimp}(t)$ and $P_{MGexp}(t)$ are both positive variables and are formulated as

$$P_{swing} = P_{MG,imp}(t) - P_{MG,exp}(t) \quad (3.5)$$

where P_{swing} is the swing bus power which can be both positive and negative.

3.2 Electric Network

In this section, the equations and the parameters that model the distribution system are presented.

3.2.1 Line Modelling

The model of a line is shown in Figure 3.1, where X is the line reactance, R is the line resistance, and Bc is the line charging.

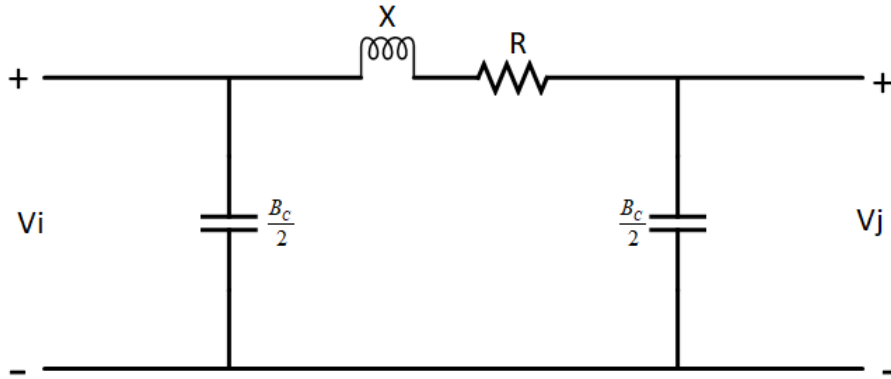


Figure 3.1: Equivalent π -model of a line.

The electrical network is modelled as n buses interconnected through complex impedances, which is denoted by Z and measured in Ω . The complex impedance is formulated as

$$Z_{i,j} = R_{i,j} + jX_{i,j} \quad (3.6)$$

and the admittance is calculated by

$$Y = \frac{1}{Z} \quad (3.7)$$

The admittance can either be expressed in its rectangular form

$$Y_{i,j} = G_{i,j} + jB_{i,j} \quad (3.8)$$

or its polar form

$$Y_{i,j} = |Y| \angle \theta_{i,j} \quad (3.9)$$

where G is the conductance, B is the susceptance, and $\theta_{i,j}$ is the admittance angle. The measurement unit of Y is Siemens (Ω^{-1}). Both i and j are indices representing the network buses. The nodal admittance matrix is given by [24]

$$\mathbf{Y}_{i,j} = \begin{pmatrix} Y_{11} & Y_{12} & \dots & Y_{1n} \\ Y_{21} & Y_{22} & \dots & Y_{2n} \\ \vdots & \vdots & \ddots & \vdots \\ Y_{n1} & Y_{n2} & \dots & Y_{nn} \end{pmatrix} \quad (3.10)$$

and the matrix is calculated as

$$\mathbf{Y}_{i,j} = \begin{cases} -Y_{i,j} & \text{if } i \neq j \\ Y_i + \sum_{j,j \neq i} Y_{i,j} & \text{if } i = j \end{cases} \quad (3.11)$$

where

$$Y_i = \frac{Bc_i}{2} \quad (3.12)$$

The admittance angle can be calculated as follows

$$\theta_{i,j} = \begin{cases} \arctan\left(\frac{B_{i,j}}{G_{i,j}}\right) & \text{if } G_{i,j} > 0 \\ \arctan\left(\frac{B_{i,j}}{G_{i,j}}\right) + \pi & \text{if } G_{i,j} < 0 \quad \& \quad B_{i,j} \geq 0 \\ \arctan\left(\frac{B_{i,j}}{G_{i,j}}\right) - \pi & \text{if } G_{i,j} < 0 \quad \& \quad B_{i,j} < 0 \\ \frac{\pi}{2} & \text{if } G_{i,j} = 0 \quad \& \quad B_{i,j} > 0 \\ \frac{-\pi}{2} & \text{if } G_{i,j} = 0 \quad \& \quad B_{i,j} < 0 \\ 0 & \text{if } G_{i,j} = 0 \quad \& \quad B_{i,j} = 0 \end{cases} \quad (3.13)$$

The admittance matrix can also be expressed in its rectangular form

$$\mathbf{Y}_{i,j} = \mathbf{G}_{i,j} + j\mathbf{B}_{i,j} \quad (3.14)$$

where $\mathbf{G}_{i,j}$ is the conductance matrix and $\mathbf{B}_{i,j}$ is the susceptance matrix.

3.2.2 Power Flow Equations

The power flow balance has to be satisfied at all buses of the system. This is described by the power flow equations

$$P_i - PD_i = |V_i| \cdot \sum_j |V_j| \cdot \left(G_{i,j} \cdot \cos(\delta_{i,j}) + B_{i,j} \cdot \sin(\delta_{i,j}) \right) \quad (3.15a)$$

$$Q_i - QD_i = -|V_i| \cdot \sum_j |V_j| \cdot \left(G_{i,j} \cdot \sin(\delta_{i,j}) - B_{i,j} \cdot \cos(\delta_{i,j}) \right) \quad (3.15b)$$

and

$$\delta_{i,j} = \delta_i - \delta_j \quad (3.15c)$$

where P_i and Q_i are the active and reactive power production, PD_i and QD_i are the active and reactive power demand, and δ_i is the voltage angle. The voltage is limited to its minimum and maximum value by

$$V_{i,min} \leq |V_i| \leq V_{i,max} \quad (3.16)$$

The power flow in the lines can be calculated as follows [25]

$$P_{i,j} = G_{i,j} \cdot (|V_j|^2 - |V_i| \cdot |V_j| \cdot \cos(\delta_{i,j})) + B_{i,j} \cdot |V_j| \cdot |V_j| \cdot \sin(\delta_{i,j}) \quad (3.17)$$

and

$$Q_{i,j} = B_{i,j} \cdot (|V_j|^2 - |V_i| \cdot |V_j| \cdot \cos(\delta_{i,j})) - G_{i,j} \cdot |V_j| \cdot |V_j| \cdot \sin(\delta_{i,j}) \quad (3.18)$$

Network losses are calculated by

$$P_{loss} = \sum_i \sum_j G_{i,j} \cdot |V_i|^2 + |V_j|^2 - 2 \cdot |V_i| \cdot |V_j| \cdot \cos(\delta_{j,i}) \quad (3.19)$$

3.3 Linearization

As explained in Chapter 2.5.1, non-linear problems are hard to solve. Therefore, linearized versions of the power flow constraints and the line currents are used in the microgrid. The linearization approach presented in [25] is adopted in this thesis and is presented in the coming sections. The linearization is based on the assumptions that the voltage is always close to the nominal voltage V_{nom} of the system and that the voltage angle difference between buses $\delta_{i,j}$ is always very small [25]. Equations (3.20) and (3.21) show the proposed linearization that was used in the methodology of this thesis.

$$|V_i| = V_{nom} + \Delta V_i \quad (3.20a)$$

$$|V_j| = V_{nom} + \Delta V_j \quad (3.20b)$$

$$\cos(\delta_{i,j}) \approx 1 \quad (3.21a)$$

and

$$\sin(\delta_{i,j}) \approx \delta_{i,j} \quad (3.21b)$$

where ΔV_i and ΔV_j is negligible in size compared to V_{nom} .

3.3.1 Linearized Power Flow Equations

The basic AC power flow equations for the active and the reactive power are presented in Equations (3.15a) and (3.15b). By using (3.20a) in (3.15a) and (3.15b) we get

$$P_i - PD_i = (V_{nom} + \Delta V_i) \cdot \sum_j |V_j| \cdot \left(G_{i,j} \cdot \cos(\delta_{i,j}) + B_{i,j} \cdot \sin(\delta_{i,j}) \right) \quad (3.22a)$$

and

$$Q_i - QD_i = -(V_{nom} + \Delta V_i) \cdot \sum_j |V_j| \cdot (G_{i,j} \cdot \sin(\delta_{i,j}) - B_{i,j} \cdot \cos(\delta_{i,j})) \quad (3.22b)$$

where ΔV_i is much smaller than V_{nom} and can be ignored. The magnitude of voltage at bus i can, therefore, be approximated to V_{nom} . Then the (3.22a) and (3.22b) can be expressed as

$$P_i - PD_i = V_{nom} \cdot \sum_j |V_j| \cdot (G_{i,j} \cdot \cos(\delta_{i,j}) + B_{i,j} \cdot \sin(\delta_{i,j})) \quad (3.23a)$$

and

$$Q_i - QD_i = -V_{nom} \cdot \sum_j |V_j| \cdot (G_{i,j} \cdot \sin(\delta_{i,j}) - B_{i,j} \cdot \cos(\delta_{i,j})) \quad (3.23b)$$

Since the voltage angle difference between bus i and bus j are small, the approximation in (3.21) can be used and (3.23a) and (3.23b) can now be expressed as

$$P_i - PD_i = V_{nom} \cdot \sum_j |V_j| \cdot (G_{i,j} + B_{i,j} \cdot \delta_{i,j}) \quad (3.24a)$$

and

$$Q_i - QD_i = -V_{nom} \cdot \sum_j |V_j| \cdot (G_{i,j} \cdot \delta_{i,j} - B_{i,j}) \quad (3.24b)$$

The Equations (3.24a) and (3.24b) can be rewritten as

$$P_i - PD_i = V_{nom} \cdot \sum_j (|V_j| \cdot G_{i,j} + |V_j| \cdot B_{i,j} \cdot \delta_{i,j}) \quad (3.25a)$$

and

$$Q_i - QD_i = -V_{nom} \cdot \sum_j (|V_j| \cdot G_{i,j} \cdot \delta_{i,j} - |V_j| \cdot B_{i,j}) \quad (3.25b)$$

Using (3.20b); (3.25a) and (3.25b) can be rewritten as

$$P_i - PD_i = V_{nom} \cdot \sum_j (|V_j| \cdot G_{i,j} + (V_{nom} + \Delta V_j) \cdot B_{i,j} \cdot \delta_{i,j}) \quad (3.26a)$$

and

$$Q_i - QD_i = -V_{nom} \cdot \sum_j ((V_{nom} + \Delta V_j) \cdot G_{i,j} \cdot \delta_{i,j} - |V_j| \cdot B_{i,j}) \quad (3.26b)$$

In (3.26a) and (3.26b), ΔV_j is comparatively small and hence can be neglected. Finally, the derived linearized power flow equations that were used for the modelling of the microgrid are

$$P_i - PD_i = V_{nom} \cdot \sum_j (|V_j| \cdot G_{i,j} + V_{nom} \cdot B_{i,j} \cdot \delta_{i,j}) \quad (3.27a)$$

and

$$Q_i - QD_i = -V_{nom} \cdot \sum_j (V_{nom} \cdot G_{i,j} \cdot \delta_{i,j} - |V_j| \cdot B_{i,j}) \quad (3.27b)$$

3.3.1.1 Linearized Current Constraints

To consider the current constraints in network lines, linearized expressions of the line currents were used. The current in the lines can be approximated by

$$Ire_{i,j} \approx \frac{P_{i,j}}{V_{nom}} \quad (3.28a)$$

$$Iim_{i,j} \approx \frac{Q_{i,j}}{V_{nom}} \quad (3.28b)$$

Combining (3.20), (3.21), and (3.28) with (3.17) and (3.18), the calculation for the real and the imaginary part of the current can be expressed as

$$Ire_{i,j} = \frac{1}{V_{nom}} \cdot (G_{i,j} \cdot ((V_{nom} + \Delta V_j) \cdot |V_j| - (V_{nom} + \Delta V_j) \cdot |V_i| \cdot 1) + B_{i,j} \cdot ((V_{nom} + \Delta V_j) \cdot (V_{nom} + \Delta V_j) \cdot \delta_{i,j})) \quad (3.29)$$

and

$$Iim_{i,j} = \frac{1}{V_{nom}} \cdot (B_{i,j} \cdot ((V_{nom} + \Delta V_j) \cdot |V_j| - (V_{nom} + \Delta V_j) \cdot |V_i| \cdot 1) - G_{i,j} \cdot ((V_{nom} + \Delta V_j) \cdot (V_{nom} + \Delta V_j) \cdot \delta_{i,j})) \quad (3.30)$$

These equations can be further rewritten as

$$Ire_{i,j} = \frac{1}{V_{nom}} \cdot (G_{i,j} \cdot ((V_{nom} + \Delta V_j) \cdot |V_j| - (V_{nom} + \Delta V_j) \cdot |V_i| \cdot 1) + B_{i,j} \cdot (V_{nom}^2 \cdot \delta_{i,j} + V_{nom} \cdot (\Delta V_j + \Delta V_j) \cdot \delta_{i,j} + (\Delta V_j \cdot \Delta V_j) \cdot \delta_{i,j})) \quad (3.31)$$

and

$$Iim_{i,j} = \frac{1}{V_{nom}} \cdot (B_{i,j} \cdot ((V_{nom} + \Delta V_j) \cdot |V_j| - (V_{nom} + \Delta V_j) \cdot |V_i| \cdot 1) - G_{i,j} \cdot (V_{nom}^2 \cdot \delta_{i,j} + V_{nom} \cdot (\Delta V_j + \Delta V_j) \cdot \delta_{i,j} + (\Delta V_j \cdot \Delta V_j) \cdot \delta_{i,j})) \quad (3.32)$$

where ΔV_j and ΔV_i are negligible compared to the other parts and can, therefore, be ignored. This leads to the linearized equations for the real and imaginary part of the current

$$Ire_{i,j} = G_{i,j} \cdot (|V_j| - |V_i|) + V_{nom} \cdot B_{i,j} \cdot \delta_{i,j} \quad (3.33)$$

and

$$Iim_{i,j} = B_{i,j} \cdot (|V_j| - |V_i|) - V_{nom} \cdot G_{i,j} \cdot \delta_{i,j} \quad (3.34)$$

The limit of the current magnitude is given by

$$\sqrt{Ire_{i,j}^2 + Iim_{i,j}^2} \leq I_{max} \quad (3.35)$$

and it is a non-linear expression. Piecewise linearization of the boundary of a circle is used to linearize the current magnitude limit [25]. The linearization is illustrated in Figure 3.2.

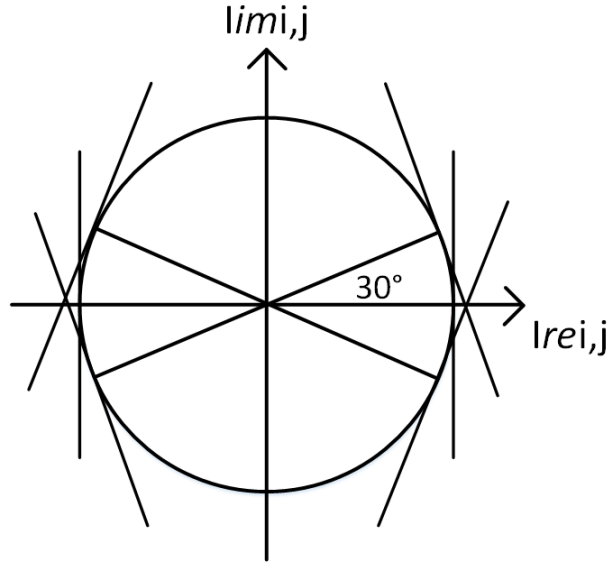


Figure 3.2: Piecewise linearization of a circle.

The linearization can also be expressed by the following equations

$$-Imax_{i,j} \leq Ire_{i,j} \leq Imax_{i,j} \quad (3.36)$$

$$-a \cdot Imax_{i,j} \leq Ire_{i,j} - b \cdot Imi_{i,j} \leq a \cdot Imax_{i,j} \quad (3.37)$$

and

$$-a \cdot Imax_{i,j} \leq Ire_{i,j} + b \cdot Imi_{i,j} \leq a \cdot Imax_{i,j} \quad (3.38)$$

where $a=1.15$ and $b=0.58$ and they represent the tangential lines of the circle.

3.4 Resource modelling

This section presents the energy resources that were used for the microgrid design and implementation. The chosen resources are batteries, PV systems, wind turbines, hydrogen ESS, and combined heat and power generation.

3.4.1 Energy Storage System

Two different types of energy storage are used, battery and hydrogen storage. The energy content (Wh) in the storage system is given by [26]

$$E(t) = E(t-1) - \frac{P_{Discharge}(t)}{n_{dc}} + n_c \cdot P_{Charge}(t) \quad (3.39)$$

where t is the time in hours, n_{dc} and n_c is the discharging and charging efficiency, $P_{Discharge}$ is the discharging power in W, and P_{Charge} is the charging power in W. The losses in the energy storage system are calculated as

$$ESS_{losses} = \sum_t (P_{Discharge}(t) \cdot \frac{1-n_{dc}}{n_{dc}} + P_{Charge}(t) \cdot (1-n_c)) \quad (3.40)$$

The discharging and charging power is limited by

$$P_{Discharge}(t) \leq P_{max} \quad (3.41)$$

$$P_{Charge}(t) \leq P_{max} \quad (3.42)$$

where P_{max} is the maximum power. The energy content of the battery is also limited between its maximum and minimum energy content

$$E_{min} \leq E(t) \leq E_{max} \quad (3.43)$$

The batteries should not be able to charge and discharge at the same time. If this restriction is included, the optimization problem becomes either non-linear or mixed-integer linear, meaning its complexity is increased. Instead of adding a constraint, the objective function is modified by adding a lower limit to the priority factor presented in Section 3.1. This makes the problem remain linear. The lower limit is chosen in such a way that the energy loss, by simultaneous discharging and charging, in the battery is lower than what is added by the priority factor. The power flow, during simultaneous charge and discharge, through the battery is

$$P_{Charge}(t) + P_{Discharge}(t) = (1 + n) \cdot P_{Charge}(t) \quad (3.44)$$

and the battery losses are

$$P_{Charge}(t) - P_{Discharge}(t) = (1 - n) \cdot P_{Charge}(t) \quad (3.45)$$

The lower limit of the priority factor is formed by dividing (3.45) by (3.44)

$$\frac{(1 - n) \cdot P_{Charge}(t)}{(1 + n) \cdot P_{Charge}(t)} = \frac{(1 - n)}{(1 + n)} \quad (3.46)$$

3.4.2 Photovoltaic System

For the PV model, the following parameters are taken into consideration: the area of each PV panel, power capacity, efficiency, and panel tilt. The panel tilt is the fixed mounting angle of the PV panel, where 0° is the horizontal position.

The power from the PV panel is calculated by,

$$P_{PV}(t) = k_{tilt}(t) \cdot GI(t) \cdot PV_{eff} \cdot PV_{area} \quad (3.47)$$

where $t = 1, 2, 3, \dots, 24$ hours, GI is the global irradiance in W/m^2 , PV_{eff} is the efficiency of each solar panel in percentage, PV_{area} is the area in m^2 of each solar panel, and $k_{tilt}(t)$ is a scaling factor corresponding to the panel tilt.

3.4.3 Wind Turbines

The wind turbine is modelled as a power source, where the generated power is given by

$$P_{wind} = f(w) \quad (3.48)$$

where w is wind speed.

3.4.4 Combined Heat and Power Generation Plant

The combined heat and power plant is modelled as a controllable power source [27], where the power output is constrained by

$$P_{chp,min} \leq P_{chp}(t) \leq P_{chp,max} \quad (3.49)$$

$P_{chp}(t)$ is the power output from the CHP plant and $P_{chp,min}$ and $P_{chp,max}$ are the minimum and maximum power output.

3.5 Solution Approach

An OPF problem is solved for the energy scheduling of the micro-grid resources, where the PCC is treated as the swing bus of the microgrid system. This is a LP problem, since the linearized power flow equations are used to model the operation of the microgrid. The power injection into the microgrid, at the PCC, which is decided from the solution of the optimization problem is used to solve the power flow in the main grid where the import bus (connection to the upstream network) is treated as the swing bus. The non-linear power flow equations are used for calculating the power flow in the main grid. After both power flow solutions (in the micro-grid and in the main distribution network) have been obtained, the results are used to calculate the losses in the grids. The simulation is run over 24 hour periods assuming that power production from RES and power consumption is known for all hours. The simulation is run for several microgrid cases.

3.5.1 Software

The software used in this thesis are General Algebraic Modelling System (GAMS) and Matrix Laboratory (MATLAB). GAMS is used to build the model and to solve the optimization problem. MATLAB is used to send data to GAMS and to initialize the parameters of the GAMS model. MATLAB is also used to process data from GAMS. Figure 3.3 illustrates how GAMS and MATLAB interact.

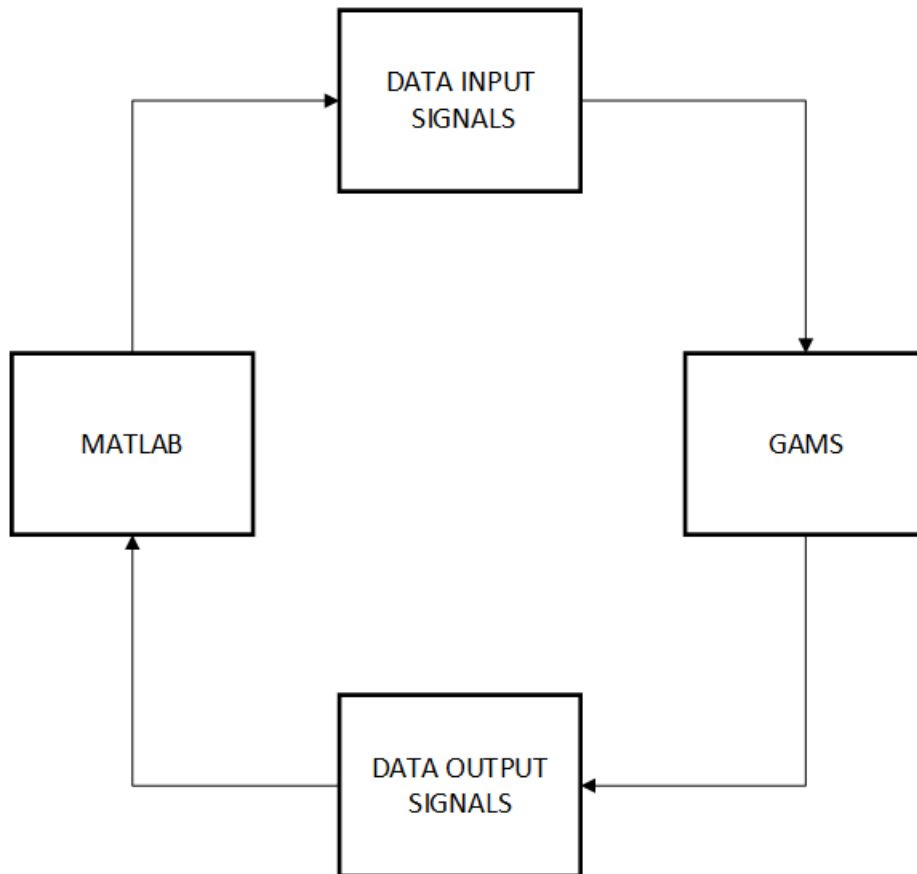


Figure 3.3: Microgrid GAMS and MATLAB simulation.

MATLAB sends data to GAMS and then initializes the 24 h period optimization. MATLAB then processes the output from GAMS and again sends data to GAMS as initial values of the next 24 h period in order to start the simulation for the next day.

4

Microgrid Scenario

This chapter presents the grid data that are used in the network model as well as the data for the parameters used in the resource modelling. This chapter also presents the microgrid cases and the mix of resources, that are used in the simulations.

The data are given in p.u values and the power factor of the load is assumed to be 95 %. All data were gathered in an hourly resolution for the year of 2017.

4.1 Location of Microgrid

A 400 V network supplying an area consisting of villas in the area of Gothenburg was considered for the microgrid scenario. The 400 V network is located in a 10 kV feeder loop, shown in Figure 4.1, with several other 400 V networks. The distribution grid data were gathered from GENAB, the DSO of this network. These data include line parameters, transformer ratings, system/operation limits and system loads. Load data and line data up to the house level were used for the 400 V network where the microgrid is considered whereas for the rest of the low voltage networks in the feeder loop aggregated load data were used at the medium voltage level.

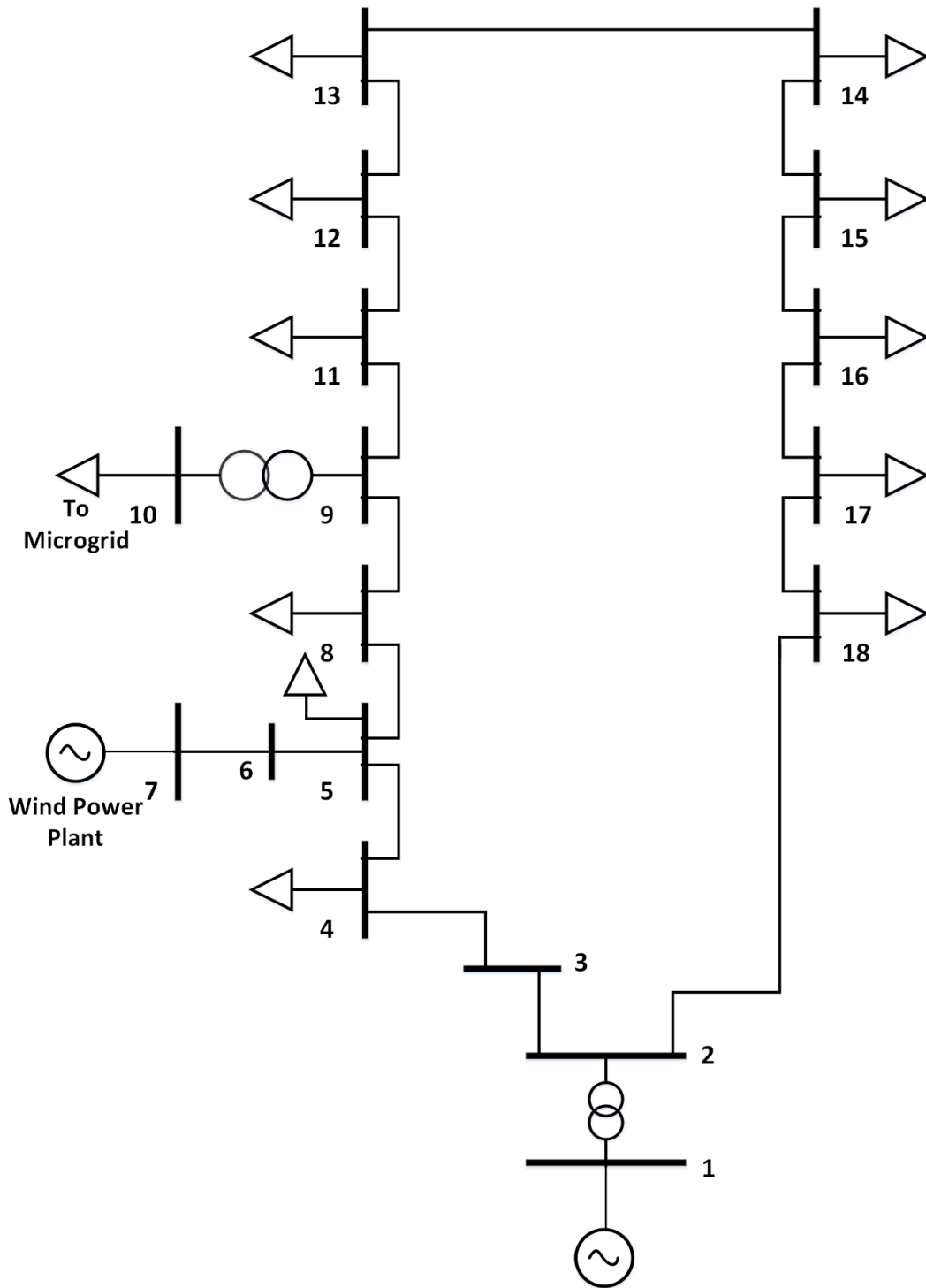


Figure 4.1: The 10 kV distribution grid that was used for the development of the microgrid model.

Bus 1 is located at the connection point to the upstream network. The 400 V network is located at bus 9 which is the only PCC of the microgrid. The 10 kV network also includes a 2 MW wind turbine located at bus 7. Bus 9 is also treated as the PCC and the voltage at this point needs to be kept within $\pm 7\%$ of the nominal voltage. The 400 V grid diagram is shown in Figure 4.2.

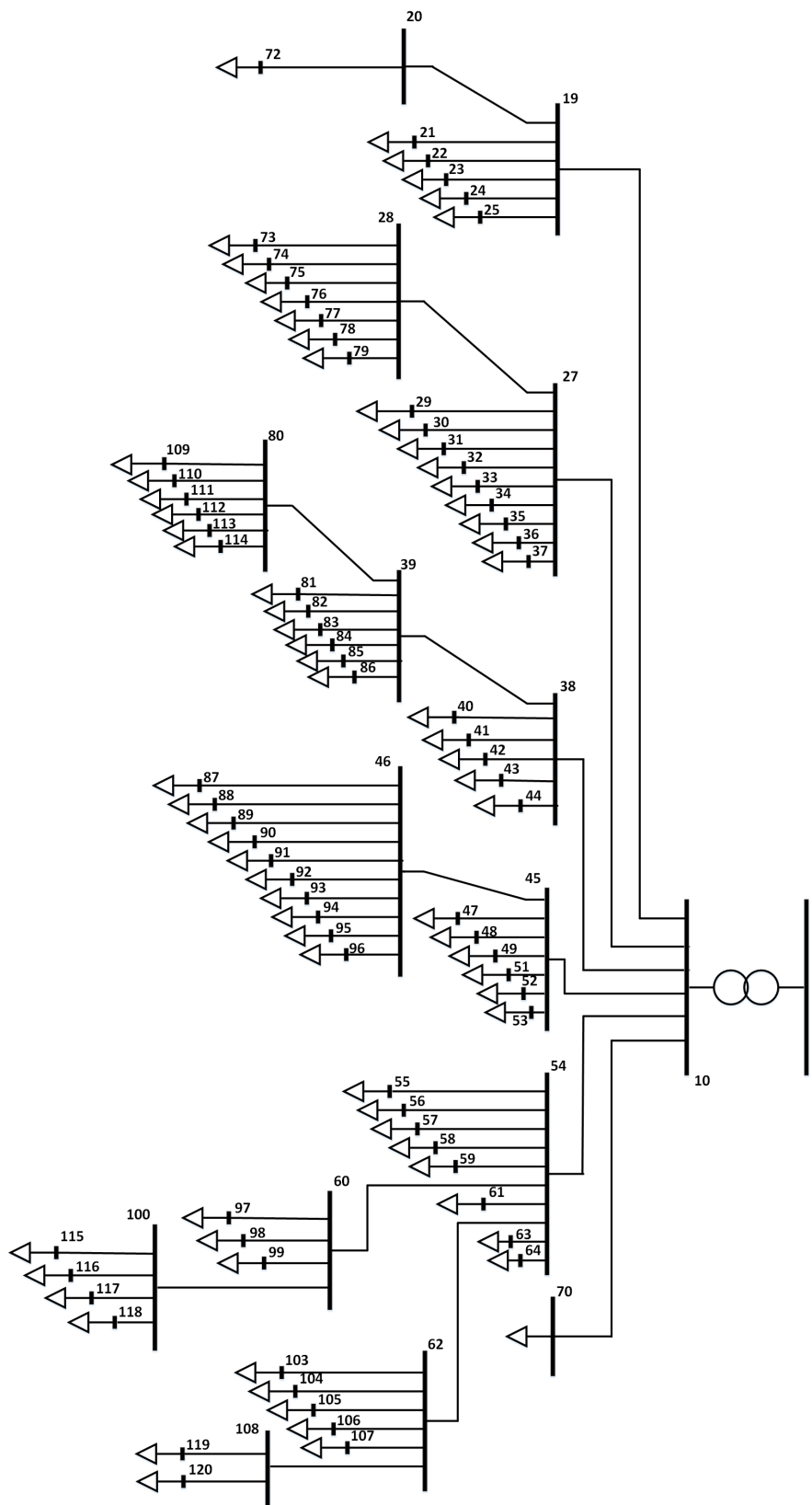


Figure 4.2: The 400 V distribution grid that was used for the development of the microgrid model.

The line parameters for the 400 V microgrid and the 10 kV distribution network can be found in Tables A.1 and A.2 in Appendix A. Capacitance is included in the 10 kV grid lines and is assumed to be negligible for 400 V grid lines. The current limit of all lines, except those connected to the houses, is 270 A. The limit of lines connected to the houses is 35 A. The rated power of the transformer at bus 9 is 800 kVA.

4.2 Energy Cost and Fees

The microgrid operation was simulated with data for the year 2017. When buying or selling energy, the payment (or profit) consists of the spot price and the energy transmission fee. The spot price data was gathered from Nordpool [28]. The spot price is shown in Figure 4.3.

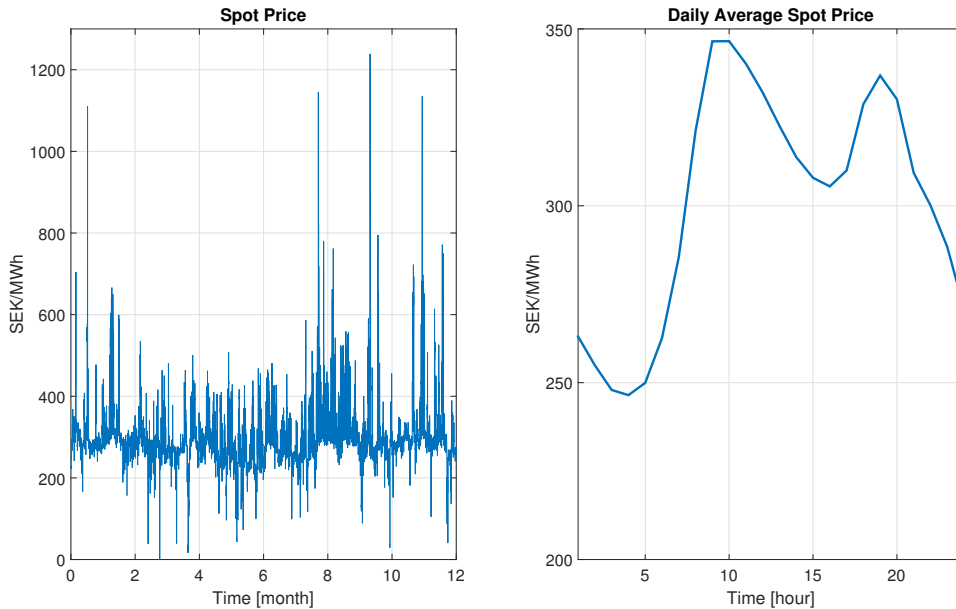


Figure 4.3: Spot price for the year 2017.

The figure shows yearly variation in cost and also the average daily cost variation. There are two energy transmission fees that the DSO charges to the end-users. In Table 4.1, the two different fees are presented.

Table 4.1: Energy subscription fees.

	Energy Transmission Fee SEK/MWh		Monthly Fee SEK
	Buy	Sell	
Household	270 [29]	270 (50-500) [30]	132.08 [29]
Company	31 [31]	30 [32]	$808.33 + (35400)/MW_{peak}$ [31]

The energy transmission fee for selling power as household varies depending on the certification of the energy production installed. The value is, therefore, assumed to be the same as the buying fee, 270 SEK. The company monthly fee depends on the monthly peak consumption. Since the resource scheduling is done on a daily basis, a new modified version of the company fee is introduced. The monthly peak consumption cost is converted into a daily peak consumption cost. The daily peak consumption cost is $\pi_{peak,daily} = \frac{35400 \cdot 12}{365} = 1163.84 \text{ SEK}/\text{MW}_{peak}$. This fee will now be called the microgrid fee.

4.3 Resources

The implementation and choices of different resources in the microgrid are explained in this section. All energy sources operate at unity power factor. The weather data, i.e., global irradiance, and wind speed were collected from SMHI open database [33].

4.3.1 Battery

The battery model characteristics are based on the Tesla Powerwall, which is a lithium-ion battery [34]. The round trip efficiency is 90% and the charging and discharging efficiency is assumed to be the same, i.e. $\sqrt{90\%} \approx 95\%$. The maximum continuous charging and discharging power is 5 kW, and the total usable energy content of the battery is 13.5 kWh. The warranty of the battery states that the battery can handle a total aggregated energy throughput of 37.8 MWh in its lifetime and the energy capacity is guaranteed to be at least 80 % during the whole lifetime [35]. Therefore, the minimum and maximum energy content in the battery model is set as $E_{min} = 0$ and $E_{max} = 0.8 \cdot 13.5 \text{ kWh} = 10.8 \text{ kWh}$ and the efficiency is assumed to remain the same for its whole life time. This is done in order to make the assumption that the battery will perform at the same level throughout its whole lifetime. In total, 78 batteries are added at each of the 78 houses in the 400 V network.

4.3.2 Hydrogen Energy Storage System

The hydrogen storage system is assumed to have a round-trip efficiency of 40 % [22]. The charging and discharging efficiency is assumed to be the same. The necessary capacity of the hydrogen energy storage system to make the grid self-sufficient will be evaluated after the simulations.

4.3.3 Photovoltaic System

The PV model characteristics are based on a 250 W mono-crystalline-silicon panel from Sharp Energy Solution Europe [19]. The efficiency of the panel is 15.2 % and the area is 1.64 m^2 . In total, 25 panels with a peak capacity of 6.25 kW are added to 60 of the 78 houses. On the remaining 18 houses, there already was a capacity of 5 kW installed. Installing 25 panels is reasonable considering the total roof area of a medium sized villa is around 100 m^2 and PVs will be installed on only one half

of the roof. The power production of 25 panels for the full year of 2017 is shown in Figure 4.4.

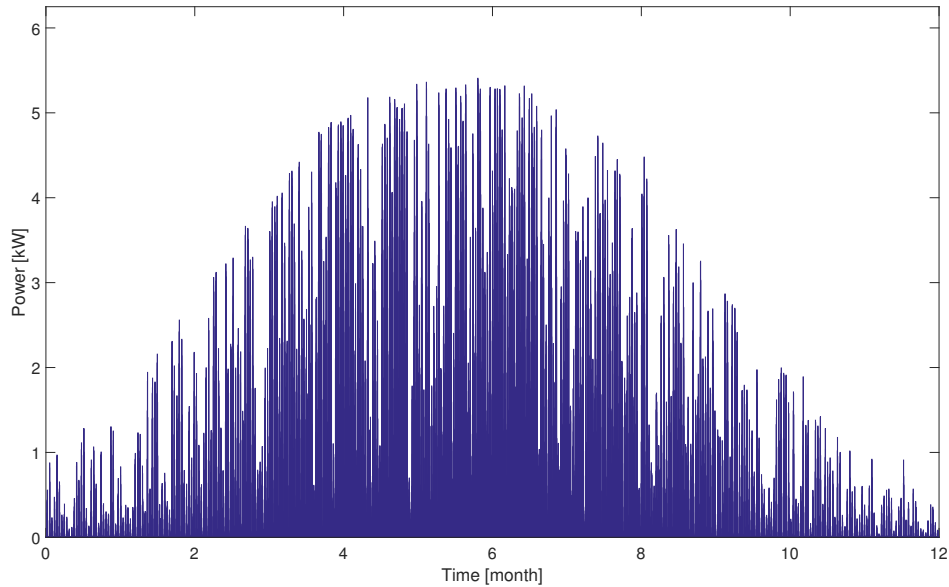


Figure 4.4: Power production from 25 Sharp PV panels.

The power production of the PV panels can be increased by tilting the panels. Table 4.2 shows the estimated average monthly increased power production for different tilt angles. The tilt is in southern direction. The values are retrieved from National Renewable Energy Laboratory PV calculator [36].

Table 4.2: Scaling factor of solar panels for different tilt angles.

Months/Scaling factor for different tilt angles (deg)	20	30	40
January	1.48	1.68	1.84
February	1.30	1.40	1.48
March	1.22	1.30	1.34
April	1.15	1.18	1.19
May	1.09	1.10	1.08
June	1.05	1.04	1.01
July	1.07	1.07	1.05
August	1.11	1.14	1.13
September	1.23	1.30	1.34
October	1.40	1.54	1.65
November	1.43	1.59	1.70
December	1.73	2.02	2.27

From Table 4.2, it can be seen that higher tilt angle increases the power production during the winter months and whereas, during the summer months, the tilt angle

has much smaller impact. The typical pitch of a house roof is 27° . Therefore, the tilt angle of the PV panels is chosen to be 30° as going higher might be unrealistic. Figure 4.5 shows the power production when the panels are tilted.

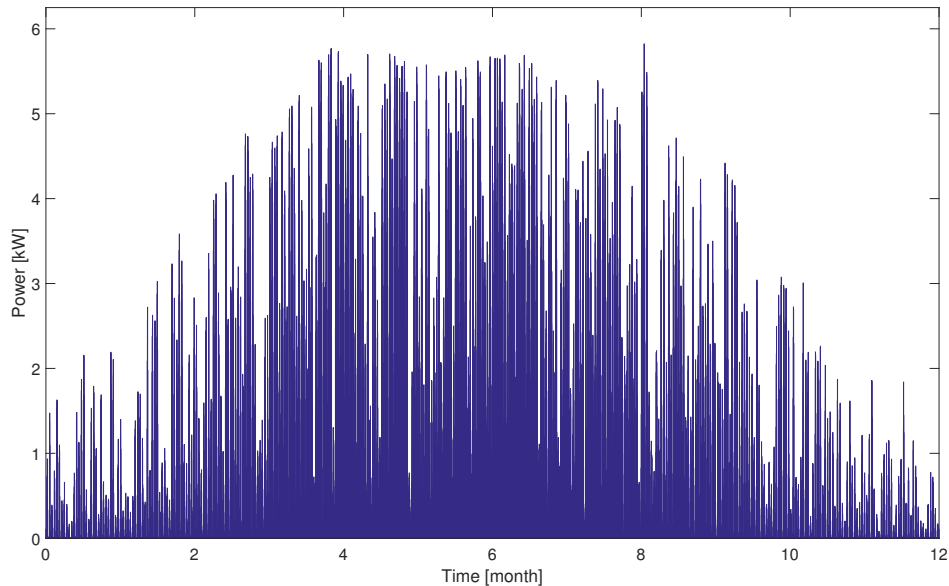


Figure 4.5: Power production from 25 Sharp PV panels with 30° tilt.

This amount of installed PV corresponds to 57 % of the annual energy consumption of the 400 V network.

4.3.4 Wind Turbine

The wind power plant that is used in the modelling is a 10 kW turbine with rotor diameter of 7 m from Bergey called Excel 10 [37]. The wind turbines need to be spaced at sufficient distance from each other due to the wake effect from the rotors. The impact of the wakes depend on the wind speed, temperature and the size of the obstacle (in this case the rotor). As the spacing increases, the impact decreases. A spacing which is 10 times bigger than the rotor diameter is sufficient to reduce the impact [18]. One Excel 10 turbine were considered to be installed at 12 of the 400 V buses of the microgrid. These buses are 19, 27, 28, 38, 39, 45, 46, 54, 60, 62, 80, and 100 which are located upstream from load buses as shown in the 400 V network diagram in Figure 4.2. The available geographic distance to install wind turbines in this area is approximately 800 m and this results in a distance spacing that is approximately 9 times bigger than the rotor diameter. Excel 10 has a rated noise level of 42.9 dB [37]. The noise level is below the limit of what should be expected from road traffic [38]. The limit that has often been used to settle court cases when the building of wind turbines have been appealed against is 40 dB [39]. This limit is measured at the location of the houses, which means that if the wind turbines are not built too close to them, it will not create noise problems. Therefore, Excel 10

wind turbines are used in the microgrid. In Figure 4.6, the production data from the data sheet of the wind turbine are plotted together with a fitted curve.

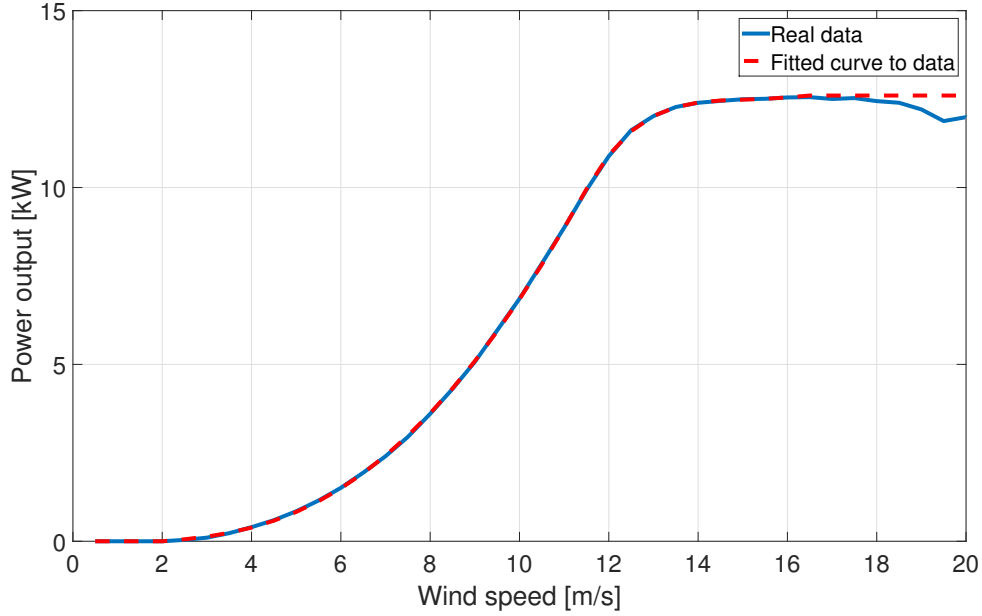


Figure 4.6: Power output as function of wind speed for the production data from the data sheet of the wind turbine and for a polynomial fitted curve.

The fitted curve is used to calculate the power production from wind data and is described by two polynomial curves of the following form

$$P_{poly} = a_4 \cdot w^4 + a_3 \cdot w^3 + a_2 \cdot w^2 + a_1 \cdot w + a_0 \quad (4.1)$$

where the two polynomial curves consist of the factors shown in Table 4.3.

Table 4.3: Factors for polynomial fitted curves.

	$P_{poly,1}$	$P_{poly,2}$
a4	-0.470247229326502	-5.990675990784808
a3	15.2428161001586	394.4693084753995
a2	-44.6702517162441	-9666.271561898999
a1	87.4307307639665	1046335.586647395
a0	-103.006142419506	-410164.2820553708

The fitted curve is then created by combining the two polynomial curves as follows

$$P_{fit} = \begin{cases} 0 & \text{if } w < 2 \text{ m/s} \\ P_{poly,1} & \text{if } 2 \text{ m/s} < w < 11.5 \text{ m/s} \\ P_{poly,2} & \text{if } 11.5 \text{ m/s} < w < 16 \text{ m/s} \\ P_{max} & \text{if } w > 16 \text{ m/s} \end{cases} \quad (4.2)$$

Where w is the wind speed in m/s , P_{fit} is the power output in W of the polynomial fitting curve, P_{max} is the maximum power output in W. The wind speed is measured at a lower height than what the wind turbine is built. Hellmann exponential law is used to correct for this [40] and it is given by

$$w = w_{measured} \cdot \left(\frac{h}{h_{measured}} \right)^a \quad (4.3)$$

where the value of a is chosen to be 0.2 which is the value that best represents the terrain in the measurement location [40]. The new height is h , and $w_{measured}$ and $h_{measured}$ is the measured wind and its measurement height. The wind speed is measured at 5 m above ground while the wind power plant is built at approximately 100 m height. The hub height of the wind power plant is 24 m. This results in $h=120$ m and $h_{measured}=5$ m. The wind speed is not measured at the exact location where the turbine is built. The distance between the locations is 10 km but the wind speed at 120 m on both places is assumed to be the same. Figure 4.7 shows the estimated power production of the wind turbine for the year 2017.

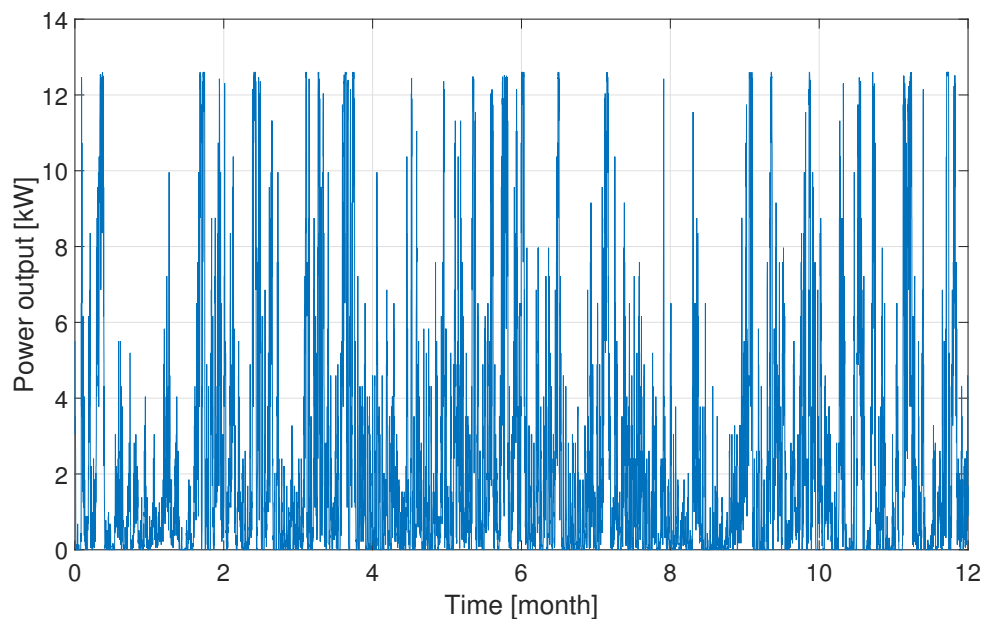


Figure 4.7: Calculated power production from Bergey wind turbine for the year 2017.

If 12 turbines are used, their total energy production corresponds to 25 % of the annual consumption in the 400 V microgrid.

4.3.5 Combined Heat and Power Generation Plant

The needed power capacity of the CHP plant to make the grid self-sufficient is evaluated after the simulation. The power production cost of the CHP plant is based on the CHP plant at Chalmers University of Technology and it is 600 SEK/MWh [41]. Benefits of using the waste heat that is produced is not considered.

4.4 Investment Costs and Cost Analysis

In Sweden, there exists government support for investing in PV, of 30 %, and for battery, of 60 % [42]. The inflation is assumed to be 2 % per year since this is Sweden's target value [43]. A 30 year period is considered for the evaluation of the total investment cost. For the long-term cost analysis, the annual energy cost will be scaled according to inflation, and the interest rate used for the energy cost is the same as inflation and for investments the interest rate used is 5 %. The government support for batteries is assumed to be in place for this whole time period. In this project the microgrid operator and the DSO is considered to be two separate entities. The microgrid operator will own and operate all of its own resources, except for the grid which will be owned by the DSO but operated by the microgrid operator. If an investment or cost is postponed in time the value of the investment will be lower. This is represented by the present value factor (PVF) which is determined by

$$PVF = \frac{1}{(1 + i)^n} \quad (4.4)$$

where n represents the year that the investment is made and i is the interest rate.

4.4.1 Battery

One Tesla Powerwall battery costs 70 500 SEK and the installation cost varies from 8 900 SEK to 22 300 SEK [44]. The total cost is, therefore, assumed to be 80 000 SEK. With the government support, the battery cost is 32 000 SEK per battery. The total battery investment cost is $32\,000 \cdot 78 = 2\,496\,000$ SEK. The battery is expected to be replaced, when it has reached its aggregated throughput limit. The cost of the battery is expected to be reduced by 30 % after approximately 10 years and by 50 % after approximately 20 years [45].

4.4.2 Hydrogen Energy Storage System

The hydrogen storage system comprises of an electrolyzer, a hydrogen tank and a fuel cell. The electrolyzer costs 8.8 MSEK/MW, the hydrogen tank costs 0.260 MSEK/MWh, and the fuel cell costs 22 MSEK/MW with a lifetime of 10, 20 and 5 years, respectively [46].

4.4.3 Photovoltaic System

The cost of PV panels is about 12 500 SEK/kWh with government support [47]. Sixty houses with installed peak capacity of 6.25 kW results in an investment cost of $12\,500 \cdot 60 \cdot 6.25 = 4\,687\,500$ SEK. The expected lifetime of a PV panel is at least 30 years [48]. The solar inverter is assumed to be replaced after 15 years for 20 % of the initial investment cost [45].

4.4.4 Wind Turbine

The investment cost of installing one Bergey Excel 10 wind turbine is between 400 300 SEK to 542 100 SEK. All the required equipment costs approximately 334 000 SEK [49]. The total investment cost is, therefore, assumed to be 800 000 SEK.

4.4.5 Combined Heat and Power Generation Plant

The investment cost of a CHP plant is approximately 10 000 SEK/kW. The annual operation and maintenance cost is approximately 400 SEK/kW and the lifetime is approximately 25 years [50].

4.4.6 Grid Ownership and Operation

The microgrid operates the grid while the DSO is the owner of the grid. The microgrid pays the maintenance fee of the grid, which is considered to be 1 % of the value of the grid. The value of the grid is 1 850 732.3 SEK.

4.5 Cases

Five cases of microgrid energy resources mix are considered and evaluated. In Table 4.4, the cases with their added resources, and operation objective are shown.

Table 4.4: Cases used in simulating the operation of the low voltage network.

	Base Case	Case 1	Case 2	Case 3	Case 4	Case 5
DER's	None	PV	PV Battery	PV Wind Battery	PV Wind Battery Hydrogen	PV Wind CHP Battery Hydrogen
Operational objective(s)	-	-	Minimize cost Minimize exchange	Minimize exchange	Minimize exchange	Minimize exchange

The base case with no added resources, and case 1 with only PV added does not include any controllable resources, meaning that in these cases, the low voltage network cannot operate as a microgrid. For each additional case additional resources are iteratively added. In case 2 batteries are introduced to the model, in case 3 wind turbines, in case 4 a hydrogen storage system, and in case 5 a CHP plant. In case 2 to 5, controllable resources have been added and these cases are, therefore, used to evaluate the operation of the microgrid. In case 2, when controllable resources first are added, two operational objectives are tested and compared. Cases 3-5 focus on reaching a self-sufficient microgrid, so the energy exchange minimization is the only objective. In the base case and case 1, the household energy fee is paid. In case 2

4. Microgrid Scenario

both fees are applied. In the cases 3-5, when only the energy exchange is minimized, the microgrid fee is used since the cost does not affect the power flow solution and also since this fee rewards the microgrid for lowering its power import. The priority of the DER is determined by setting the penalty factors as

$$K_{ESS,battery} < K_{ESS,hydrogen} < K_{CHP} \quad (4.5)$$

5

Result and Analysis

This chapter illustrates the results for all the microgrid cases. The analysis of the results is also carried out in this section. Lastly, the cost analysis is presented.

5.1 Base Case

In the base case, no DER are included in the low voltage network. Figure 5.1 shows the power import for the year 2017. The base case represents the present operation of the low voltage network in the distribution system and in this case no optimization can be done as there are no controllable resources.

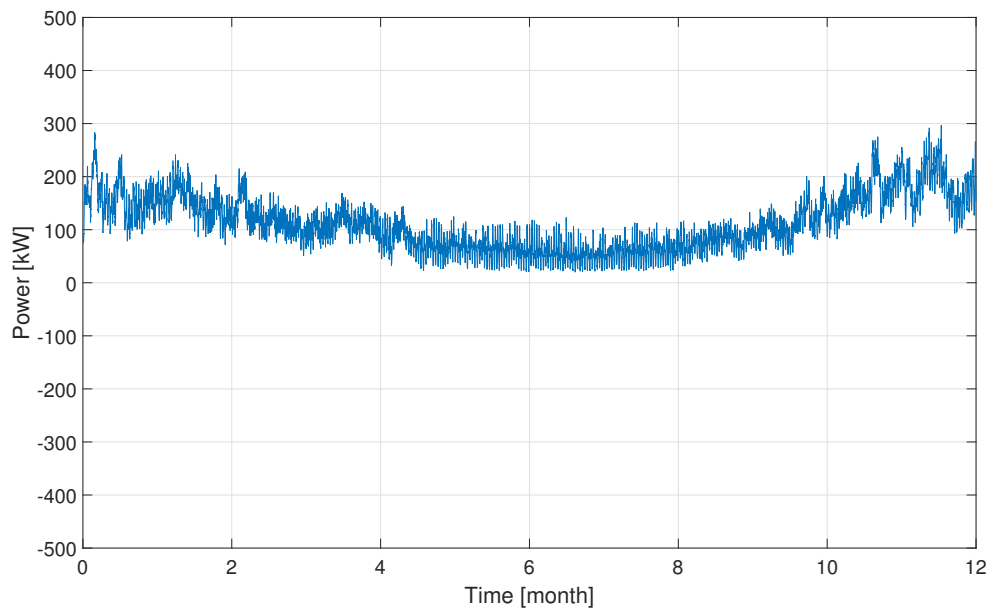


Figure 5.1: Power import for the base case for year 2017.

As can be seen from Figure 5.1, the import is highest during winter, when the energy consumption is the highest. The energy import slightly decreases during the summer following the decrease in consumption that time of the year. It can also be seen that the energy export, throughout a year, is zero as there is almost no local production of energy, only a few houses with PV, in the low voltage network. In Figure 5.2, the average daily energy import profile is shown. The consumption is lowest in the morning.

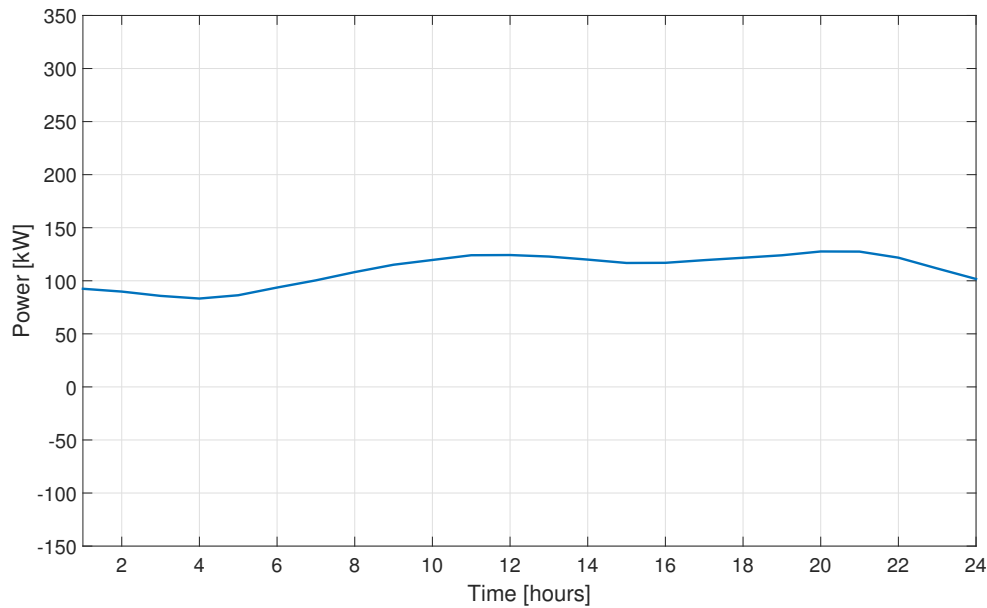


Figure 5.2: Average power import for the base case for a day.

Table 5.1 shows the annual results for the base case. Two power flow calculations have been performed, one for the low voltage network and the other for the main grid.

Table 5.1: Annual results for the base case.

	Low voltage network	Medium voltage network
Energy cost (SEK)	685 349	-
Total energy import (MWh)	968.9	15 311
Total energy export (MWh)	0	19.7
Losses (MWh)	3.4	108.4
Peak import (MW)	0.297	3.9

As shown in Table 5.1, it can be seen that the annual energy cost is 685 349 SEK. The total energy import in the low and medium voltage network is 968.9 MWh and 15 311 MWh, respectively. In the medium voltage network the total energy export is 19.7 MWh because of the presence of the 2 MW wind turbine in the main grid. The losses in the low voltage network are 3.4 MWh and in the medium voltage network is 108.4 MWh.

5.2 Case 1

In case 1, PVs are considered to be installed in the low voltage network. Figure 5.3 shows the power import for a year using consumption data from 2017.

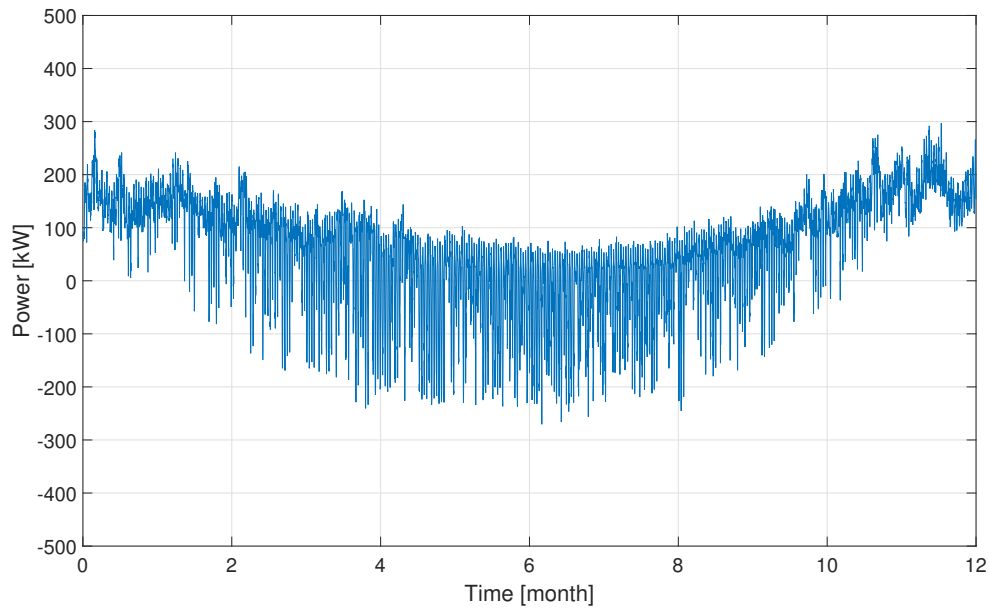


Figure 5.3: Annual power import for case 1.

By comparing Figure 5.3 and 5.1, it can be seen that there is a mismatch between consumption and production. The consumption is highest during the winter while the production is highest during the summer. There is a surplus of energy production from PV panels during the summer, which is exported. Figure 5.4 shows the daily average power import.

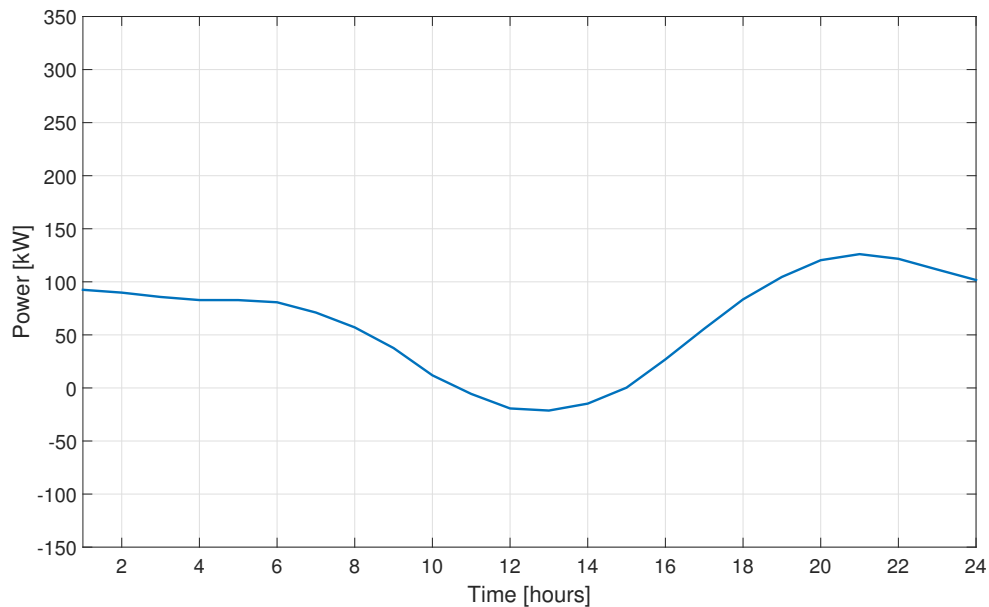


Figure 5.4: Average power import for a day for case 1.

Figure 5.4 shows that the energy is imported in the starting few hours of the day. During the mid-day there is less need of importing energy as energy from PV panels

is sufficient and it again imports energy in the evening. Table 5.2 shows the annual results for case 1.

Table 5.2: Annual results for case 1.

	Low voltage network	Medium voltage network
Energy cost (SEK)	434 185	-
Total energy import (MWh)	719.5	14 884
Total energy export (MWh)	178.1	24.4
Losses (MWh)	3.4	105
Peak import (MW)	0.297	3.9

Comparing the results from Table 5.1 and Table 5.2 it can be seen that the annual energy cost reduces by 37 % due to the installation of new PV panels in the low voltage network as compared to the base case. The energy import in the low voltage and medium voltage network is also decreased by 26 % and 2.8 % respectively. The energy export for low and medium voltage network is increased as shown in Table 5.2. In case 1, no difference is observed in the losses in the low voltage network and whereas in the medium voltage network they are decreased by 3.1 %. It can also be seen that the peak power import remains the same for the base case and case 1. This can be explained from the fact that the peak in the imported power occurs during the winter, when there is low production from the PV panels.

5.3 Case 2

In case 2, PVs and batteries are installed in the low voltage network. In this case, two operational objectives are used in the operation of the microgrid. One is minimizing energy cost and the other is minimizing power exchange. The microgrid fee and the household fee are both used in scheduling with the two operational objectives.

5.3.1 Energy Cost Minimization Considering the Household Fee

Figure 5.5 shows the power import for a year. Where again the consumption data is taken from 2017.

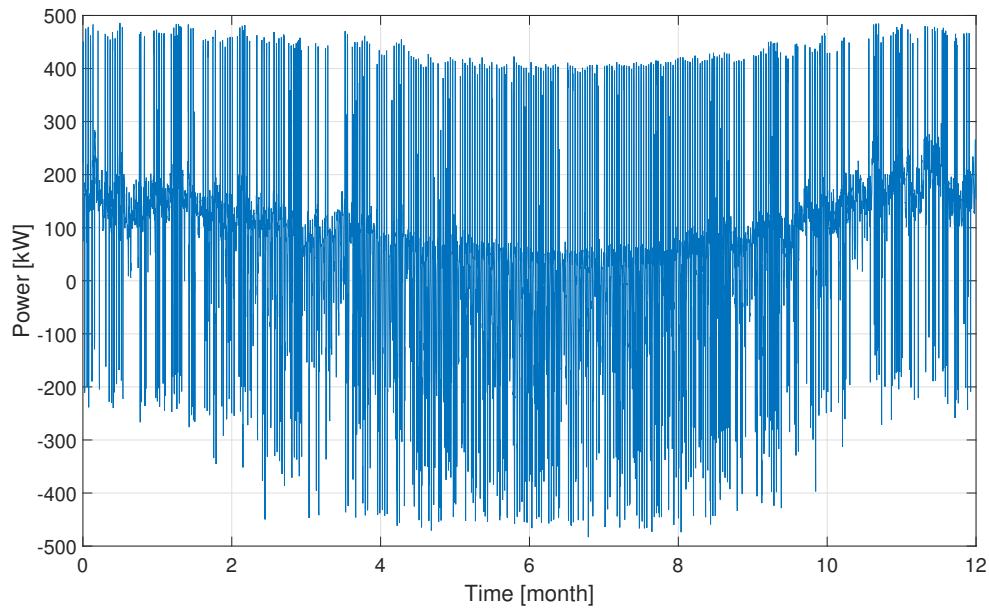


Figure 5.5: Annual power import when energy cost is minimized considering the household fee (case 2).

In Figure 5.5, it can be seen that there is a lot of energy exchange, energy is imported and exported continuously. The import profile, seen in Figure 5.5, is not desirable by the DSO because it exchanges a lot of energy and the uncertainties in the hourly variation of power import is high. Figure 5.6 shows the daily average power import and the average daily total charging and discharging of the batteries.

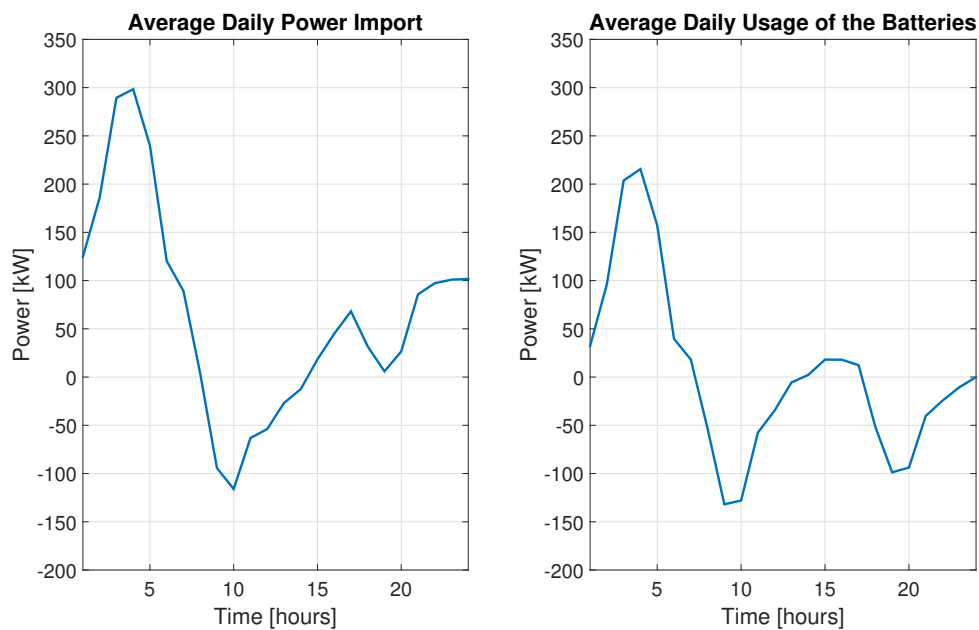


Figure 5.6: Daily average power import and battery usage when energy cost is minimized considering the household fee (case 2).

In Figure 5.6, it can be seen that the low voltage network trades a lot of energy with the medium voltage network. The batteries are used to import energy when the price is low and export energy when the price is high, they engage in energy arbitrage. It can be seen that the power import follows the daily average spot price, shown in Figure 4.3. The network lines of the microgrid are in case 2 operated close to the current limits. Table 5.3 shows the annual results from the simulation of the microgrids optimal operation considering energy cost minimization with household fee, and it also shows the calculated values for the main grid.

Table 5.3: Annual results for energy cost minimization considering the household fee for case 2.

	Low voltage network	Medium voltage network
Energy cost (SEK)	407 097	-
Total energy import (MWh)	960.7	14 908
Total energy export (MWh)	389.0	17.7
Losses (MWh)	7.9	104.7
Peak import (MW)	0.486	3.9
Total battery losses (MWh)	30.3	-
Total aggregated energy through each battery (MWh)	7.6	-

By installing batteries and PV panels in the low voltage network, the annual energy cost is decreased by 6.2 % as illustrated in Table 5.3 when compared to case 1. The power exchange between the microgrid and the distribution grid is increased considerably because even though the energy import remains almost unchanged, the microgrid now exports a lot of energy. The total aggregated energy through each battery is on average 7.6 MWh which means that the batteries will have reached the warranty limit after only 5 years. If the microgrid seeks to minimize the energy cost daily this is not a viable way to schedule the batteries. Therefore a fee with a peak import penalty could be introduced, which is done in the section.

5.3.2 Energy Cost Minimization Considering the Microgrid Fee

To restrict the big amount of energy exchange observed in Figure 5.5, the microgrid fee with penalty on peak import can be used. Figure 5.7 shows the power import for the year 2017 when the energy cost is minimized considering the microgrid fee.

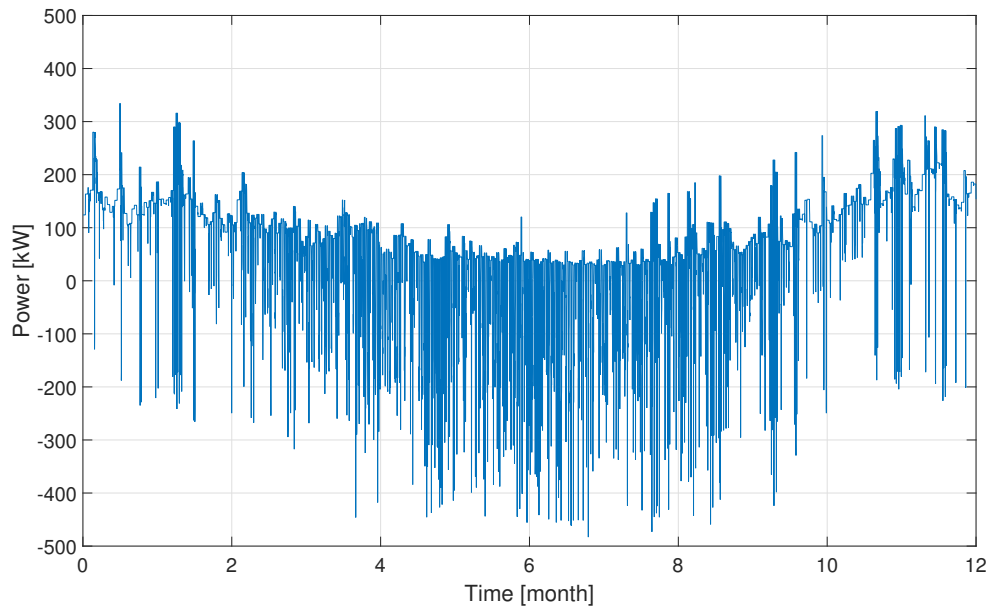


Figure 5.7: Power import for 2017 for case 2 minimizing cost with microgrid fee.

In this case, Figure 5.7 shows that the daily peak import has been reduced because of the peak import penalty. Figure 5.8 depicts the average daily power import and the average daily total charging and discharging of the batteries and it can be seen that on a daily level the power import has been flattened out and the batteries are used to reschedule the microgrid consumption by importing energy when it is cheap, i.e., during the morning.

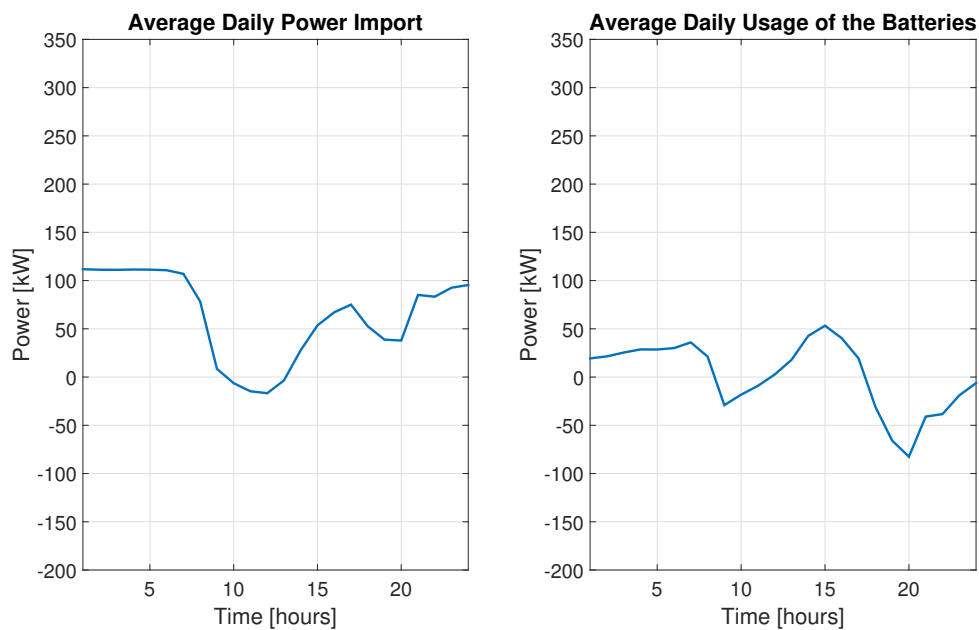


Figure 5.8: Average power import and battery usage for daily energy cost minimization considering the microgrid fee for case 2.

The energy import is shifted to the beginning of the day compared to the base case, as depicted in Figure 5.8, when energy is cheaper to buy. This import profile is much more desirable by the DSO since the energy exchange and the hourly variations in power import is decreased. Table 5.4 shows the annual results from the simulation of the microgrids optimal operation considering energy cost minimization with microgrid fee, and it also shows the calculated values for the main grid.

Table 5.4: Annual results for energy cost minimization considering the microgrid fee for case 2.

	Low voltage network	Medium voltage network
Energy cost (SEK)	225 554	-
Total energy import (MWh)	775.6	14 900
Total energy export (MWh)	217.3	23.0
Losses (MWh)	4.2	104.8
Peak import (MW)	0.334	3.8
Total battery losses (MWh)	16.9	-
Total aggregated energy through each battery (MWh)	4.2	-

The annual energy cost considering the microgrid fee for low voltage network is decreased by 45 % as compared when the household fee is implemented. The total energy exchange between low voltage network and medium voltage network is decreased by 26 %. The losses are reduced by 47 % in the low voltage network because the network is used less. Medium voltage network losses remains almost unchanged. The battery losses decrease by 44 %. The total aggregated energy through each battery is on average 4.2 MWh which means that the batteries will have reached the warranty limit after 9 years. If the microgrid seeks to minimize the energy cost daily this can be considered a viable way to schedule the batteries.

5.3.3 Minimization of Energy Exchange

In this case a different operational objective, minimizing energy exchange, is applied. And since this operational objective is not affected by the energy fee both energy fees are used in calculating the annual energy cost. Figure 5.9 shows the power import for 2017.

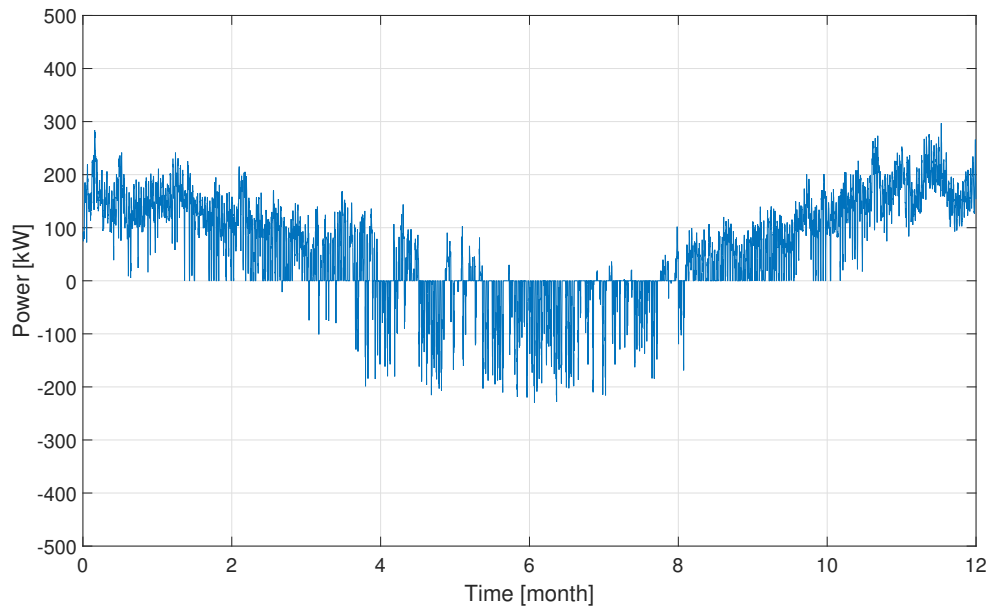


Figure 5.9: Power import for a year when minimizing energy exchange for case 2.

It can be noted that no energy is imported for several weeks during the summer months. However, a lot of energy is still exported since there is not enough capacity in the batteries to store the excess energy that is produced. Figure 5.10 shows the average daily energy import and the average daily total charging and discharging of the batteries.

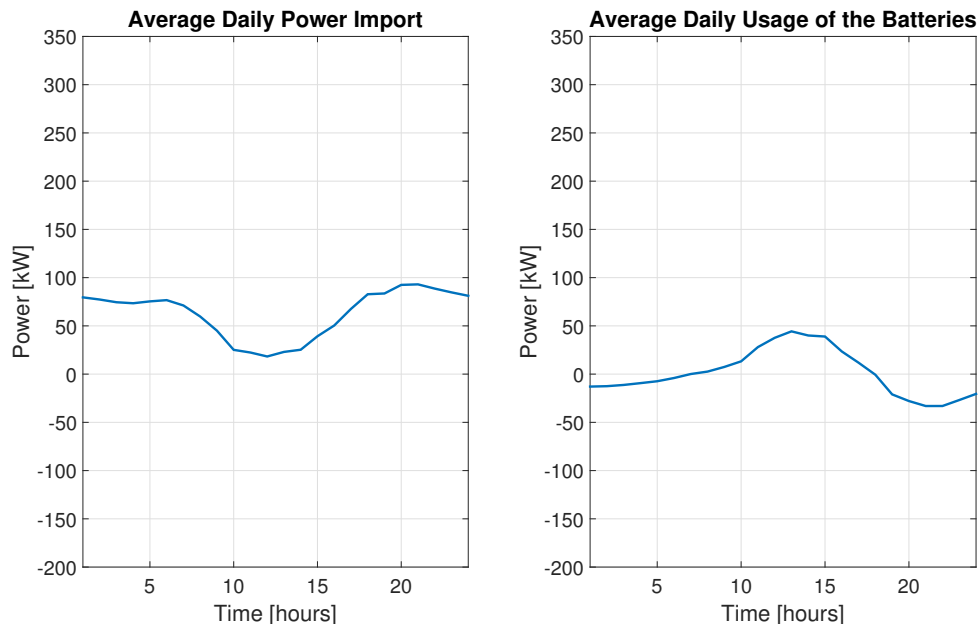


Figure 5.10: Average power import and battery usage for a day when minimizing energy exchange for case 2.

The batteries discharge during morning and night when the PV production is low

and they charge during the day when the PV production is high. Table 5.5 shows the numerical results.

Table 5.5: Annual results for minimization of energy exchange for case 2.

		Low voltage network	Medium voltage network
Energy cost (SEK)	Microgrid fee	244 241	-
	Household fee	441 992	
Total energy import (MWh)		628.5	14 894
Total energy export (MWh)		77.2	24.5
Losses (MWh)		3.0	105.0
Peak import (MW)		0.297	3.9
Total battery losses (MWh)		9.9	-
Total aggregated energy through each battery (MWh)		2.5	-

The annual energy cost calculated with the microgrid fee is 244 241 SEK. The annual energy cost is increased by 7.6 % compared to when the operational objective is the energy cost minimization. When minimizing exchange, the total energy import in the low voltage network is reduced by 18.9 % and the energy export is decreased by 64.4 %. The annual energy cost is 441 922 SEK when calculated with household fee. The cost is even bigger than the cost in case 1, when no microgrid optimal operation is considered. The total aggregated energy through each battery is on average 2.5 MWh which means that the batteries will have reached the warranty limit after 15 years. If the microgrid seeks to minimize the energy exchange daily this would be a viable way to schedule the batteries.

5.4 Case 3

In case 3, PVs, batteries, and wind turbines are considered to be installed in the low voltage network. In this case, the operational objective to minimize the energy exchange is used considering the microgrid fee, since the purpose in this case and the two next cases are to investigate the requirements for the microgrid to be self-sufficient. Figure 5.11 shows the power import for a year considering the minimization of energy exchange. The consumption data is taken from the year 2017.

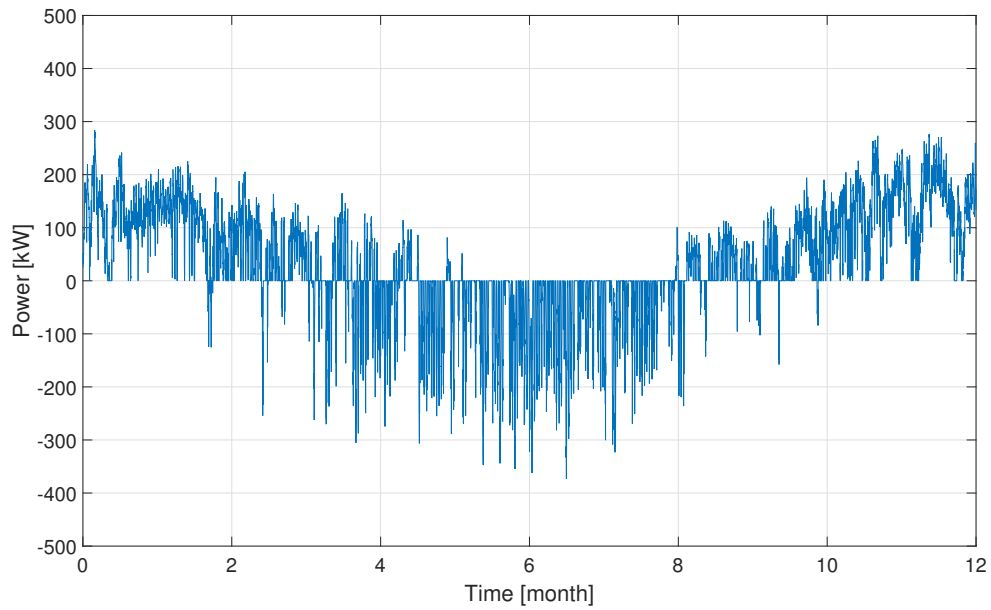


Figure 5.11: Power import for a year considering minimization of energy exchange for case 3.

In this case, the microgrid is self-sufficient for approximately 2 months longer time, during summer, than in case 2 when exchange is minimized. The energy storage capacity is not big enough to store all the excess energy produced. Therefore, the microgrid also exports a lot of energy during the summer. In Figure 5.12, the average daily power import is presented.

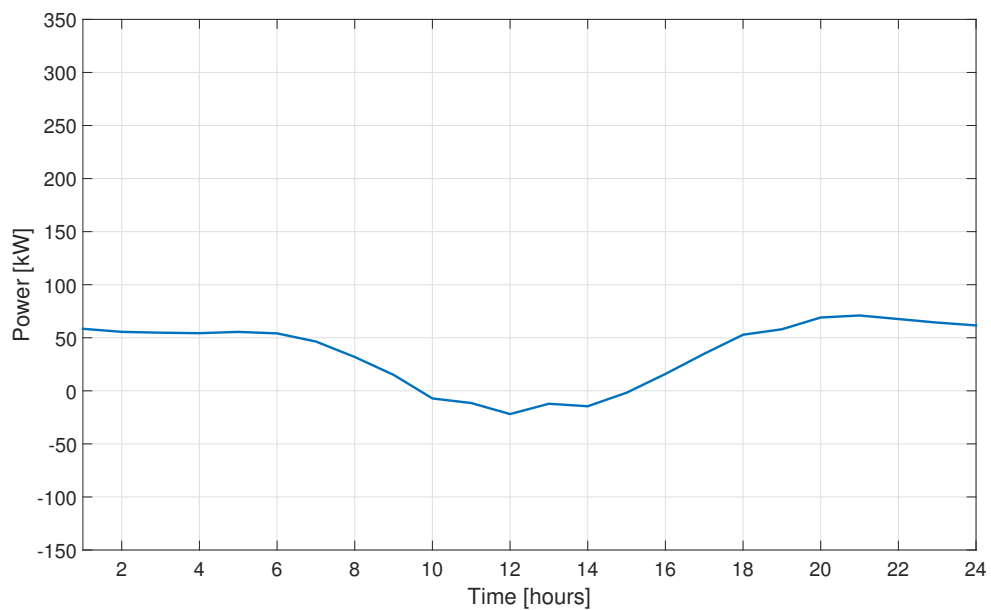


Figure 5.12: Average daily power import for minimization of the energy exchange for case 3.

It can be noted that the microgrid imports energy during morning and night, and it exports energy during daytime when the energy production from PV panels is higher. Table 5.6 shows the annual results for the minimization of energy exchange considering the microgrid fee.

Table 5.6: Annual results for the minimization of energy exchange for case 3.

	Low voltage network	Medium voltage network
Energy cost (SEK)	162 695	-
Total energy import (MWh)	482.9	14 672
Total energy export (MWh)	171.7	43.7
Losses (MWh)	2.67	103.7
Peak import (MW)	0.283	3.9
Total battery losses (MWh)	10.7	-
Total aggregated energy through each battery (MWh)	2.9	-

The annual energy cost is decreased by 33 % when compared to case 2 (minimization of energy exchange), since more local production has been added. The total energy import in the low and medium voltage network is decreased by 23 % and 0.01 %, respectively. However, as more energy is produced more energy is exported since the batteries do not have enough storage capacity. The increase in the total energy export in the low and medium voltage network is 55 % and 44 % respectively. The losses in both low and medium voltage network are decreased by approximately 11 % and 1.3 %. The battery losses are slightly higher compared to case 2 (minimization of energy exchange). This is because the batteries are utilized more in this case where there is an average aggregated energy throughput of 2.9 MWh in each battery. The batteries will have reached the warranty limit after 13 years, and if the microgrid seeks to minimize the energy exchange daily this would still be a viable way to schedule the batteries.

5.5 Case 4

In case 4, hydrogen storage system is installed along with PVs, batteries and wind turbines in the low voltage network. In this case, the operational objective for minimization of energy exchange using the microgrid fee is implemented. Figure 5.13 depicts the energy import for a year. The consumption data is taken from 2017.

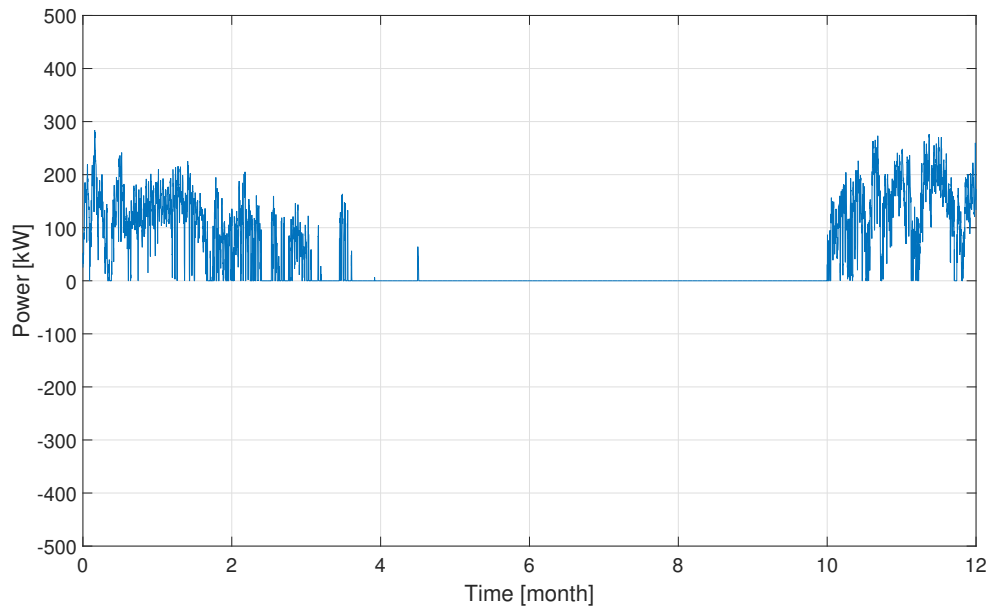


Figure 5.13: Power import for a year for case 4.

As shown in Figure 5.11, there is excess production of energy, which is exported due to the low storage capacity of the batteries. Therefore, a hydrogen ESS is installed to create a microgrid that is self-sufficient for a longer period during the year. It can be seen from Figure 5.13, that the microgrid is self-sufficient for almost half a year. Figure 5.14 shows the average daily power import for minimization of energy exchange.

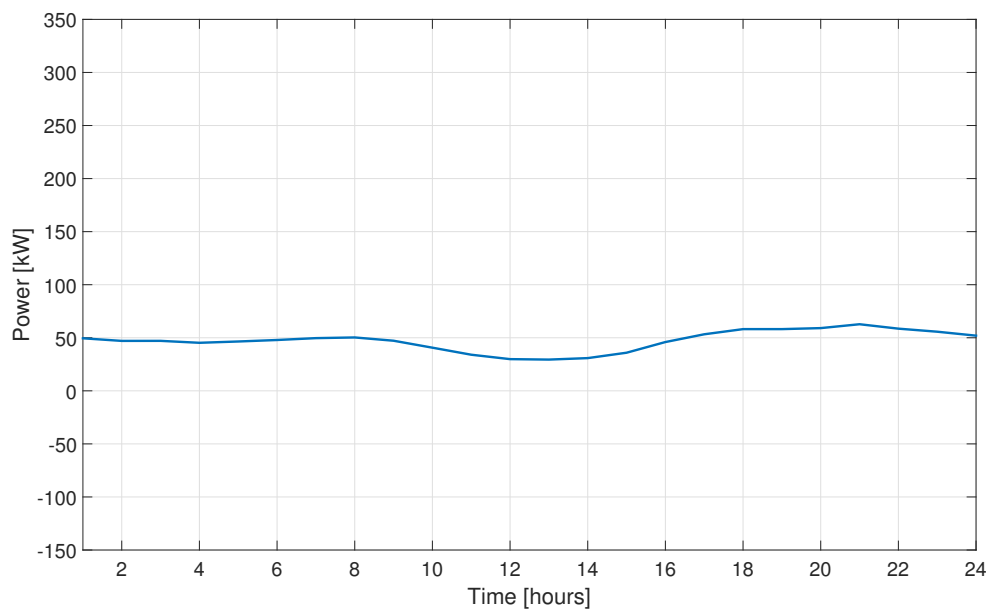


Figure 5.14: Average daily power import for the minimization of energy exchange for case 4.

Due to the added storage capacity the daily import profile has become flatter and now no energy is needed to be exported during day time. Figure 5.15 shows the stored energy in the hydrogen storage system throughout the year.

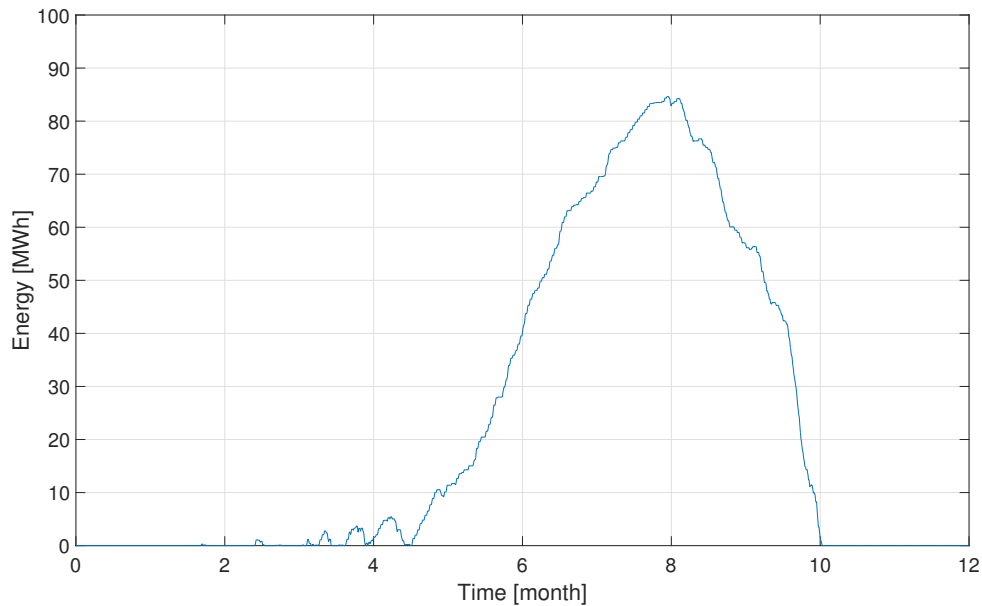


Figure 5.15: Stored energy in the hydrogen tank in case 4.

Excess energy produced during the summer is stored in the hydrogen storage system and used during the autumn. However, the microgrid still imports reactive power since it is assumed that the microgrid resources do not produce its own. Table 5.7 presents the annual results for the low and medium voltage network.

Table 5.7: Annual results for the minimization of energy exchange for case 4.

	Low voltage network	Medium voltage network
Energy cost (SEK)	186 580	-
Total energy import (MWh)	414.2	14 762
Total energy export (MWh)	0	30.1
Losses (MWh)	2.3	104.0
Peak import (MW)	0.284	3.86
Energy storage losses (MWh)	113.7	-
Total aggregated energy through each battery (MWh)	2.7	-

The annual energy cost of the low voltage network is increased by 13 % compared to case 3. The annual cost is increased when adding hydrogen storage, because the efficiency of the hydrogen energy storage system is low. The total energy import into the low voltage network is more than halved compared to the base case, meaning that the microgrid supplies more than 50 % of its own energy. The total energy

export is zero due to the addition of hydrogen storage system in the low voltage network. The energy storage losses in the low voltage network are 113.7 MWh. The total aggregated energy through each battery is on average 2.7 MWh which means that the batteries are expected to last for about 14 years. Table 5.8 shows the various components in the hydrogen storage system, their size, investment cost and their life expectancy

Table 5.8: Components of the Hydrogen energy storage system.

	Size	Investment cost (MSEK)	Lifetime (Years)
Hydrogen tank	84.6 MWh	22	20
Electrolyzer	0.373 MW	3.3	10
Fuel cell	0.196 MW	4.3	5

5.6 Case 5

In case 5, PVs, batteries, wind turbines, a hydrogen ESS and a CHP plant are included in the energy resources mix in the low voltage network. In this case, again the operational objective for the minimization of energy exchange including the microgrid fee is implemented. A CHP plant is installed to make up for the lack of energy production during the winter. In Figure 5.16, the power import for a year is presented. The consumption data is taken from 2017.

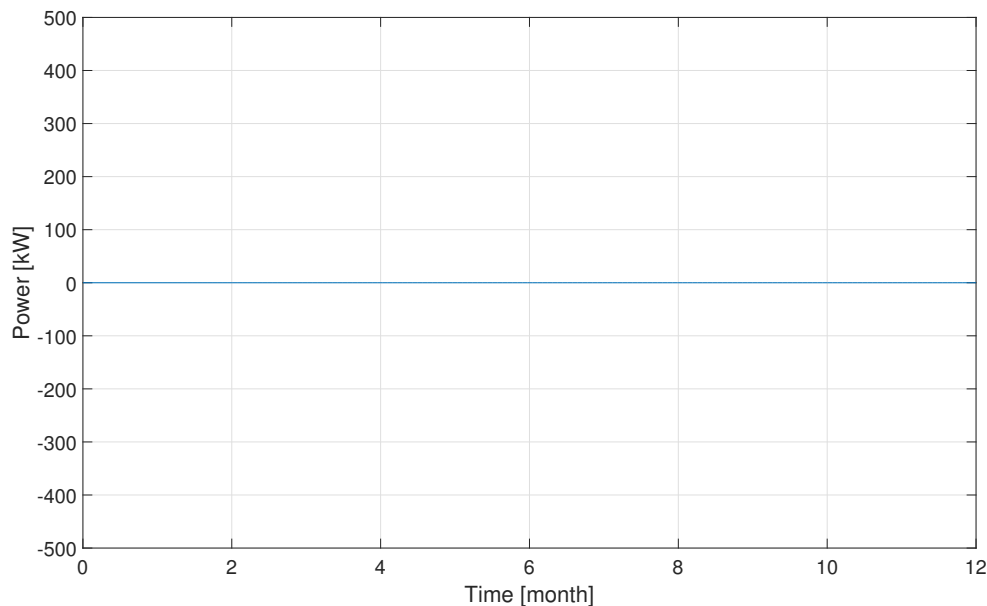


Figure 5.16: Power import for a year for minimization of energy exchange for case 5.

From Figure 5.16 it can be seen that the energy import is zero after the installation

of a CHP plant. The microgrid is self-sufficient regarding the active power supply. Figure 5.17 shows the power production for a year from the CHP plant.

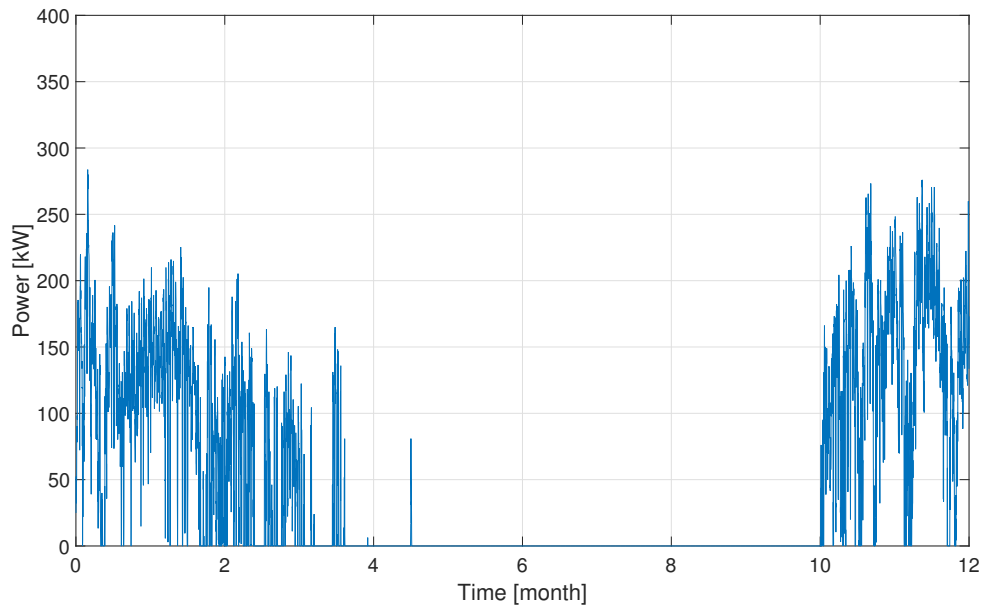


Figure 5.17: Power production for a year from the CHP plant.

Figure 5.18 depicts the energy stored in the hydrogen tank. The surplus energy produced during the summer is stored, just as in case 4.

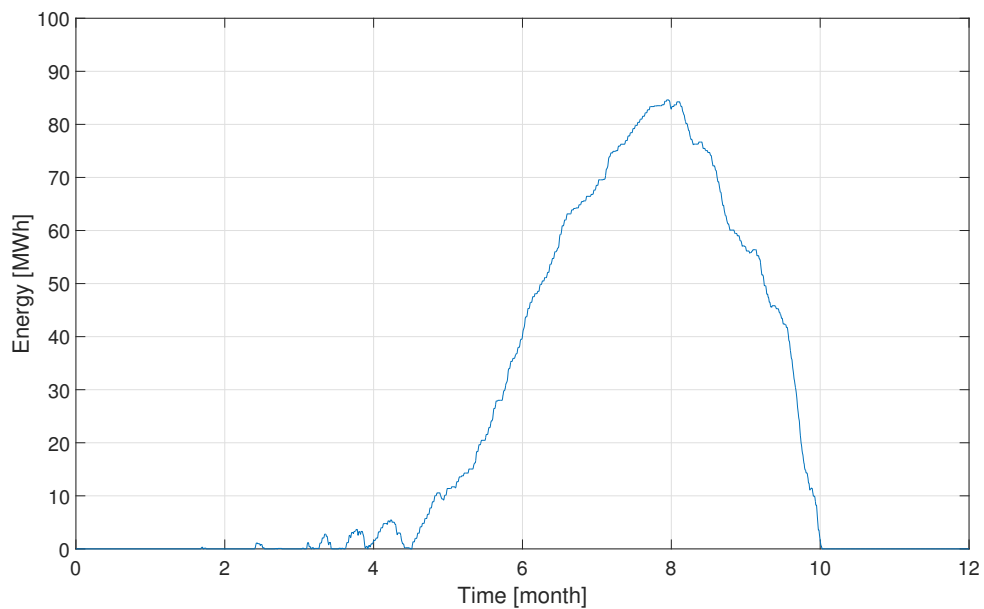


Figure 5.18: Stored energy in hydrogen tank in case 5.

The various components in the hydrogen storage system, their sizes, investment costs and its life expectancy are in case 5 of the same dimensions as in case 4. In

Table 5.9, the annual results for the minimization of energy exchange for case 5 is shown.

Table 5.9: Annual results for the minimization of energy exchange for case 5.

	Low voltage network	Medium voltage network
Energy cost (SEK)	258 219	-
Total energy import (MWh)	0	14 344
CHP energy production (MWh)	414.2	-
CHP peak production (MW)	0.284	-
Total energy export (MWh)	0	31.1
Losses (MWh)	1.3	99.6
Peak import (MW)	0	3.6
Energy storage losses (MWh)	113.7	-
Total aggregated energy through each battery (MWh)	2.7	-

The annual energy cost is increased by 38 % as compared to case 4. This increase is because it is more expensive to produce energy in the CHP plant than to buy it from the main grid. The energy production from CHP plant is 414.2 MWh. The peak production of the CHP plant is 284 kW resulting in an investment cost of 2 840 000 SEK with a yearly maintenance cost of 113 600 SEK. The total energy import, the total energy export and the peak import are zero as illustrated in Table 5.9. The losses in the low and medium voltage network are reduced by 43 % and 4.2 % when compared with case 4. Compared to the base case the medium voltage network losses are reduced by 8.1 %. The energy storage losses are the same as in case 4. The total aggregated energy through each battery is on average 2.7 MWh which means that the batteries will have reached the warranty limit after 14 years, if the microgrid seeks to minimize the energy exchange daily. Therefore, this would also be a viable way to schedule the batteries.

5.7 Cost Analysis

The cost considered in the analysis consist of the annual energy cost, the investment cost, the replacement cost, and the grid maintenance cost. The cost analysis is performed for the base case, case 1, and case 2 in order to illustrate the reduction in the cost considering a long term operation of the microgrid. In case 2, both microgrid operational objectives are considered but only for the microgrid fee. Household fee is excluded since the results showed that when this fee is considered in case 2, the reduction in annual energy cost cannot compensate for the high investment cost. Cases 3-5 are also excluded because the focus of these cases was to make a self-sufficient microgrid by adding necessary resources step by step. In these cases, it is also shown that the the reduction in annual energy cost cannot compensate for the high investment cost. Figure 5.19 shows the actual costs for the base case, case 1, and case 2 considering the two microgrid operational objectives.

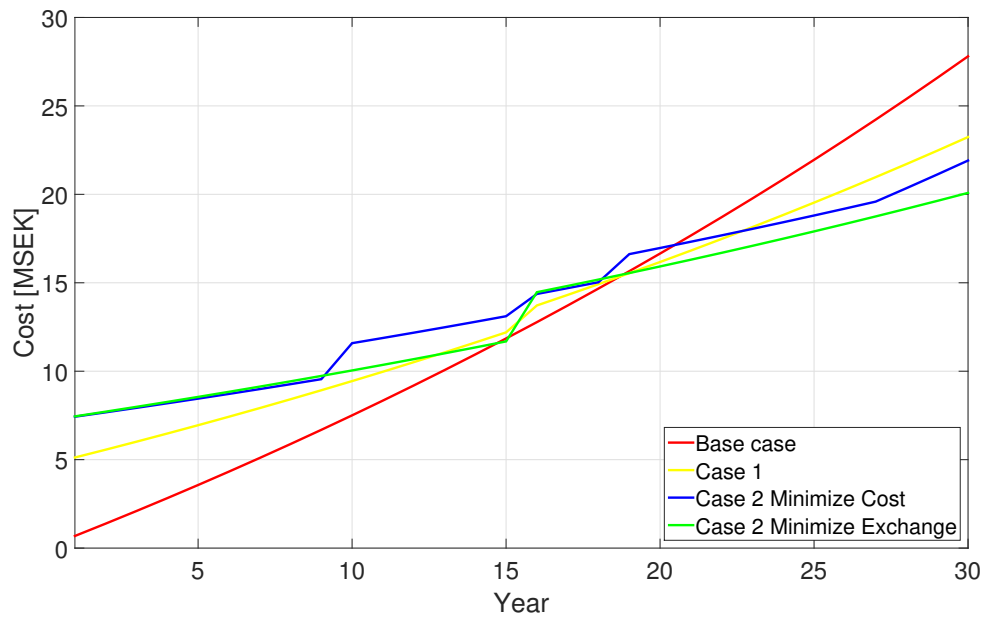


Figure 5.19: Cost analysis comparison.

The cost of installing only PV (case 1) can be compensated for in about 18 years. When installing batteries, as in case 2, it takes longer time to compensate for the total cost. However, by the end of the 30 year period, the microgrid operation as in case 2 saves more money than in case 1. The microgrid operational objective does not have much impact on the annual energy cost, however it has a big impact on the battery lifetime. When minimizing exchange, the lifetime of the batteries is 15 years and the batteries only have to be replaced once. Therefore, the total cost savings are bigger, when minimizing exchange as compared to when minimizing cost, with the total cost saving after 30 years being approximately 6 MSEK, compared to the base case. In order to evaluate the cost of an investment, the present worth cost can be calculated. In Table 5.10 the present worth of the energy cost, scaled with inflation, and the total investment cost, scaled using an interest rate of 5 %, is shown.

Table 5.10: Present worth of energy and investment costs for a 30-year period.

	Energy Cost (SEK)	Investment Cost (SEK)	Total Cost (SEK)
Base case	20 157 000	0	20 157 000
Case 1	12 770 000	5 423 000	18 193 000
Case 2 Minimize exchange	7 184 000	8 639 000	15 823 000
Case 2 Minimize cost	6 634 000	9 564 000	16 198 000

From the table it can be seen that the microgrid, in case 2, seeking to minimize energy exchange makes the biggest total cost savings. However, minimizing energy

cost is almost as good. In Figure 5.20 The present worth cost is plotted for each year.

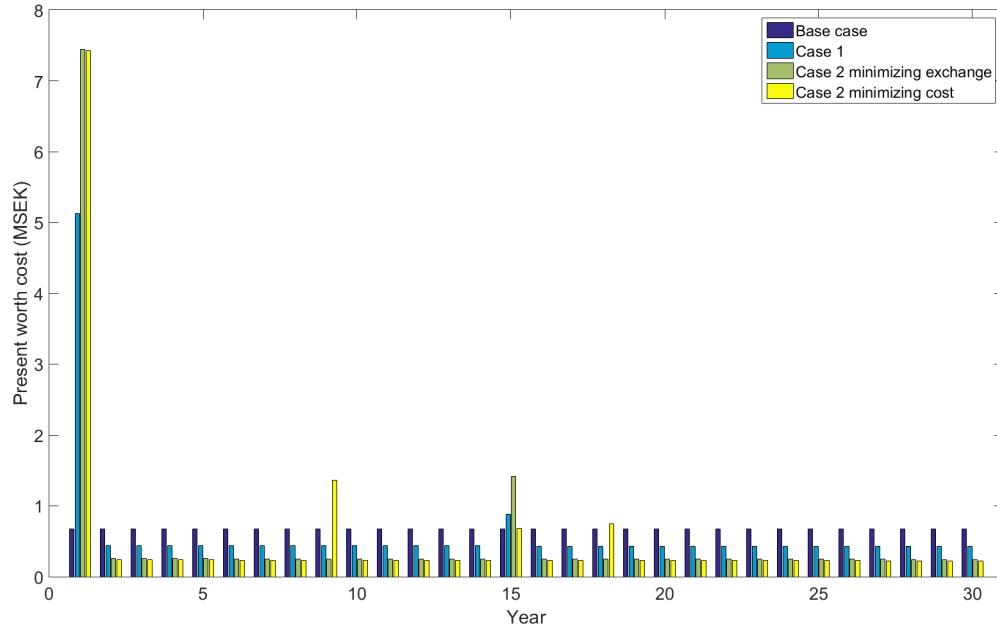


Figure 5.20: The total of present worth of energy and investment costs for a each year for 30 year period.

In Figure 5.20 it can be seen that the biggest investments are in the first year.

5.8 Accuracy of Linearization

The error of the linearization is compared for two extreme cases. One case is that all loads consume 5 kW and there is no production in the microgrid. The load consumption of 5 kW is chosen because the maximum total peak demand at bus 10 is 336.4 kW and when this splits on 78 household consumptions, it results in 4.3 kW on each load. For pushing the limit further, 5 kW is chosen. The other case is that there is no consumption and that all PV panels produce at maximum level, i.e., 6.25 kW. The voltage, voltage angle, current magnitude, power flow, and losses are compared for these two extreme cases. For these two cases, the current is close to the current limits of the lines in the grid. The average absolute value of the error when solving using the linearized equations compared to the non-linear equations is presented in Table 5.11.

Table 5.11: Average absolute value of the error of linearized model compared to non-linear model.

	Average error (%)	
	High Consumption	High Production
Voltage	0.060	0.086
Voltage Angle	0.160	0.823
Active power flow	0.035	0.039
Reactive power flow	0.090	-
Current magnitude	0.205	0.960
Power losses	0.811	2.52

As can be seen from Table 5.11 the error is always sufficiently small (less than 3 %) and the linearization can be considered valid.

5.9 Summary

In this section, a summary of the key results for all cases is presented. The voltage deviation from steady-state voltage at the PCC for each case is shown in Table 5.12.

Table 5.12: Maximum voltage deviation for different test cases in percentage.

	Maximum voltage deviation %
Base case	-0.4/+0.39
Case 1	-0.44/+0.51
Case 2	-0.39/+0.49
Case 3	-0.4/+0.48
Case 4	-0.4/+0.4
Case 5	-0.32/+0.4

As can be noted from Table 5.12, the voltage is practically not affected and is always well within the limit of $\pm 7\%$. The energy cost, energy losses, medium voltage energy import, energy exchange, and battery lifetime for all cases are shown in Table 5.13.

Table 5.13: Summary of the key results for different test cases.

	Cost (SEK)	Medium voltage network energy losses (MWh)	Medium voltage network energy import (MWh)	Energy exchange at PCC (MWh)	Battery lifetime (Years)
Base case	685 349	108.4	15 311	968.9	-
Case 1	434 185	105.0	14 884	897.6	-
Case 2	407 097	104.8	14 908	1349.7	5
Minimize cost household fee					
Case 2	225 554	104.8	14 900	992.9	9
Minimize cost microgrid fee					
Case 2	244 241	105.0	14 894	705.7	15
Minimize exchange	441 922				
Case 3	162 695	103.7	14 672	654.6	13
Case 4	186 580	104.0	14 762	414.2	14
Case 5	258 219	99.6	14 344	0	14

6

Discussion

This chapter discusses the results and analysis and explains the impacts of the found results.

6.1 Network Losses

The share of local energy production in the microgrid plays the most significant role in the reduction of the energy losses in the upstream main grid. This can be seen in case 5, when the microgrid produces all the energy required to cover the demand locally. In this case, the losses in the 10 kV network are the lowest. However, if the total losses in the interconnected system (main grid and micro-grid) are considered then the losses are increased in all microgrid cases. This is because of the losses in the ESS.

6.2 Energy Storage System Strategies

As stated in the previous section, the total losses are increased due to the ESS losses. However, the purpose of the ESS is not to reduce losses but to manage energy, e.g., energy arbitrage, reschedule consumption, and store excess energy. The batteries usage depend on the operational strategy of the microgrid and the usage can be a combination of, e.g., both energy arbitrage and excess energy storage. Using the whole energy capacity of the batteries for energy arbitrage is not an economically efficient way of operation due to the low size of profit versus investment. In addition, the batteries are worn out up to three times faster compared to when they are used only for storing excess energy.

6.3 Microgrid Operational Strategies

If the microgrid operates with the aim to minimize the daily energy cost, as in case 2, it would be more beneficial for the DSO to enforce a tax that includes a peak import penalty, as the proposed microgrid fee that is applied here. This forces the microgrid to limit its peak import and flatten out its import profile. The resulting import profile is much better for the DSO for two reasons, lower peaks and much smaller variations in hourly power import. Lower overall loading of the 10 kV network gives the DSO the opportunity to supply power to more customers within

the area without reinforcing the grid and that way increasing their income. This way of operation is also much better for the microgrid for several reasons; lower cost, longer battery lifetime, and the lines in the 400 V network will be less loaded, releasing capacity for a future increase in the load consumption. When minimizing daily energy cost, without any peak import penalty, the batteries are used for energy arbitrage. The energy exchange is increased significantly because this microgrid operational objective forces all batteries to fully charge when the price is low so that the microgrid can sell back the stored energy, when the price is higher. This means that the lines will be operated close to their current limits during these hours.

In case 2, when the exchange is minimized with the application of the microgrid fee the annual energy cost is slightly higher than when cost is minimized. However, the lifetime of the batteries is increased from 9 to 15 years. Therefore, this case proposes the most economically viable way of operation. Implementing an EMS to minimize exchange is also much simpler and requires less aspects to be considered when scheduling than when implementing an EMS to minimize cost. When minimizing exchange the energy scheduling practically follows the priority order of the resources. The basic idea is that the ESS should charge when there is an overproduction and discharge when there is an underproduction. When minimizing cost forecasts of weather conditions, price, and consumption is required which will also introduce a lot of uncertainties.

6.4 Microgrid Economics

A PV and battery based microgrid, like in case 2, can be an economically viable investment. After a 30 year period, approximately 6 MSEK can have been saved in total costs when exchange is minimized. The annual energy cost can be reduced significantly for the microgrid. The investment cost is the biggest problem but with advancements in technology (battery, PV, etc.) leading to reduced investment costs, the microgrid could make even bigger total cost savings.

The purpose of the development and the operation of a microgrid can have other benefits apart from cost saving, such as energy loss reduction, increased penetration of renewable, more secure and reliable energy supply and release of network capacity. The microgrid could also provide ancillary services to the main distribution grid. Such ancillary services could be e.g., the production of reactive power or regulating power.

6.5 Off-grid Operation

In a microgrid with a large penetration of PV systems, there is a mismatch between energy production and consumption throughout the year. The PV production reaches the highest values during the summer, while the consumption is highest

during winter. Due to this mismatch, a microgrid with a large proportion of PV will have a lot of overproduction during the summer, more than what the batteries can store. This creates the need to invest in long-term storage. A microgrid based on a lot of wind energy would most likely be more suitable in Sweden. However, building PV is much simpler in a living area which is the location of this project. Adding hydrogen storage is a good way to store the excess energy. The stored energy can be consumed later when needed, this effectively increases the amount of time that the microgrid can supply its own energy. However, it is not profitable to invest in a hydrogen storage system, because they are expensive and have a low efficiency meaning that it is always, in a stable energy market, more profitable to sell the energy than to store it as hydrogen. Introducing hydrogen storage is not sufficient to supply the microgrid with power throughout the whole winter. To counteract this problem, another source of energy needs to be added. A CHP plant is a good compliment to PV. The CHP plant can produce energy during winter for a price that is comparable to the market price. There is also the possibility of utilizing the heat production from the CHP plant, when the heat demand is high during the winter. From case 4, it can be noted that the microgrid has the capability to go off-grid for about half a year and in case 5 for the whole year. In cases 2 and 3, one can also see that the microgrid can supply its own energy for weeks or months, but in these cases, the microgrid still needs the connection to the main grid to export its excess energy. In order to go completely off-grid, the microgrid would have to start producing its own reactive power. This can easily be done through the inverters of the PVs, wind turbines, batteries, and fuel cells. The CHP plant could also produce reactive power. To add reactive power production from the inverter-based resources of the microgrid, a linear model of power factor control would need to be developed. A suitable reactive power fee would also need to be developed in order to analyze the cost savings from producing reactive power versus buying it.

7

Conclusions and Future Work

This section includes the conclusion remarks of the project and it also offers suggestions for future work on the area.

7.1 Conclusions

The main purpose of this thesis was to evaluate the effects of having a grid-connected microgrid in the distribution network. This was done for several different microgrid cases.

The grid-connected microgrid in the distribution grid can offer a lot of benefits for the DSO. By having a grid-connected microgrid within the distribution grid, the losses in the upstream medium voltage network can be reduced by up to 8.1 %. It was shown that the microgrid could help reduce congestion by reducing the power import from the upstream 135 kV network by up to 6.3 %. This reduction in power import could provide an opportunity to the distribution system operator to release network capacity, which could support the supply of more loads in the future. The implementation of the microgrid does not have a significant impact on the steady-state voltage at the PCC. In terms of investment and energy cost, a PV and battery based microgrid operating to minimize energy exchange seemed to be the best option for this network, since after a 30-year period this microgrid could have saved up to 6 MSEK.

If the household fee would be applied to the microgrid, it would never be beneficial for the microgrid owner to invest in installing batteries. Minimizing energy cost with household fee results in a very short, 5 years, lifetime of the batteries for a very small profit gain. In this case, the batteries are used for energy arbitrage and the microgrid exchanges a lot of energy with main the grid. This is not good for either the DSO or the microgrid. This problem can be mitigated by enforcing a fee that penalizes daily peak import, the proposed microgrid fee. This decreases the annual energy cost for the microgrid and increases the lifetime of the batteries as well as reduces the energy exchange. When the microgrid operates to minimize energy exchange considering the household fee, the annual energy cost is increased and there is no profit from investing in batteries. However, if the microgrid fee is enforced then minimizing exchange is a viable option. This means that if the DSO enforces a fee penalizing peak import, like the microgrid fee, it gives the microgrid incentive to minimize its exchange with the main grid. The batteries last longer if the microgrid

operates with the aim to minimize the energy exchange instead of minimizing cost, meaning that this operational objective should be preferred for optimal long term results. As a result of these conclusions the proposed strategy for the DSO is to enforce peak penalizing energy fee.

A microgrid based on PV, wind, and batteries can avoid importing power for several months during summer. The batteries used in this project, however, do not have sufficient storage capacity to store all the energy that is produced during this time since batteries are in terms of energy storage capacity expensive. This makes it necessary to invest in energy storage with higher capacity to store the excess energy. Adding hydrogen storage, which has a high energy storage capacity makes it a good alternative for storing the excess produced energy. Hydrogen storage, however, has a low efficiency making it most suitable for long-term storage. Being able to supply its own power, using only intermittent energy sources, during winter is a challenge. Using a CHP plant to compensate for low power production during winter is an effective, although expensive, solution.

In summary, a grid-connected microgrid can offer a lot of benefits for the microgrid operator and, therefore, its customers as well as the DSO and the main grid, however, the investment costs involved are high given the present conditions.

7.2 Future Work

The following points offer suggestions for future research as an extension of the work carried out in this thesis.

- **Optimal sizing and choices of DERs:** Investigate which and what resources are the optimal selection in order to maximize the benefits versus the investment cost.
- **Increase time resolution of data:** Gather all data on a higher time resolution in order to optimize the operation of the microgrid in shorter time-periods.
- **Reactive power production:** Evaluate the cost for the microgrid to produce its own reactive power. A reactive power fee should also be developed.
- **Multiple microgrids:** Introduce more microgrids to the grid. Investigate how the microgrids interact with each other and how the the main grid is affected.
- **Heat modelling:** Model the heating system for a microgrid that includes cogeneration.
- **Ancillary services:** Investigate what kind of ancillary services the microgrid could provide and also what is the profit that they could offer to the microgrid.

- **Detailed battery model:** Model the batteries with more details in terms of aging where, e.g., efficiency is dependent on battery age and the aging of the batteries is dependent on the depth of charge.

Bibliography

- [1] F. Katiraei, R. Iravani, N. Hatziargyriou, and A. Dimeas, "Microgrids management," *IEEE Power and Energy Magazine*, vol. 6, no. 3, pp. 54–65, May 2008.
- [2] N. Hatziargyriou, H. Asano, R. Iravani, and C. Marnay, "Microgrids," *IEEE Power and Energy Magazine*, vol. 5, no. 4, pp. 78–94, July 2007.
- [3] C. Marnay, F. J. Rubio, and A. S. Siddiqui, "Shape of the microgrid," Ernest Orlando Lawrence Berkeley National Laboratory, Berkeley, CA (US), Tech. Rep., 2000.
- [4] W. Su and J. Wang, "Energy management systems in microgrid operations," *The Electricity Journal*, vol. 25, no. 8, pp. 45–60, 2012.
- [5] "Introduction to microgrids," *Introduction to Microgrids - What is a Microgrid / ABB*, accessed: 2018-04-23. [Online]. Available: <http://new.abb.com/distributed-energy-microgrids/introduction-to-microgrids>
- [6] R. Lasseter, A. Akhil, C. Marnay, J. Stephens, J. Dagle, R. Guttromson, A. S. Meliopoulos, R. Yinger, and J. Eto, "Integration of distributed energy resources. the certs microgrid concept," 2002.
- [7] N. Hatziargyriou, A. Anastasiadis, J. Vasiljevska, and A. Tsikalakis, "Quantification of economic, environmental and operational benefits of microgrids," in *PowerTech, 2009 IEEE Bucharest*. IEEE, 2009, pp. 1–8.
- [8] C. Chen, S. Duan, T. Cai, B. Liu, and G. Hu, "Smart energy management system for optimal microgrid economic operation," *IET renewable power generation*, vol. 5, no. 3, pp. 258–267, 2011.
- [9] J. P. Lopes, C. Moreira, and A. Madureira, "Defining control strategies for microgrids islanded operation," *IEEE Transactions on power systems*, vol. 21, no. 2, pp. 916–924, 2006.
- [10] E. Rokrok, M. Shafie-khah, and J. P. Catalão, "Review of primary voltage and frequency control methods for inverter-based islanded microgrids with distributed generation," *Renewable and Sustainable Energy Reviews*, 2017.
- [11] Y.-S. Kim, E.-S. Kim, and S.-I. Moon, "Frequency and voltage control strategy of standalone microgrids with high penetration of intermittent renewable generation systems," *IEEE Transactions on Power systems*, vol. 31, no. 1, pp. 718–728, 2016.
- [12] A. Bidram and A. Davoudi, "Hierarchical structure of microgrids control system," *IEEE Transactions on Smart Grid*, vol. 3, no. 4, pp. 1963–1976, 2012.
- [13] L. Che, M. Khodayar, and M. Shahidehpour, "Microgrids for distribution system restoration," *IEEE Power and Energy Mag*, 2013.

- [14] D. E. Olivares, A. Mehrizi-Sani, A. H. Etemadi, C. A. Cañizares, R. Iravani, M. Kazerani, A. H. Hajimiragha, O. Gomis-Bellmunt, M. Saeedifard, R. Palma-Behnke *et al.*, “Trends in microgrid control,” *IEEE Transactions on smart grid*, vol. 5, no. 4, pp. 1905–1919, 2014.
- [15] “Direkt från simris,” *Lokala energisystem | Direkt från Simris - E.ON*, accessed: 2018-04-19. [Online]. Available: <https://www.eon.se/om-e-on/innovation/lokala-energisystem/direkt-fran-simris.html#/produktion>
- [16] “Abb microgrid to power robben island,” *Robben Island microgrid / ABB*, accessed: 2018-04-23. [Online]. Available: <http://new.abb.com/distributed-energy-microgrids/projects/robben-island>
- [17] “World’s most powerful wind turbine successfully installed in scottish waters,” *Vattenfall*, accessed: 2018-04-18. [Online]. Available: <https://corporate.vattenfall.co.uk/about-vattenfall/news-and-media/press-releases/2018/worlds-most-powerful-wind-turbine/>
- [18] H. L. Wegley, J. V. Ramsdell, M. M. Orgill, and R. L. Drake, “Siting handbook for small wind energy conversion systems,” Battelle Pacific Northwest Labs., Richland, WA (USA), Tech. Rep., 1980.
- [19] *Sharp: NU series*, Sharp Energy Solution Europe, datasheet.
- [20] P. A. Breeze, *Combined heat and power*. Amsterdam Academic Press, 2018.
- [21] O. Gandhi, W. Zhang, C. D. Rodriguez-Gallegos, M. Bieri, T. Reindl, and D. Srinivasan, “Analytical approach to reactive power dispatch and energy arbitrage in distribution systems with ders,” *IEEE Transactions on Power Systems*, p. 1, 2018.
- [22] IEC, *Electrical Energy Storage White Paper*.
- [23] X.-S. Yang, E. C. (e-book collection), and I. ebrary, *Introduction to mathematical optimization: from linear programming to metaheuristics*. Cambridge, UK: Cambridge International Science Publishing, 2008;2007;.
- [24] T. K. Nagsarkar, M. S. Sukhija, and K. (e-book collection), *Power System Analysis: Power System Analysis*, 2nd ed. Oxford;New Delhi;: Oxford University Press India, 2016.
- [25] N. Cai, *Linearized and distributed methods for power flow analysis and control in smart grids and microgrids*. Michigan State University, 2014.
- [26] H. Hao, D. Wu, J. Lian, and T. Yang, “Optimal coordination of building loads and energy storage for power grid and end user services,” *IEEE Transactions on Smart Grid*, 2017.
- [27] Z. Liang and Y. Guo, “Optimal energy management for microgrids with cogeneration and renewable energy sources,” in *Smart Grid Communications (SmartGridComm), 2015 IEEE International Conference on*. IEEE, 2015, pp. 647–652.
- [28] “Historical market data,” *Nord Pool*. [Online]. Available: <https://www.nordpoolgroup.com/historical-market-data/>
- [29] “Elnätspriser i göteborg 2017,” *Göteborg Energi*, accessed: 2018-04-18. [Online]. Available: https://www.goteborgenergi.se/Privat/Produkter_och_priser/Elnat/Elnatspriser/Elnatspriser_i_Goteborg/Elnatspriser_i_Goteborg_2017

-
- [30] “Solel,” *Göteborg Energi*, accessed: 2018-04-18. [Online]. Available: https://www.goteborgenergi.se/Privat/Produkter_och_priser/Elhandel/Gor_din_egen_el/SolEl
- [31] “Elnätspriser i göteborg 2017,” *Göteborg Energi*, accessed: 2018-04-18. [Online]. Available: https://www.goteborgenergi.se/Foretag/Produkter_och_tjanster/Elnat/Elnatspriser/Elnatspriser_i_Goteborg/Elnatspriser_i_Goteborg_2017
- [32] “Ersättningar och avgifter för produktion av el 2017,” *Göteborg Energi*, accessed: 2018-04-18. [Online]. Available: https://www.goteborgenergi.se/Foretag/Produkter_och_tjanster/Elnat/Ersattningar_och_avgifter_for_produktion_av_el/Produktion_av_el_Goteborg/Produktion_av_el_Goteborg_2017
- [33] *SMHI Öppna Data | Meteorologiska Observationer*. [Online]. Available: <http://opendata-download-metobs.smhi.se/explore/#>
- [34] *Powerwall:Litium-ion Battery*, Tesla, datasheet.
- [35] “Powerwall support,” *Powerwall Support | Tesla Sverige*, Mar 2018, accessed: 2018-04-25. [Online]. Available: https://www.tesla.com/sv_SE/support/powerwall#warranties-home-owners
- [36] “Pvwatts,” *PVWatts Calculator*, accessed: 2018-03-15. [Online]. Available: <http://pvwatts.nrel.gov/index.php>
- [37] *Excel 10kW wind turbine*, Bergey, datasheet.
- [38] P. Andersson, “Riktvärden för buller från väg- och spårtrafik vid befintliga bostäder,” *Naturvårdsverket*, accessed: 2018-03-13. [Online]. Available: <http://www.naturvardsverket.se/Stod-i-miljoarbetet/Vagledninga/Buller/Buller-fran-vag--och-spartrafik-vid-befintliga-bostader/>
- [39] “Buller,” *Vindlov*, accessed: 2018-03-16. [Online]. Available: <https://www.vindlov.se/sv/lagar--regler/rattsfall/buller/>
- [40] F. Bañuelos-Ruedas, C. Angeles-Camacho, and S. Rios-Marcuello, “Methodologies used in the extrapolation of wind speed data at different heights and its impact in the wind energy resource assessment in a region,” in *Wind Farm-Technical Regulations, Potential Estimation and Siting Assessment*. InTech, 2011.
- [41] N. L. Martin Göransson, “Development of an energy managementmodel for Chalmers’ microgrid: Application for cost-benefit analysis of battery energy storage,” Master’s thesis, Chalmers University of Technology, Gothenburg, Sweden, 2016.
- [42] “Stöd och bidrag,” *Energimyndigheten*, accessed: 2018-04-20. [Online]. Available: <http://www.energimyndigheten.se/fornybart/stod-och-bidrag-pa-fornybartomradet/>
- [43] Riksbanken, “Inflationsmålet,” *Sveriges Riksbank*, accessed: 2018-04-23. [Online]. Available: <https://www.riksbank.se/sv/penningpolitik/inflationsmalet/>
- [44] “Tesla powerwall,” *Powerwall | The Tesla Home Battery*, accessed: 2018-04-18. [Online]. Available: https://www.tesla.com/sv_SE/powerwall
- [45] S. Rodrigues, R. Torabi, H. G. Ramos, and F. Morgado-Dias, “Powerwall 2.0 economic feasibility in australia,” in *2017 International Conference in Energy*

- and Sustainability in Small Developing Economies (ES2DE)*, July 2017, pp. 1–7.
- [46] C.-H. Li, X.-J. Zhu, G.-Y. Cao, S. Sui, and M.-R. Hu, “Dynamic modeling and sizing optimization of stand-alone photovoltaic power systems using hybrid energy storage technology,” *Renewable energy*, vol. 34, no. 3, pp. 815–826, 2009.
- [47] “Solcellspaket – priser och produkter,” *Solcellspaket priser - en helhetslösning för ditt hus - Vattenfall*, accessed: 2018-04-20. [Online]. Available: <https://www.vattenfall.se/solceller/solcellspaket/>
- [48] “Solcellspaket och batterier,” *Solcellspaket | Skräddarsytt för ditt hus - E.ON*, accessed: 2018-04-20. [Online]. Available: <https://www.eon.se/privat/for-hemmet/solceller/solcellspaket.html#/hoegre-elfoerbrukning>
- [49] “Residential wind energy systems - bergey wind power,” *Bergey Wind Power*. [Online]. Available: <http://bergey.com/wind-school/residential-wind-energy-systems>
- [50] I. ETSAP, “Combined heat and power,” *Energy technology systems analysis programme*, 2010.

A

Line Data

Table A.1: 10 kV network line data.

p.u	R	X	Bc
240 mm^2 Al			
1.2	0.00016597	0.00305008	0
2.3	0.00186	0.00131375	0.010787915
3.4	0.0015554	0.0001745	0.0001047
4.5	0.00060125	0.00042325	0.0034755
5.6	0.00039375	0.00027715	0.00227605
6.7	0.0002272	0.0000825	0.00033455
5.8	0.0008125	0.00057195	0.00469665
8.9	0.000635	0.000447	0.0036706
9.10	0.01678875	0.08841	0
9.11	0.00038125	0.00026835	0.0022038
11.12	0.00093	0.00065465	0.00537585
12.13	0.0008925	0.0006284	0.0051591
13.14	0.00055625	0.00039155	0.0032154
14.15	0.00044625	0.0003141	0.00257955
15.16	0.00026875	0.00018915	0.0015535
16.17	0.000315	0.0002217	0.00182085
17.18	0.000325	0.00022875	0.00187865
18.2	0.004125	0.00290385	0.02384465

Table A.2: 400 V network line data.

p.u	R	X
240 mm^2 Al		
10.19	0.010625	0.006675884
10.27	0.0185	0.011623893
10.38	0.011625	0.007304203
10.45	0.027125	0.01704314
10.54	0.020875	0.013116149
10.65	0.0053125	0.003337942
10.70	0.001375	0.000863938
19.20	0.00875	0.005497787
20.71	0.01025	0.006440265
27.28	0.017	0.010681415
38.39	0.01125	0.007068583
39.80	0.010625	0.006675884
45.46	0.0115	0.007225663
54.60	0.012875	0.008089601
60.100	0.009875	0.006204645
54.62	0.014125	0.008874999
62.108	0.011	0.006911504
10 mm^2 Cu		
10.69	0.1098	0.005219442
19.21	0.05307	0.00252273
19.22	0.04209	0.002000786
19.23	0.17934	0.008525089
19.24	0.07686	0.003653609
19.25	0.04026	0.001913795
19.26	0.00183	0.00008699
27.29	0.11163	0.005306433
27.30	0.08784	0.004175554
27.31	0.05856	0.002783702
27.32	0.02745	0.001304861
27.33	0.12993	0.00617634
27.34	0.12078	0.005741386
27.35	0.07869	0.0037406
27.36	0.07137	0.003392637
27.37	0.08235	0.003914582
38.40	0.0549	0.002609721
38.41	0.03477	0.001652823
38.42	0.04392	0.002087777
38.43	0.12078	0.005741386
38.44	0.0732	0.003479628
45.47	0.01098	0.000521944
45.48	0.11529	0.005480414
45.49	0.08601	0.004088563

p.u	R	X
45.50	0.04209	0.002000786
45.51	0.06405	0.003044675
45.52	0.1281	0.006089349
45.53	0.03843	0.001826805
54.55	0.04758	0.002261758
54.56	0.08784	0.004175554
54.57	0.12261	0.005828377
54.58	0.15738	0.0074812
54.59	0.16104	0.007655182
54.61	0.11346	0.005393423
54.63	0.05673	0.002696712
54.64	0.08418	0.004001572
65.66	0.26718	0.012700642
65.67	0.19215	0.009134024
65.68	0.12444	0.005915368
20.72	0.0549	0.002609721
28.73	0.06039	0.002870693
28.74	0.03843	0.001826805
28.75	0.07686	0.003653609
28.76	0.09699	0.004610507
28.77	0.13176	0.00626333
28.78	0.07137	0.003392637
28.79	0.04941	0.002348749
39.81	0.04392	0.002087777
39.82	0.04026	0.001913795
39.83	0.06588	0.003131665
39.84	0.08967	0.004262544
39.85	0.07869	0.0037406
39.86	0.09516	0.004523516
46.87	0.08052	0.003827591
46.88	0.05307	0.00252273
46.89	0.07686	0.003653609
46.90	0.03294	0.001565833
46.91	0.02379	0.001130879
46.92	0.02562	0.00121787
46.93	0.04758	0.002261758
46.94	0.08052	0.003827591
46.95	0.08235	0.003914582
46.96	0.0549	0.002609721
60.97	0.04392	0.002087777
60.98	0.0366	0.001739814
60.99	0.08052	0.003827591
60.101	0.05856	0.002783702
60.102	0.04941	0.002348749

A. Line Data

p.u	R	X
62.103	0.05307	0.00252273
62.104	0.02745	0.001304861
62.105	0.04026	0.001913795
62.106	0.08784	0.004175554
62.107	0.0549	0.002609721
80.109	0.05307	0.00252273
80.110	0.08784	0.004175554
80.111	0.04209	0.002000786
80.112	0.02013	0.000956898
80.113	0.06954	0.003305647
80.114	0.10065	0.004784489
100.115	0.06039	0.002870693
100.116	0.06405	0.003044675
100.117	0.0732	0.003479628
100.118	0.02379	0.001130879
108.119	0.02379	0.001130879
108.120	0.06405	0.003044675
108.121	0.02013	0.000956898

B

GAMS Code Case 5

```
Option work=100000000
option decimals=4;
option reslim=36000

set t time;
$GDXIN MtoG.gdx
$LOAD t
$GDXIN

** microgrid buses
set i bus /9, 10, 19*120/;
alias(i,j);
set iL(i) /10, 19, 27, 28, 38, 39, 80, 45, 46, 54, 60, 100, 62/;
set jL(i) /10, 19, 27, 28, 38, 39, 80, 45, 46, 54, 60, 100, 62/;

** starting battery energy.
parameter Estart(i,t);
$GDXIN Enitial.gdx
$LOAD Estart
$GDXIN CHPin.gdx
$LOAD PchpStart
$GDXIN

* SET Distribution Grid
set Di DIST Bus /1*9, 11*18/
alias(Di,Dj);

set head1 /Pmin, Pmax, Vmin, Vmax, Qmin, Qmax, Pris/
set head2 /R, X, C/;
set BattHead /Emax, Pmin, Pmax/;
scalars phi /3.141592654 /
        Sb Power base /1000000/
        PVeff PV efficiency /0.152/
        PVarea PV panel size m^2 /1.642088/
        PVamount PV panels per house /25/
        MGhouses Houses with PV /100/
        PF Load Power Factor /0.95/
        Vmin Minimum Voltage /0.97428571428/
        Vmax Maximum Voltage /1.12095238095/
        Vswing Swing bus voltage /1.03/
        nb Battery Efficiency /0.95/
        Vbaselow Low voltage base /381.81818181/
        Vbasemed medium voltage base /10000/
        IbaseMed Medium voltage Current base /100/
        Imax Max current /270/
        Day /100/;
```

B. GAMS Code Case 5

Parameter Time 'Total time in hours';

Time = card(t);
display Time, PchpStart2;

* Grid Data

* Microgrid swing bus

Table SwingMG(i, head1)

	Pmin	Pmax	Qmin	Qmax
9	-0.8	0.8	-100	100

* Microgrid Linedata

Table LineData(i, j, Head2) network data

	R	X
9.10	0.01678875	0.08841
10.19	0.010625	0.006675884
10.27	0.0185	0.011623893
10.38	0.011625	0.007304203
10.45	0.027125	0.01704314
10.54	0.020875	0.013116149
10.70	0.001375	0.000863938
19.20	0.00875	0.005497787
27.28	0.017	0.010681415
38.39	0.01125	0.007068583
39.80	0.010625	0.006675884
45.46	0.0115	0.007225663
54.60	0.012875	0.008089601
60.100	0.009875	0.006204645
54.62	0.014125	0.008874999
62.108	0.011	0.006911504
19.21	0.05307	0.00252273
19.22	0.04209	0.002000786
19.23	0.17934	0.008525089
19.24	0.07686	0.003653609
19.25	0.04026	0.001913795
27.29	0.11163	0.005306433
27.30	0.08784	0.004175554
27.31	0.05856	0.002783702
27.32	0.02745	0.001304861
27.33	0.12993	0.00617634
27.34	0.12078	0.005741386
27.35	0.07869	0.0037406
27.36	0.07137	0.003392637
27.37	0.08235	0.003914582
38.40	0.0549	0.002609721
38.41	0.03477	0.001652823
38.42	0.04392	0.002087777
38.43	0.12078	0.005741386
38.44	0.0732	0.003479628
45.47	0.01098	0.000521944
45.48	0.11529	0.005480414
45.49	0.08601	0.004088563
45.51	0.06405	0.003044675
45.52	0.1281	0.006089349
45.53	0.03843	0.001826805
54.55	0.04758	0.002261758
54.56	0.08784	0.004175554
54.57	0.12261	0.005828377

```

54.58      0.15738      0.0074812
54.59      0.16104      0.007655182
54.61      0.11346      0.005393423
54.63      0.05673      0.002696712
54.64      0.08418      0.004001572
20.72      0.0549       0.002609721
28.73      0.06039      0.002870693
28.74      0.03843      0.001826805
28.75      0.07686      0.003653609
28.76      0.09699      0.004610507
28.77      0.13176      0.00626333
28.78      0.07137      0.003392637
28.79      0.04941      0.002348749
39.81      0.04392      0.002087777
39.82      0.04026      0.001913795
39.83      0.06588      0.003131665
39.84      0.08967      0.004262544
39.85      0.07869      0.0037406
39.86      0.09516      0.004523516
46.87      0.08052      0.003827591
46.88      0.05307      0.00252273
46.89      0.07686      0.003653609
46.90      0.03294      0.001565833
46.91      0.02379      0.001130879
46.92      0.02562      0.00121787
46.93      0.04758      0.002261758
46.94      0.08052      0.003827591
46.95      0.08235      0.003914582
46.96      0.0549       0.002609721
60.97      0.04392      0.002087777
60.98      0.0366       0.001739814
60.99      0.08052      0.003827591
62.103     0.05307      0.00252273
62.104     0.02745      0.001304861
62.105     0.04026      0.001913795
62.106     0.08784      0.004175554
62.107     0.0549       0.002609721
80.109     0.05307      0.00252273
80.110     0.08784      0.004175554
80.111     0.04209      0.002000786
80.112     0.02013      0.000956898
80.113     0.06954      0.003305647
80.114     0.10065      0.004784489
100.115    0.06039      0.002870693
100.116    0.06405      0.003044675
100.117    0.0732       0.003479628
100.118    0.02379      0.001130879
108.119    0.02379      0.001130879
108.120    0.06405      0.003044675
;
*****
* Reading data from GDX: Loads, PV, Wind, and battery
parameters Pload(t,i), Qload(t,i), GI(t,i),Psun(i,t),Pbergey(t,i),
BattData(i,BattHead), Price(t,head1),PriceBuy(t), PriceSell(t),
n(i), PriceCHP, CHPramp, CHPmax;

$GDXIN 2017_MG.gdx
$LOAD Pload
$GDXIN 2017_GI_Tilt.gdx
$LOAD GI
$GDXIN 2017_bergey.gdx

```

B. GAMS Code Case 5

```

$LOAD Pbergey
$GDXIN Battery_AllHouses.gdx
$LOAD BattData
$GDXIN 2017_Price.gdx
$LOAD Price
$GDXIN

Pload(t,i)=Pload(t,i)/1000;
Qload(t,i)=sqrt((Pload(t,i)/PF)**2-(Pload(t,i))**2);
Psun(i,t)=GI(t,i)*PVeFF*PVarea*PVamount/Sb;
Pbergey(t,i)= Pbergey(t,i)/Sb;

PriceBuy(t)=31+Price(t,"Pris");
PriceSell(t)=30+Price(t,"Pris");
n(i)=nb;

* Add hydrogen here
BattData("10","Emax")=150000000000000000;
BattData("10","Pmin")=-10;
BattData("10","Pmax")=10;
n("10")=0.63245553203;

*CHP DATA
PriceCHP=600;
CHPmax=10;

*****
$offorder
*CREATE Y-matrix for microgrid
Parameter Z(i,j), GG(i,j), BB(i,j);
Parameter G(i,j), B(i,j), Y(i,j), ZI(i,j), Theta(i,j);

LineData(j,i,"R")$(LineData(i,j,"R") gt 0.00) = LineData(i,j,"R");
LineData(j,i,"X")$(LineData(i,j,"X") gt 0.00) = LineData(i,j,"X");

Z(i,j) = (LineData(i,j,"R"))**2 + (LineData(i,j,"X"))**2 ;
GG(i,j)$(Z(i,j) ne 0.00) = LineData(i,j,"R")/Z(i,j) ;
BB(i,j)$(Z(i,j) ne 0.00) = -LineData(i,j,"X")/Z(i,j);

B(i,i) = sum(j, BB(i,j));
G(i,i) = sum(j, GG(i,j));
G(i,j)$(ord(i) ne ord(j)) = -GG(i,j);
B(i,j)$(ord(i) ne ord(j)) = -BB(i,j);
Y(i,j) = sqrt(G(i,j)*G(i,j) + B(i,j)*B(i,j));
ZI(i,j)$(G(i,j) ne 0.00) = abs(B(i,j))/abs(G(i,j)) ;

Theta(i,j) = arctan(ZI(i,j));
Theta(i,j)$( (B(i,j) eq 0) and (G(i,j) gt 0) ) = 0.0 ;
Theta(i,j)$( (B(i,j) eq 0) and (G(i,j) lt 0) ) = phi ;
Theta(i,j)$( (B(i,j) gt 0) and (G(i,j) gt 0) ) = Theta(i,j) ;
Theta(i,j)$( (B(i,j) lt 0) and (G(i,j) gt 0) ) = 2*phi - Theta(i,j) ;
Theta(i,j)$( (B(i,j) gt 0) and (G(i,j) lt 0) ) = phi - Theta(i,j);
Theta(i,j)$( (B(i,j) lt 0) and (G(i,j) lt 0) ) = phi + Theta(i,j);
Theta(i,j)$( (B(i,j) gt 0) and (G(i,j) eq 0) ) = 0.5*phi;
Theta(i,j)$( (B(i,j) lt 0) and (G(i,j) eq 0) ) = -0.5*phi;
Theta(i,j)$( (B(i,j) eq 0) and (G(i,j) eq 0) ) = 0.0 ;

Display G, B, Theta;
** end of Y-MATRIX

```

```

$onorder
*****

*Variables
free variable      PswingMG(i,t)  Active power
free variable      QswingMG(i,t)  Reactive power
positive variable  VMG(i,t)       Micro grid Bus Voltage
free variable      delta(i,t)    Bus Voltage Angle
positive variable  Pbdc(i,t)     Battery discharge power
positive variable  Pbc(i,t)     Battery charge power
positive variable  E(i,t)       Battery energy
positive variable  MGimp(t)     Microgrid power import
positive variable  MGexp(t)     Microgrid power export
free variable      MGexT      Total Microgrid power exchange in MW
free variable      Cost       Total microgrid energy cost in SEK
free variable      IreL(iL,jL,t)
free variable      IimL(iL,jL,t)
positive variable  Pchp(i,t)   Power output from CHP
;

* fixed constraints
PswingMG.Lo(i,t) = SwingMG(i,"Pmin");
PswingMG.Up(i,t) = SwingMG(i,"Pmax");
QswingMG.Lo(i,t) = SwingMG(i,"Qmin");
QswingMG.Up(i,t) = SwingMG(i,"Qmax");
VMG.Lo(i,t) = Vmin;
VMG.Up(i,t) = Vmax;
E.Up(i,t)= 0.8*BattData(i,"Emax");
E.Up("10",t)= BattData("10","Emax");
Pbdc.Up(i,t)=BattData(i,"Pmax");
Pbc.Up(i,t)=-BattData(i,"Pmin");
IreL.up(iL,jL,t)=Imax;
IreL.lo(iL,jL,t)=-Imax;
Pchp.up(i,t)=0;
Pchp.up("10",t)=CHPmax;

* fixed values
delta.fx("9",t)=0;
VMG.fx("9",t)=Vswing;
PswingMG.fx(iL,t)=0;
QswingMG.fx(iL,t)=0;
E.l(i,t)=0;

*****
* Microgrid equations
EQUATIONS
PPowerflowMG      Active Powerflow equations
QPowerflowMG      Reactive Powerflow equations
Battery           Battery equation
MGPowerImport     Microgrid power exchange
MGCost            Microgrid profit
MGexTOT
*IMPandEXP
Ire
Iim
Iconst1
Iconst2
Iconst3
Iconst4
;

```

B. GAMS Code Case 5

```

* Power flow equations
PpowerflowMG(i,t)..          PswingMG(i,t)+Pbergey(t,i)+Pchp(i,t)+Psun(i,t)
+Pbdc(i,t)-Pbc(i,t)- Pload(t,i)  =e=
1.03*sum(j, VMG(j,t)*G(i,j)+1.03*B(i,j)*(delta(i,t)-delta(j,t)));

QpowerflowMG(i,t)..          QswingMG(i,t)- Qload(t,i) =e=
-1.03*sum(j, 1.03*G(i,j)*(delta(i,t)-delta(j,t))-VMG(j,t)*B(i,j));

* Battery equations
Battery(i,t)..          E(i,t)=e=E(i,t-1)-(Pbdc(i,t)/n(i)-Pbc(i,t)*n(i))+Estart(i,t);

* Current constraint
Ire(iL,jL,t)..          IreL(iL,jL,t)=e=(G(iL,jL)*(VMG(jL,t)-VMG(iL,t))
+1.03*B(iL,jL)*(delta(iL,t)-delta(jL,t)))*Sb/Vbaselow;

Iim(iL,jL,t)..          IimL(iL,jL,t)=e=(B(iL,jL)*(VMG(jL,t)-VMG(iL,t))
-1.03*G(iL,jL)*(delta(iL,t)-delta(jL,t)))*Sb/Vbaselow;

Iconst1(iL,jL,t)..      IreL(iL,jL,t)-0.58*IimL(iL,jL,t)=l=1.15*Imax;
Iconst2(iL,jL,t)..      IreL(iL,jL,t)-0.58*IimL(iL,jL,t)=g=-1.15*Imax;
Iconst3(iL,jL,t)..      IreL(iL,jL,t)+0.58*IimL(iL,jL,t)=l=1.15*Imax;
Iconst4(iL,jL,t)..      IreL(iL,jL,t)+0.58*IimL(iL,jL,t)=g=-1.15*Imax;

* Power import/exchange equations
MGPowerImport(t)..      MGimp(t)-MGexp(t) =e= PswingMG("9",t);
MGexTOT..              MGexT=e=sum(t, MGimp(t)+MGexp(t))
+0.2*sum(t, sum(i, Pbc(i,t)+Pbdc(i,t))-Pbc("10",t)-Pbdc("10",t))
+0.7*sum(t, Pbc("10",t)+Pbdc("10",t))+0.8*sum(t, Pchp("10",t));

*initial values
PswingMG.l(i,t) = 0;
QswingMG.l(i,t) = 0;
VMG.l(i,t) = 0;
IreL.l(iL,jL,t)=0;
IimL.l(iL,jL,t)=0;

delta.l(i,t)=0;

MODEL Microgrid
/
PpowerflowMG
QpowerflowMG
Battery
MGPowerImport
MGexTOT
Ire
Iim
Iconst1
Iconst2
Iconst3
Iconst4
/

option MINLP=dicopt;
option DNLP=Minos;
option NLP=Minos
option Mip=cplex
option lp=cplex

SOLVE Microgrid using LP Minimize MGexT;
parameter statusMG, statusDBG ;

```

```

statusMG=microgrid.modelStat;

** Post solution calculations
Cost.l=sum(t,MGimp.l(t)*PriceBuy(t)-MGexp.l(t)*PriceSell(t))
+smx(t,MGimp.l(t)*1164+26.575+sum(t,PriceCHP*Pchp.l("10",t));

parameter BatteryLosses(t) kW, BatteryLossesTotal kW,
MGloss(t) kW, MGlossTotal kW;

BatteryLosses(t)=sum(i,Pbdc.l(i,t)*((1-n(i))/n(i))+Pbc.l(i,t)*(1-n(i)));
BatteryLossesTotal=sum(t, BatteryLosses(t));

MGloss(t)= 0.5*(sum(i, sum(j,abs(G(i,j))*(VMG.l(i,t)*VMG.l(i,t)
+VMG.l(j,t)*VMG.l(j,t)
-2*VMG.l(i,t)*VMG.l(j,t)*cos(delta.l(j,t)-delta.l(i,t))))));

*****
*****DISTRIBUTION GRID MODEL*****

*Distribution grid line data
Table LineDataDBG(Di,Dj,Head2) network data
      R          X          C
1.2    0.00016597    0.00305008    0
2.3    0.00186      0.00131375    0.010787915
3.4    0.0015554    0.0001745     0.0001047
4.5    0.00060125    0.00042325    0.0034755
5.6    0.00039375    0.00027715    0.00227605
6.7    0.0002272     0.0000825     0.00033455
5.8    0.0008125     0.00057195    0.00469665
8.9    0.000635      0.000447      0.0036706
9.11   0.00038125    0.00026835    0.0022038
11.12  0.00093         0.00065465    0.00537585
12.13  0.0008925       0.0006284     0.0051591
13.14  0.00055625     0.00039155    0.0032154
14.15  0.00044625     0.0003141     0.00257955
15.16  0.00026875     0.00018915    0.0015535
16.17  0.000315       0.0002217     0.00182085
17.18  0.000325        0.00022875    0.00187865
18.2   0.004125        0.00290385    0.02384465
;

$offorder
*CREATE Y-matrix for distribution grid lines
Parameter ZDBG(Di,Dj), GGDBG(Di,Dj), BBDBG(Di,Dj), YCLDBG(Di);
Parameter GDBG(Di,Dj), BDBG(Di,Dj), YDBG(Di,Dj), ZIDBG(Di,Dj), ThetaDBG(Di,Dj);

LineDataDBG(Dj,Di,"R")$(LineDataDBG(Di,Dj,"R") gt 0.00)
= LineDataDBG(Di,Dj,"R");

LineDataDBG(Dj,Di,"X")$(LineDataDBG(Di,Dj,"X") gt 0.00)
= LineDataDBG(Di,Dj,"X");

LineDataDBG(Dj,Di,"C")$(LineDataDBG(Di,Dj,"C") gt 0.00)
= LineDataDBG(Di,Dj,"C")/2;

ZDBG(Di,Dj) = (LineDataDBG(Di,Dj,"R"))**2 + (LineDataDBG(Di,Dj,"X"))**2 ;
GGDBG(Di,Dj)$(ZDBG(Di,Dj) ne 0.00) = LineDataDBG(Di,Dj,"R")/ZDBG(Di,Dj) ;

```

```

BBDBG(Di,Dj)$ (ZDBG(Di,Dj) ne 0.00) = -LineDataDBG(Di,Dj,"X")/ZDBG(Di,Dj);
YCLDBG(Di) = sum(Dj, LineDataDBG(Di,Dj,"C"));
BDBG(Di,Di) = sum(Dj, BBDBG(Di,Dj)) + YCLDBG(Di);
GDBG(Di,Di) = sum(Dj, GGDBG(Di,Dj));
GDBG(Di,Dj)$ (ord(Di) ne ord(Dj)) = -GGDBG(Di,Dj);
BDBG(Di,Dj)$ (ord(Di) ne ord(Dj)) = -BBDBG(Di,Dj);
YDBG(Di,Dj) = sqrt(GDBG(Di,Dj)*GDBG(Di,Dj) + BDBG(Di,Dj)*BDBG(Di,Dj));
ZIDBG(Di,Dj)$ (GDBG(Di,Dj) ne 0.00) = abs(BDBG(Di,Dj))/abs(GDBG(Di,Dj));

ThetaDBG(Di,Dj) = arctan(ZIDBG(Di,Dj));
ThetaDBG(Di,Dj)$ ((BDBG(Di,Dj) eq 0) and (GDBG(Di,Dj) gt 0)) = 0.0 ;
ThetaDBG(Di,Dj)$ ((BDBG(Di,Dj) eq 0) and (GDBG(Di,Dj) lt 0)) = phi ;

ThetaDBG(Di,Dj)$ ((BDBG(Di,Dj) gt 0) and (GDBG(Di,Dj) gt 0))
= ThetaDBG(Di,Dj) ;

ThetaDBG(Di,Dj)$ ((BDBG(Di,Dj) lt 0) and (GDBG(Di,Dj) gt 0))
= 2*phi - ThetaDBG(Di,Dj) ;

ThetaDBG(Di,Dj)$ ((BDBG(Di,Dj) gt 0) and (GDBG(Di,Dj) lt 0))
= phi - ThetaDBG(Di,Dj);

ThetaDBG(Di,Dj)$ ((BDBG(Di,Dj) lt 0) and (GDBG(Di,Dj) lt 0))
= phi + ThetaDBG(Di,Dj);

ThetaDBG(Di,Dj)$ ((BDBG(Di,Dj) gt 0) and (GDBG(Di,Dj) eq 0))
= 0.5*phi ;

ThetaDBG(Di,Dj)$ ((BDBG(Di,Dj) lt 0) and (GDBG(Di,Dj) eq 0))
= -0.5*phi ;

ThetaDBG(di,Dj)$ ((BDBG(Di,Dj) eq 0) and (GDBG(Di,Dj) eq 0))
= 0.0 ;
*****
$onorder
Table SwingDBG(Di,head1)
      Pmin      Pmax      Qmin      Qmax
1      -100      100      -100      100

Parameters Pwind(t,Di),Qwind(t,Di),PloadDBG(t,Di), QloadDBG(t,Di);
$GDXIN 2017_Wind_P.gdx
$LOAD Pwind
$GDXIN 2017_Wind_Q.gdx
$LOAD Qwind
$GDXIN 2017_DBG.gdx
$LOAD PloadDBG
$GDXIN

PloadDBG(t,Di)= PloadDBG(t,Di)/1000;
QloadDBG(t,Di)=sqrt((PloadDBG(t,Di)/PF)**2-(PloadDBG(t,Di))**2);

* Variables
free variable      PswingDBG(Di,t)      Active power
free variable      QswingDBG(Di,t)      Reactive power
positive variable  VDBG(Di,t)      DistriGrid Bus Voltage
free variable      deltaDBG(Di,t)      Bus Voltage Angle
free variable      D      dummy
;

* fixed constraints
PswingDBG.Lo(Di,t) = SwingDBG(Di,"Pmin");

```

```

PswingDBG.Up(Di,t) = SwingDBG(Di,"Pmax");
QswingDBG.Lo(Di,t) = SwingDBG(Di,"Qmin");
QswingDBG.Up(Di,t) = SwingDBG(Di,"Qmax");
VDBG.Lo(Di,t) = Vmin;
VDBG.Up(Di,t) = Vmax;

* fixed values
deltaDBG.fx("1",t)=0;
VDBG.fx("1",t)=Vswing;
VDBG.l(Di,t) = 1;

PloadDBG(t,"9")=PswingMG.l("9",t);
QloadDBG(t,"9")=QswingMG.l("9",t);

Distribution grid equations
QpowerflowDBG
PpowerflowDBG
Dummy
;

PpowerflowDBG(Di,t)..          PswingDBG(Di,t)+Pwind(t,Di)/1000 - PloadDBG(t,Di)
=e= VDBG(Di,t)*sum(Dj,VDBG(Dj,t)*(GDBG(Di,Dj)*cos(deltaDBG(Di,t)-deltaDBG(Dj,t))
+BDBG(Di,Dj)*sin(deltaDBG(Di,t)-deltaDBG(Dj,t))));

QpowerflowDBG(Di,t)..          QswingDBG(Di,t)+Qwind(t,Di)/1000 - QloadDBG(t,Di)
=e=-VDBG(Di,t)*sum(Dj,VDBG(Dj,t)*(GDBG(Di,Dj)*sin(deltaDBG(Di,t)-deltaDBG(Dj,t))
-BDBG(Di,Dj)*cos(deltaDBG(Di,t)-deltaDBG(Dj,t))));

Dummy..                        D=e=1;

Model DistributionGrid
/
PpowerflowDBG
QpowerflowDBG
Dummy
/

SOLVE DistributionGrid using NLP Minimize D;
statusDBG=DistributionGrid.modelstat
parameter DBGLoss(t) kW,DBGLossTotal kW, VPPCmax, VPPCmin, PimpT MW;

DBGLoss(t)= 1000*0.5*(sum(Di ,sum(Dj,abs(GDBG(Di,Dj))*(VDBG.l(Di,t)*VDBG.l(Di,t)
+VDBG.l(Dj,t)*VDBG.l(Dj,t)-2*VDBG.l(Di,t)*VDBG.l(Dj,t)*cos(deltaDBG.l(Dj,t)
-deltaDBG.l(Di,t))))));

DBGLossTotal=1000*(sum(t,PswingDBG.l("1",t)+Pwind(t,"7")/1000)
-sum(Di,sum(t,PloadDBG(t,Di))));

VPPCmax=smax(t,VDBG.l("9",t));
VPPCmin=smin(t,VDBG.l("9",t));
PimpT=sum(Di,sum(t,PswingDBG.l(Di,t)));

```